UNIVERSITY OF NAPLES

FEDERICO II

SCHOOL OF MEDICINE AND SURGERY

DEPARTMENT OF PUBLIC HEALTH

DOCTOR OF PHILOSOPHY IN CLINICAL AND PATHOLOGICAL MORPHOLOGY

CYCLE XXIX

COORDINATOR: PROF. STEFANIA MONTAGNANI

DISSERTATION ON

MINIMALLY INVASIVE TUBULAR RETRACTION AND TRANSTUBULAR APPROACHES IN NEUROSURGERY

SUPERVISOR:

PROF. STEFANIA MONTAGNANI

CANDIDATE:

DR. ALEXANDER I. EVINS

ACADEMIC YEAR 2016/2017

MINIMALLY INVASIVE TUBULAR RETRACTION AND TRANSTUBULAR APPROACHES IN NEUROSURGERY

Alexander I. Evins

Department of Neurological Surgery, Weill Cornell Medical College, Cornell University

Department of Public Health, School of Medicine and Surgery, University of Naples Federico II

Minimally invasive surgical approaches have revolutionized surgical care and are becoming increasingly common and sought after in neurosurgery. Despite significant advancements in these techniques and associated technologies, the use of spatulas, that remain essentially unchanged since the late 1800s, for brain retraction endures as a mainstay of neurosurgical practice. In the last decade, tubular retractors have been successfully used in the management of deep-seated intraparenchymal and intraventricular lesions but have yet to be used to minimize brain retraction in skull base surgery.

In order to determine the full applicability of transtubular techniques in neurosurgery, we compare brain retraction pressures between tubular retractors and brain spatulas in common neurosurgical approaches, assess the feasibility of performing minimally invasive transtubular skull base and general neurosurgical approaches, and introduce a novel technique for closure of transtubular minicraniectomies with maintenance of anatomic integrity.

In all approaches assessed, tubular retraction resulted in average brain retraction pressures that were 57% less collectively than those resulting from spatula retraction. Tubular retractors demonstrated more consistent average retraction pressures between approaches and required 50% less mean retraction distance

compared to spatula retractors, while cortical tearing was observed microscopically in 39% of cases following spatula retraction.

Transtubular supraorbital, anterior transpetrosal, interhemispheric transcallosal, retrosigmoid, and supracerebellar infratentorial approaches are safe and effective surgical corridors to their respective intracranial targets, with ample surgical exposure, freedom, and maneuverability and minimal retraction of brain tissue. The tubular retractor provided sufficient working space for standard bimanual surgical technique without obstruction of the visual field and permitted sufficient surgical freedom while allowing for constant monitoring of retracted tissues. Adequate preoperative planning of the surgical trajectory was critical for facilitating a safe, direct, and practicable surgical corridor. Closure of transtubular minicraniectomies could be accomplished by rapid on-demand 3D printing of patient-specific cranioprostheses which was found to be a novel, feasible, and inexpensive option that was accomplished with minimal technical difficulty.

Tubular retraction in neurosurgery provides a safe and effective conduit for the application of percutaneous minimally invasive approaches while inducing substantially reduced brain retraction pressures than conventional spatula retractors. Advances in neuronavigation and surgical robotics will continue to expand the indications for tubular retraction in neurosurgery.

BIOGRAPHICAL SKETCH

Alexander I. Evins is currently the Chief Research Fellow and an Instructor in the Microneurosurgery Skull Base and Surgical Innovations Laboratory in the Department of Neurological Surgery of Weill Cornell Medical College of Cornell University where he spearheads the development of new operative techniques in microneuosurgery, skull base surgery, and neuroendoscopy. As a doctoral candidate, Alexander worked with neurosurgery fellows from around the world to expand the current boundaries of neurosurgical practice through the development of novel technologies, techniques, and procedures that have rapid clinical applicability; and to enhance neurosurgical training through the integration of cadaveric dissections with 3D visualization, virtual reality, and computer simulation. Alexander has published a large number of peer-reviewed studies on a range of neurosurgical topics and is regularly invited to speak at neurosurgical conferences around the world. His previous research on epilepsy surgery complications helped to widen the indications for the surgical management of epilepsy, and his pioneering work on minimally invasive transtubular neurosurgery has been featured on the cover of the Journal of Neurosurgery. Recently, Alexander was awarded a grant from the National Center for Advancing Translational Sciences of the U.S. National Institutes of Health to develop techniques for integrating 3D printing into the neurosurgical operating room. Alex is also a recipient of the Outstanding Young Alumnus Award from Tulane University, from which he was graduated from their Neuroscience Program. In addition to his academic research activities, Alex instructs the Weill Cornell Clinical and Surgical Neuroanatomy program for medical students and serves as a clinical research consultant in several countries. Alexander is a native of New Yok City, where he currently resides.

To my parents, for their unending love and support, and for whom without this would not have been possible, I am eternally grateful—especially to my Mom, whose fortitude and tenacity inspire me each and every day.

To Jessica—whose kind passion and dedication know no bounds—in the vastness of space and the immensity of time, there is no one else with whom I could imagine taking this journey.

And to all patients who may benefit from this work.

ACKNOWLEDGMENTS

I would like to express my deepest thanks and appreciation to my longtime teacher, mentor, advisor, and friend Dr. Antonio Bernardo. Without his constant support, encouragement, inspiration, and medical insight, I would not have been able to accomplish what I have thus far professionally. I deeply admire his enthusiasm for the pursuit of increasingly better solutions to basic problems in surgery, his passion for unadulterated excellence in neuroanatomy and skull base surgery, and his all-too-rare no nonsense approach to medical pedagogy. His mentorship has allowed me to grow into a focused and accomplished clinical scientist, and I am forever grateful for the opportunity to work under such a talented and dedicated neurosurgeon.

I would also like to especially thank Dr. Clotilde Castaldo who provided invaluable support, expertise, feedback, and reassurance. Her warm and welcoming advice and direction were instrumental throughout this process, and I am exceptionally grateful for her guidance as well as for her and her mother's extraordinary cooking.

Furthermore, I would like to thank Prof. Stefania Montagnani, for without her assistance and leadership none of this would be possible. I am deeply grateful for her enthusiastic support and willingness to take on an outsider, as well as that of the Department of Public Health and the faculty, staff, and students of the School of Medicine and Surgery.

I sincerely thank all of the members of the doctoral selection, advisory, and thesis committees—who enabled and fostered this pursuit of knowledge—for investing their time and providing thoughtful and indispensable feedback while continuously reminding me of the boundless diversity, complexity, and wonder of this specialty.

I am immensely grateful to my neurosurgical colleagues around the world who

helped shape these ideas and who provided meaningful discourse over the years, as well as to my longtime friend and collaborator, Justin Burrell, who willingly listens to my crazy ideas at even the most unthinkable of hours.

Additionally, I would like to express my sincere gratitude to all of the medical students, residents, and fellows who assisted in the production of this body of work and to those who provided support, comments, and assistance. I would also like to thank the Department of Neurological Surgery at Weill Cornell Medical College/NewYork–Presbyterian Hospital for their valued and continued support.

TABLE OF CONTENTS

LIST OF FIGURES

LIST OF TABLES

LIST OF ABBREVIATIONS

3D	Three-dimensional
ACOM	Anterior communicating artery
CI	Confidence interval
cm	Centimeter
CN	Cranial nerve
CT	Computed tomography
ELF	Economical load and force
FLAIR	Fluid-attenuated inversion recovery
g	Gram
GSPN	Greater superficial petrosal nerve
IAC	Internal auditory canal
ICH	Intracerebral hemorrhage
MiSPACE	Minimally Invasive Subcortical Parafascicular Transsulcal Access for Clot Evacuation
mm	Millimeter
mmHg	Millimeters of mercury
MRD	Mean retraction distance
MRI	Magnetic resonance imaging
MRP	Mean retraction pressure
PEEK	Polyether ether ketone
PMMA	Polymethyl methacrylate
SD	Standard deviation
SE	Standard error
STL	Standard triangle language
VBAS	ViewSite Brain Access System

LIST OF SYMBOLS

α	Alpha
°	Degree
®	Registered trademark
™	Trademark

PREFACE

"In examining disease, we gain wisdom about anatomy and physiology and biology. In examining the person with disease, we gain wisdom about life."

—Oliver Sacks M.D.

Skull base surgery developed as a neurosurgical subspecialty in the 1980s with the aim of expanding bone removal in cranial approaches to the skull base in order to minimize brain retraction and injury, while providing enhanced exposure of the neurovasculature and lesions located at the base of the skull. The 1990s saw rapid growth and adoption of skull base surgery, as well as significant development of its techniques. Despite these advances in surgical access, neurosurgery has for over a century relied and continues to rely on retractors, which remain essentially unchanged since their development in the late 19th century, to displace brain tissue in order to enhance surgical exposure of deeper targets.

In the last two decades, minimally invasive surgical approaches have revolutionized neurosurgical care and are becoming increasingly common and sought after by both practitioners and patients. Endoscopic procedures performed through smaller corridors, as opposed to large traditional openings of the skull, are gentler on the brain and cause less total tissue damage. As the incisions and surgical corridors are small, patients tend to have faster recovery times and less discomfort compared with conventional surgery.

The last several years have marked a period of transition from maximal bone removal and exposure to minimally invasive and endoscopic surgical techniques, however there remains a significant challenge in attempting to merge the goals of open surgery with the benefits of minimally invasive techniques using existing surgical

technologies, instruments, and tools.

Three years ago, during a spine surgery case involving a lumbar microdiscectomy a colleague made a seemingly innocent observation about the metal tube being used to retract the patient's skin and muscle that would change the course of my professional life. We subsequently postulated on the benefits of using such a system for accessing lesions at the base of the skull while minimizing the risk of retraction injury caused by neural damage from disruption of cortical microcirculation.

This body of work is the result of that conversation, and many others, which ultimately led to the development of a set of minimally invasive transtubular surgical techniques. This work describes that process of development, from incision to closure, beginning with a comparison of retraction force between retractor types, followed by an extensive demonstration of the surgical feasibility of transtubular retraction in a number of common neurosurgical approaches, and ultimately defines a novel method for closure of the associated miniature craniectomies.

I firmly believe that transtubular approaches in neurosurgery can safely bridge the gaps both between open and endoscopic skull base surgery, as well as between the bimanual surgery of today and the robotic surgery of tomorrow—by providing a corridor through which a robot can safely work. This set of transtubular approaches, combined with the emerging surgical technologies of white matter tractographic navigation and robotic exoscopy, will expand the minimally invasive neurosurgical armamentarium while improving patient outcomes and satisfaction.

The work described herein was completed in full at the Skull Base Microneurosurgery and Surgical Innovations Laboratory of Weill Cornell Medical College. To the best of my knowledge, this dissertation is original work, except where references are made to outside sources. This, nor any substantially similar dissertation, has been or is being submitted for any other degree, diploma, or qualification at any

other university. Extensions of this project have been published in the Journal of Neurosurgery and World Neurosurgery, and select portions have been presented at several scientific meetings, including but not limited to those of the American Association of Neurological Surgeons, the Congress of Neurological Surgeons, and the North American Skull Base Society.

INTRODUCTION

Brain Retraction in Neurosurgery

The history of brain retraction in neurosurgery began on November 25, 1884, when Sir Rickman Godlee performed the first primary intracranial brain tumor operation for a glioma and first introduced a brain retractor to surgery.[1–2] In 1886, in The London Medical Record, Bennett and Godlee described using a small malleable spatula to separate the tumor from the brain parenchyma,[3] and in doing so ushered in the modern era of spatula-based brain retraction. By 1890, references to brain retractors began appearing in medical texts,[4] and in 1909 American neurosurgeon Charles Frazier, in a text edited by William Williams Keen, described using the handles of ordinary spoons, which he bent to provide visualization of deeper intracranial structures (Figure 1).[5–6]

During this period, varying types of brain spatulas were introduced by German surgeon Lothar Heidenhain and later by Fraizer, who developed an elevator for operations at the base of the brain, often used in conjunction with spoon handles.[1,7] In 1906, pioneering English neurosurgeon Sir Victor Horsley provided the first review of brain retraction, associated techniques, and retraction injury in an address to the British Medical Association, in which he concluded that retraction was effective, but also posited the important question of "What happens to the hemisphere compressed?"[1,8] According to a recent review by Assina et al.,[1] this began a paradigm shift in neurosurgery at the time, and retraction soon became the preferred method, compared to excision of obstructing brain tissue as proposed by Frazier.

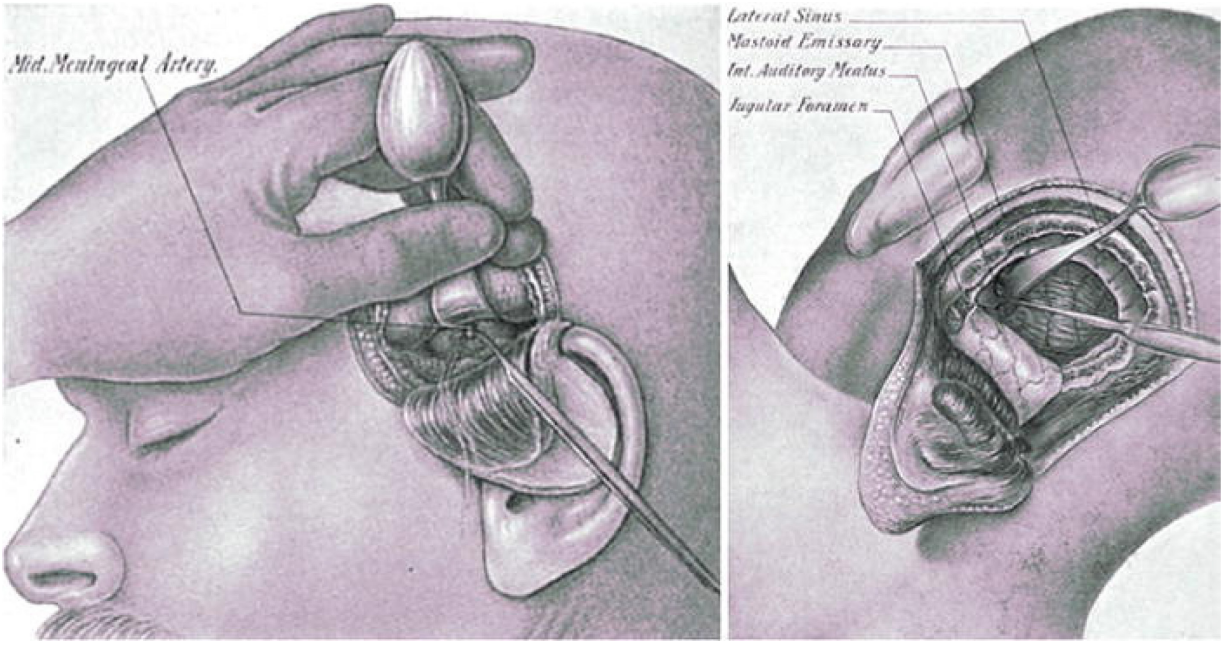

Figure 1. Spoon Handle Retractors. A bent teaspoon handle is used to elevate the temporal lobe in the subtemporal approach (left) and retract the cerebellum to visualize the facial and auditory nerves (right). Illustrations from the 1909 text, Surgery: Its Principles and Practice, Vol. 5, by various authors.[1,6]

Three years later, in 1909, the father of American neurosurgery, William Harvey Cushing, subsequently described his use of a "spoon-shaped, round-edged spatula" that reportedly caused less damage to cortical vessels than flat retractors.[1,9] Both Cushing and Horsley introduced varying sized malleable handheld retractors, in the shape of rectangular ribbons with one narrow end known as a taper, that could be bent and shaped as needed (Figure 2).[1,10] This design endured and saw only slight modifications in the 1920s, where some retractors took the form of small shovels.[10]

In the 1930s, the first skull-mounted retractors were introduced, but due to their invasiveness and requirement for drilling additional holes, as well as inherent variabilities in the thickness of the skull, they were replaced by skin-mounted, then table-mounted, and ultimately headrest-mounted retractor systems. Table-mounted retractors were popularized in the late 1970s

by renown Turkish neurosurgeon Gazi Yaşargil, who introduced a table-mounted flexible arm that held a brain spatula, and named it the Leyla retractor, after his daughter.[10–11] While effective, this system allowed for the possibility of independent movement of the patient's head and the retractor arm, so that any movement of the head or table could result in uncontrolled movement at the brain-retractor interface.[1] This issue was solved with the introduction of self-retaining headrest-mounted retractor systems by Greenberg, Sugita, Fukushima, and others.[1,12-13]

These skull clamp mounted retractor systems generally consisted of clamps, secondary clamps, flexible rod holders, retractor blades, and hand rests for instrument stabilization.[1] In 1981, Richard Budde and Jim Day developed the currently popular Budde Halo Brain Retractor System, comprised of a ring that is suspended over a patient's head by two support rods connected to the skull clamp, which allows for 360° retractor arm placement while providing a hand rest for the surgeon. Current Budde Halo systems are lightweight, made from carbon fiber, and radiolucent.[14]

Despite these advancements, the brain spatula itself—also known today as a malleable brain retractor or retractor blade—remains essentially unchanged since its original incarnation in the late 1800s. Today's retractor blades are thin, firm or malleable bands of steel and other metal alloys, with abrupt or well defined edges and a limited surface area (Figure 2).[15] Malleable retractors can be easily bent by hand and are placed, under direct observation, on top of brain parenchyma or dura to retract tissue out of the surgical field. Retractors are often placed over cottonoid strips to protect the underlying tissue, and the handle of the retractor is kept dry to avoid slippage while the distal end is moistened in order to prevent adherence to and/or tearing of the surface tissue.[16] Care must be taken as cottonoid can also adhere to brain tissue, bruise underlying tissue, become entangled in the surgical drill, and obstruct the surgeons' visual

field.[17] Additionally, the uneven transmission and apportionment of the forces applied to the brain tissue can cause retractor-mediated injury.

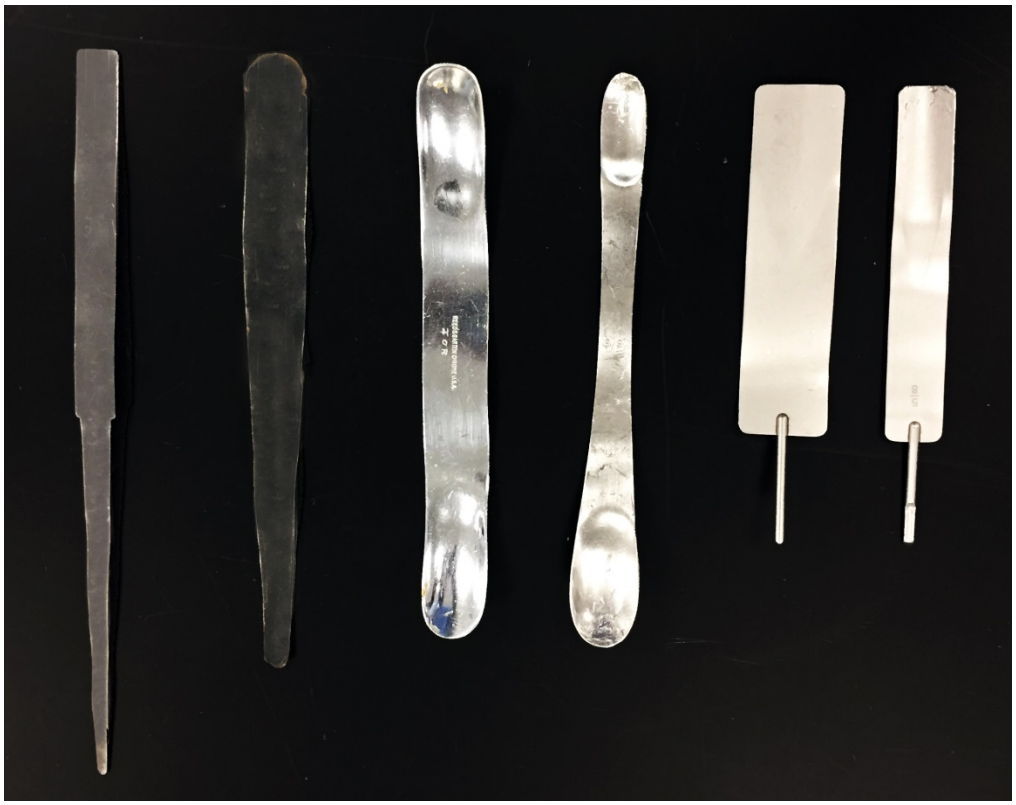

Figure 2. Modern Malleable Brain Retractors. An assortment of varying types of modern retractor blades.

Retraction Injury

Application of a brain retractor induces direct deformation of the underlying parenchyma, which can cause retractor-mediated ischemia by a reduction or cessation of local perfusion that can lead to cell death or long term neuronal atrophy and cortical thinning (Figure 3).[18-24] Venous thrombosis and infarction can also result from compression of cortical venous networks and stretching of bridging veins by provoking local venous congestion.[25–26] Direct induction of a focal area of high pressure by a low surface area retractor creates surrounding areas of low

pressure that can cause tissue to protrude around the edges of the retractor, limiting visualization, necessitating additional retraction, and potentially causing target shift, and can result in direct parenchymal injury, including cortical tearing and compromise of the blood–brain barrier.[20,27–31] A number of studies have attempted to quantify the pressure and duration thresholds for retraction injury.[21,32–35] In a clinical study of 37 patients, Hongo et al. found average neurosurgical brain retraction pressure to be 26.6 mmHg.[36] Using an animal model, Rosenørn and Diemer revealed that focal ischemic damage can occur from retractors held in place for just 15 minutes with 20 mmHg of pressure.[37]

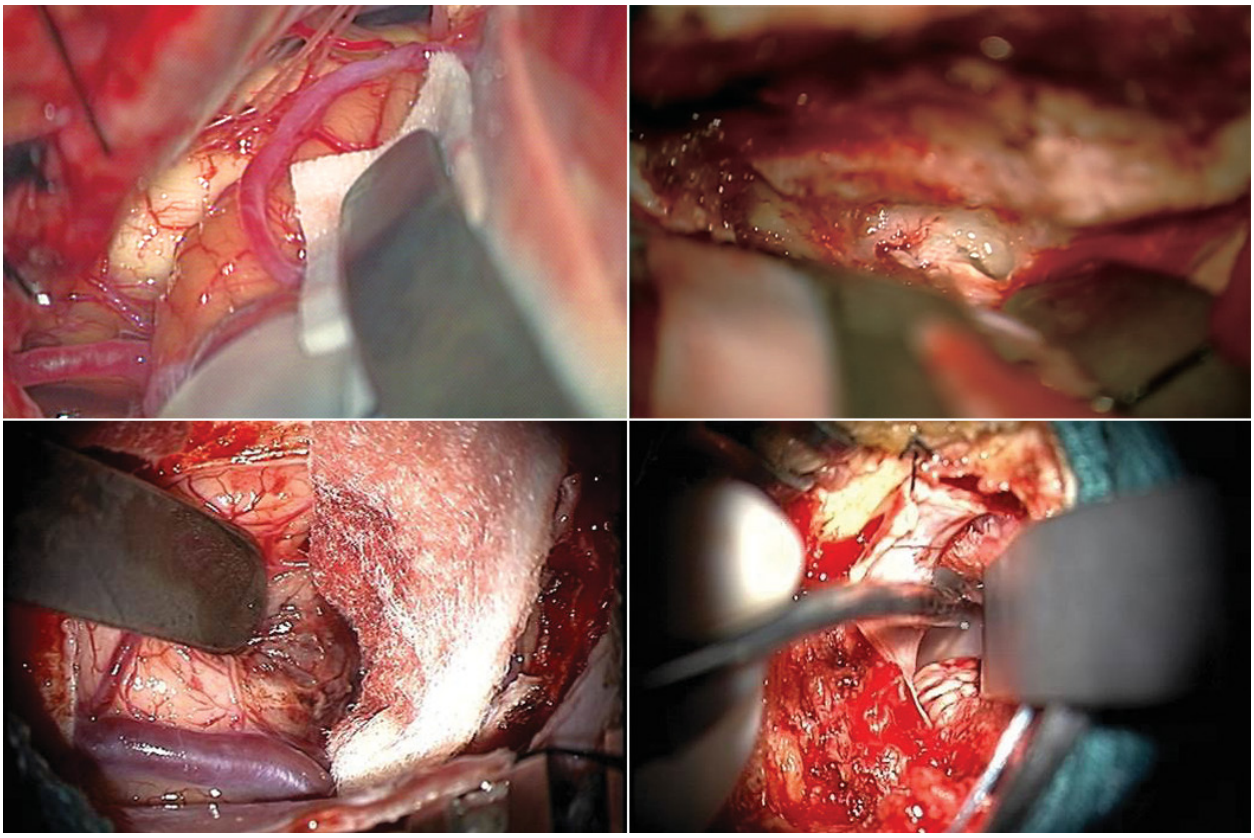

Figure 3. Clinical Application of Malleable Brain Spatulas. Retraction of brain tissue in the far lateral (top, left) and middle fossa (top, right) neurosurgical approaches. Discoloration of brain parenchyma around the retractor (bottom, left) and pulling of tissue (bottom, right) can be seen.

The severity of parenchymal damage, contusion, or infarction is dependent on the type and number of the retractors as well as the pressure, location, and duration of retraction.[21–22,38] Direct retractor-induced brain compression activates inflammatory responses that can exacerbate the initial injury and cause secondary brain damage.[14,31–32,39–41] The specific effects of these responses, the pathogenic roles of matrix metalloproteinase and tyrosine kinases, and the complex cascade of metabolic, oxidative, and electrical events that precede retraction injury have been studied extensively in both human and animal models, including in the setting of induced hypotension, using a wide array of techniques including autoradiography,[34,37] tissue microdialysis,[24,42–43] mechanical transduction,[31,38] somatosensory evoked potential mapping,[43–44] intraoperative functional mapping,[45] single-photon emission computed tomography,[46] and laser Doppler cerebral blood flow analysis.[35,47–48]

Analysis of regional cerebral blood flow by Bell et al. indicated a perfusion need of greater than 10–13 mL/100 g/minute to prevent focal hypoxic-ischemic injury.[49] Laha et al. additionally showed that maintenance of mean arterial pressure at 200 mmHg above brain retraction pressure would be sufficient to counteract retractor-mediated ischemia,[50] however in most intraoperative conditions the inverse is true, as patients often experience iatrogenically-induced or hypovolemic hypotension, which increases susceptibility to retraction injury.[34] Additionally, associated systemic conditions including hypoxemia and hypercapnia can compound the risk of damage.[22]

Biochemical analyses during retraction have revealed metabolic changes further consistent with ischemic conditions, including considerably elevated levels of glutamate and glycerol, indicative of tissue damage and cell membrane degradation, an increased

lactate/pyruvate ratio, indicative of cerebral ischemia, and reduced pH; all of which returned to normal levels upon cessation of retraction.[22,24]

Positron emission tomography studies have confirmed a primary reduction in metabolism in finding a 45% decrease in regional cerebral metabolic rate for oxygen and a 32% reduction in regional oxygen extraction fraction in the retracted regions without change in the opposite hemisphere, similar to findings reported after ischemic stroke and traumatic brain injury.[51] In a recent series of 36 patients undergoing surgery for clipping of an intracranial aneurysm, 11.1% showed magnetic resonance imaging (MRI) signs of postoperative parenchymal signal hyperintensities consistent with retraction injury in fluid-attenuated inversion recovery (FLAIR) and T2 sequences in the location of retraction.[52] These patients all presented with edema and no changes in diffusion weighted or perfusion sequences in the area of the approach.[52–53]

Clinical manifestations of retraction injury largely depend on the region of damage, but often include parenchymal hematomas, aphasia, hemiparesis, and/or paresthesia.[22] In the occipital transtentorial approach, transient and permanent hemianopia from retraction of the occipital lobes have been observed.[54] In the subfrontal approach to the sellar region, anosmia has been observed following retraction of the frontal lobe and olfactory tracts.[55] Seizures and edema are not uncommon following temporal lobe retraction, and cerebellar retraction has been known to manifest as dysmetria, dysdiadochokinesia, and ataxic gait.[55–56] In general, retraction injury should be considered in patients with postoperative development of lateralizing signs, pupillary abnormalities, visual disturbances, and/or seizures.[57]

Incidence of brain retraction injury is difficult to determine, as parenchymal damage may not be immediately evident postoperatively and delayed or subclinical intracerebral hematomas may first be detected on high-resolution computed tomography (CT) or MRI several days

postoperatively.[19,58] A number of clinical studies published in the late 1980s and early 1990s found widely varying rates of postoperative retraction injury detected by postoperative imaging and/or clinical presentation, with several studies reporting a retraction injury rate in brain tumor and intracranial aneurysm surgery between 0.5% and 10%,[58–65] while other studies from the same period reported rates between 60% and 100% with smaller subsets developing clinically significant or permanent postoperative deficits.[66–68] More recent studies have reported rates between 11% and 36% for aneurysm surgery and 79% from cerebellar retraction.[53–54,69] These considerable variations may be the result of heterogeneity in procedure difficulty, intraoperative monitoring resources, surgical skill, sensitivity of detection methods, and criteria used to define retraction injury.[22]

Given that, as previously mentioned, focal ischemic damage has been shown to occur from just 15 minutes of retraction at 20 mmHg of pressure,[37] and, according to a 2011 survey from the American Association of Neurological Surgeons, there are approximately 580,000 cranial procedures performed per year in the United States with average operative times of 327 minutes for aneurysms and 198 minutes for tumors,[70–71] it is likely that focal tissue damage from retraction injury occurs in the vast majority of cases and a significant number of those patients, around 10-15%, develop clinically significant manifestations.

Minimally Invasive Neurosurgery

In order to help mitigate the need for retraction, skull base surgery developed as a neurosurgical subspecialty in the 1980s with the aim of expanding bone removal in cranial approaches to the base of the skull in order to minimize brain retraction and injury.[72] While neurosurgical dogma, since the inception of the specialty, had previously dictated that cranial

openings be as large as possible in order to mitigate the risk of intracranial hypertension, or brain swelling, and safely control hemorrhage, skull base techniques began to transform this belief with the development of well-defined surgical corridors that allowed for more deliberate placement of cranial osteotomies. Openings evolved from generally large vascularized osteoplastic flaps, placed around the temporalis or occipitalis muscles, into large but targeted and strategic openings that minimized brain retraction and provided access to lesions of the complex neurovasculature at the base of the skull.[72–73]

The 1990s saw rapid growth and adoption of skull base surgery as well as significant development of its techniques and the integration of surgical technologies that paved the way for minimally invasive refinements. Individual tailored approaches lessened the reliance on predefined surgical corridors; computerized surgical planning, intraoperative imaging, and neuronavigation allowed for increased surgical orientation without the need to rely solely on visual markers; special instrumentation facilitated the use of narrow surgical corridors; and endoscope-assisted angled visualization provided enhanced visual control.[74–75]

The first wave of modern minimally invasive neurosurgery occurred in the mid-1990s after endoscopic sinus surgery had gained significant popularity amongst otolaryngologists for the treatment of inflammatory sinonasal disorders.[76] The excellent visualization and surgical results provided by the endoscope prompted the development of the, now popular, purely endoscopic endonasal transsphenoidal route to the sellar region by Paolo Cappabiana and Enrico Diviitis in Naples in the late 1990s.[76–80] At the same time, endoscope-assisted transcranial surgery began to evolve, initially as an adjunct that provided views out of the line of sight of the microscope that could only be achieved previously with the use of angled mirrors.[76,80–81]

Axel Perneczky, who pioneered the use of the endoscope in intracranial neurosurgery,[80,82–84] so-called endoscope-assisted neurosurgery, went on to develop the concept of keyhole approaches in neurosurgery, and in his eponymous 2008 text aptly defined this concept in that:

> *The aim of keyhole neurosurgery is not the limited craniotomy, but the limited brain exploration and minimal brain retraction. In this way, the limited craniotomy is not the goal but the result of the philosophy of minimally invasiveness in neurosurgery. The craniotomy should be as limited as possible to offer minimal brain trauma, although as large as necessary to achieve a safe surgical dissection.*[74]

The term "minimally invasive surgery" was first described by Fitzpatrick and Wickham in 1990* and became popular in general surgery with the development of modern endoscopic and laparoscopic techniques.[85] In 1991, at the first international workshop entitled "Contemporary Update on Endoscopic Neurosurgery and Stereotaxy" in Marburg, Germany, the term "minimally invasive neurosurgery" was coined with respect to the work of Fitzpatrick and Wickham.[86]

Today, minimally invasive neurosurgery, as described by Proctor and Black in their text on the subject, attempts to deal with complex lesions in a manner that minimizes blood loss and trauma to normal tissues, and is comprised by two fundamental tenets: a precise definition of the operative anatomy and a minimally invasive surgical corridor to the target.[75] The techniques that make up minimally invasive—and in some cases non-invasive—neurosurgery are varied, extend beyond keyhole approaches, and include endoscopic surgery, image-guided surgery, interventional neuroradiology and endovascular techniques, robotic neurosurgery, and

* Fitzpatrick and Wickham were the first to describe the concept of minimally invasive surgery as it is currently understood, however the term was first used by Chapple and colleagues in 1989 in: Chapple CR, Gelister J, Miller RA. Minimally Invasive Surgery for the Retrieval of Complex Fractured Double J Stents. *Br J Surg*. 1989;76(7):680.

radiosurgery including Gamma Knife, as well as conformal radiation, laser ablation, and focused ultrasound.[75,87]

Despite these advances, and minimizing of the cranial opening, brain retraction and the risk of retraction injury remains unchanged, and there now exists the challenge of merging effective transcranial skull base techniques with keyhole and minimally invasive concepts using novel instruments, tools, imaging, and visualization modalities. While some authors have advocated for the use of retractorless surgery to further this goal, others have sought an alternative that provides surgical maneuverability while minimizing surrounding tissue damage.[88]

Tubular Retraction in Neurosurgery[†]

Stereotactic cylindrical retractors were first introduced by Kelly et al. in 1988 for the excision of deep intraparenchymal lesions, and consisted of thin-walled hollow cylinders 2–3 cm in diameter.[89–90] In 1990, Otsuki and colleagues expanded on this concept by introducing an endoscope into this system for resection of intra-axial tumors.[91] Concurrently, metallic tubular retractors were introduced into spine surgery in 1991 by Faubert and Caspar, and helped form the basis of minimally invasive spine surgery which evolved rapidly and independently over the next decade.[92–95] Over the next six years, a number of reports on the application of mostly metal stereotactic cylindrical retractors for deep-seated intraparenchymal lesions, including colloid cysts, appeared in the literature.[96–100]

As endoscopic neurosurgery began to gain prominence in the early 2000s, several surgeons began to investigate the integration of minimally invasive retraction. In 2005, Harris

[†]A complete timeline of the evolution and adoption of tubular retraction in cranial surgery as seen through published research is provided in Appendix A.

and colleagues first proposed using a modified thoracic port—an 11.5 mm diameter plastic peg-shaped blunt-tipped obturator—for accessing intraventricular lesions, which they dubbed a "ventriculoport."[101] Subsequently in 2007, Schwartz and Anand expanded on this technique which later became more commonly known as an "endoport,"[102] and in 2008 co-authored a study with Greenfield and colleagues on the use of the spinal Minimal Exposure Tubular Retractor system (METRx®, Medtronic, Minneapolis, MN)—comprised of sequentially larger 14–22 mm diameter metal tubes—for the resection of 10 deep-seated intracranial lesions.[103] This ushered in the next generation of transtubular techniques, comprised mainly of microscopic and endoscope-assisted transcranial resection of deep intraparenchymal and intraventricular lesions, during which the tubular retractor evolved from a rigid metal cylinder into an oval-shaped transparent plastic tube.[104–121] At the same time, a number of authors also described the application of self-made tubular retractors, often due to the high costs associated with commercially available systems.[97,99,122–128]

In 2011, Recinos and Jo independently reported the first series of pediatric patients who underwent transtubular resection of deep-seated tumors,[107,129] and in 2015 a number of cases of transtubular evacuation of intracerebral hemorrhage (ICH) and hematoma were reported, including one report on transtubular retrieval of intracranial foreign bodies.[130–135] These studies ultimately led to a multicenter clinical trial on minimally invasive transtubular evacuation of ICH.

The Minimally Invasive Subcortical Parafascicular Transsulcal Access for Clot Evacuation (MiSPACE) trial began in 2013 and evaluated outcomes following transtubular transcortical evacuation of symptomatic and CT-confirmed supratentorial primary ICH.[136–141] Results of the pilot study presented in 2015 showed a 90% evacuation rate with neurologic

improvement in 89% of patients.[142–143] As of the time of writing, the trail is ongoing and currently recruiting patients to obtain additional information regarding clinical outcomes and the economics of the MiSPACE procedure (ClinicalTrials.gov Identifier: NCT02331719).[136,143]

Currently, the scope of practicable neurosurgical applications of transtubular techniques is expanding with the development of novel surgical technologies, including minimally invasive and flexible instruments, exoscopic visualization, surgical robotics, white matter tractography, and neuronavigation, which are facilitating the use of tubular retractors in more restricted surgical corridors as well as allowing for drilling of bone and micromanipulation of delicate tissues through the retractor.[144–146]

Characteristics of Tubular Retractors

Several iterations of tubular retractors are currently commercially available and the two most common of which are the ViewSite Brain Access System (VBAS) (Vycor Medical Inc., Boca Raton, FL) and BrainPath® (NICO Corporation, Indianapolis, IN).

The Vycor VBAS is set of single-use clear plastic, polished polycarbonate tubes comprised of an inner introducer and an outer working channel port that are connected by a spring-loaded latch and can be fixed to a Leyla retractor via an extension arm (Figure 4).[147] The system is available in four different distal port sizes—12×8 mm, 17×11 mm, 21×15 mm, 28×20 mm—each of which are available in 3 cm, 5 cm, and 7 cm lengths (Appendix B). The introducer fits inside of the working channel port and has a blunt rounded tip with a small 2 mm aperture designed to mitigate intracranial pressure spikes during insertion by allowing drainage of cerebrospinal fluid. The VBASMini are miniaturized, 6 mm wide and 5 or 7 mm long, versions of the VBAS designed as alternatives to endoscopic sheaths and for use in pediatric patients.

Figure 4. Vycor Medical ViewSite Brain Access System (VBAS). The full range of VBAS sizes including VBASMini.

The NICO BrainPath® is a set of 13.5 mm diameter single-use 50 mm, 60 mm, and 75 mm long semitransparent sheaths with corresponding reusable large aluminum obturators, equipped with 8 mm or 15 mm pointed tips with no opening and incremental depth markings printed on both the sheath and obturator (Figure 5).[148]

Versions of both the Vycor and NICO devices can be easily integrated with neuronavigation pointers. The BrainPath® device is the subject of the MiSPACE trial. Several other tubular retractors are available in China, including the Goldbov Brain Access System (Goldbov Photoelectronics Co., Ltd., Wuhan, China)—nearly identical to the VBAS—and the Disposable Tissue Duct Expander (VDY20115, Jingcheng Medical Instruments, Shanghai, China).[149]

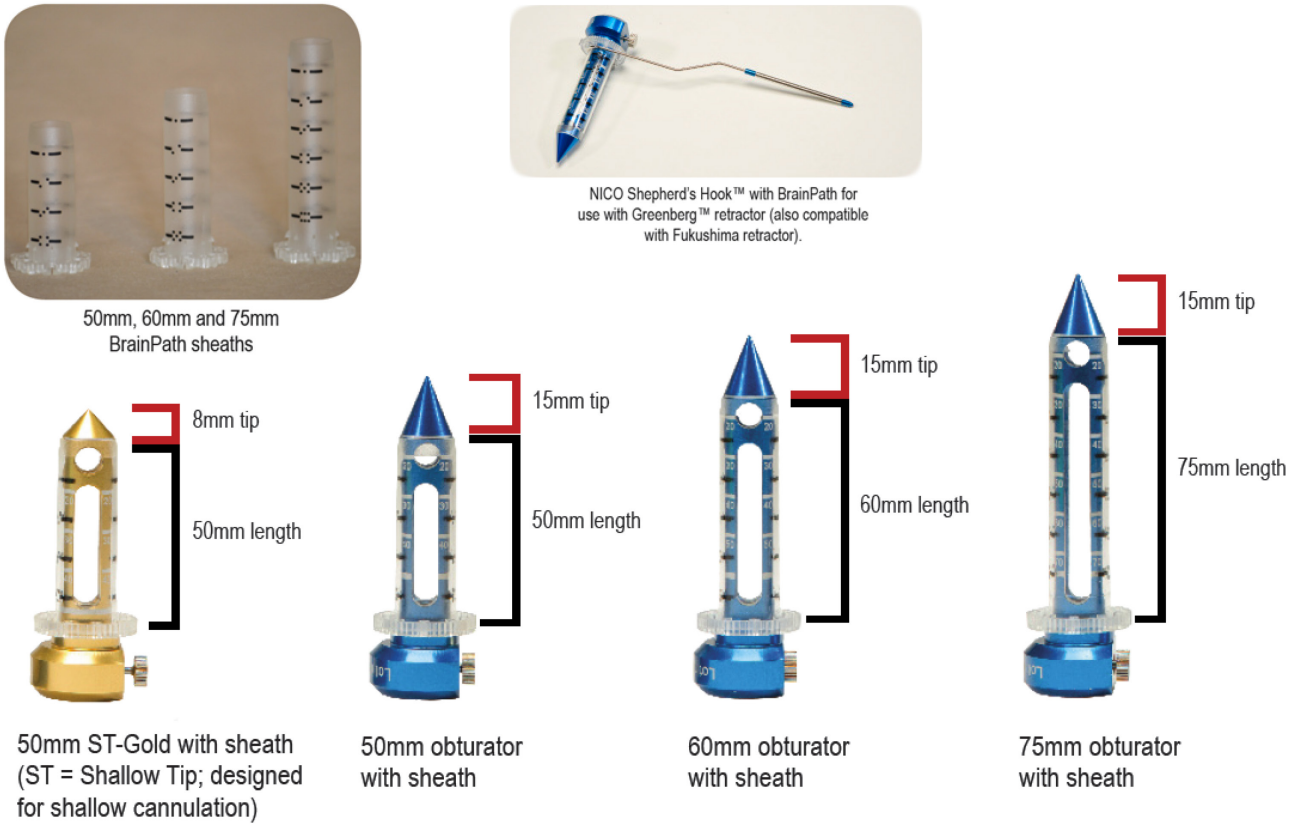

Figure 5. NICO BrainPath®. Image courtesy of NICO Corporation.

Scope of Objectives

Despite the significant advancements in skull base and minimally invasive surgical techniques described previously, developments in associated surgical technology, and the use of tubular retraction in transcortical surgery, tubular retractors have yet to be used to minimize brain retraction in skull base surgery. In order to determine the full applicability of transtubular techniques in neurosurgery, we (a) compare brain retraction pressure between tubular retractors and brain spatulas in the most common neurosurgical approaches, (b) assess the feasibility of performing minimally invasive transtubular skull base and general neurosurgical approaches, and (c) introduce a novel technique for closure of transtubular mini-craniectomies with maintenance of anatomic integrity.

COMPARISON OF RETRACTION FORCE

Rationale and Objective

In order to determine the difference in applied brain retraction pressure between tubular and spatula retractors, we assess and compare the mean retraction force exerted by each to achieve minimum adequate visualization of a given target in a series of common neurosurgical corridors using a cadaveric model. Additionally, we visually and qualitatively evaluate the cortical surface tissue for damage following removal of each retractor.

Experimental Design and Methods

Surgical Approach Selection and Classification

Standard supraorbital, middle fossa, retrosigmoid, supracerebellar infratentorial, interhemispheric, and transcortical neurosurgical approaches were selected in order to sample an array of different cranio-geometric openings and retracted surfaces, and were performed on 3 preserved adult cadaveric heads (6 sides) without arteriovenous injection. Each approach was classified based on the anatomical placement of the retractor as either between brain/dura and bone, between brain and dura, or within brain. All surgical corridors were intradural except for the middle fossa approach, where the retractors were placed extradurally underneath the temporal lobe dura.

Intracranial target structures were defined for each approach in order to provide a standard and consistent means for retractor comparison (Table 1). Each retractor was placed into

the surgical corridor and the minimum amount of brain retraction required to visually expose the given target structure was applied.

Surgical Approach	Retractor Placed Between	Surgical Corridor Between	Intracranial Target
Supraorbital	Brain and bone	Frontal lobe and roof of the orbit	Anterior communicating artery
Middle Fossa	Dura and bone	Temporal lobe dura and middle fossa floor	Petrous apex
Retrosigmoid	Brain and bone	Cerebellum and occipital bone	Trigeminal nerve (CN V)
Supracerebellar Infratentorial	Brain and dura	Cerebellum and falx cerebri	Pineal gland
Interhemispheric	Brain and dura	Frontal lobe and tentorium cerebelli	Corpus callosum
Transcortical	Within brain	Fenestration of cortical tissue	Lateral ventricle

Table 1. Intracranial Targets and Retractor Placement by Approach.

Estimation of Mean Retraction Pressure

A digital force measurement system (FlexiForce Economical Load & Force Measurement [ELF™] System, Tekscan, Inc., South Boston, MA) was used to measure the brain retraction force applied by each retractor. The ELF system comprised of software, a plastic handle that connected to a sensor, and a FlexiForce™ Sensor (B201, Tekscan) that functioned as a force sensitive resistor, translating specific applied forces to corresponding output voltages (Figures 6–7). The sensor was calibrated a using linear calibration technique with weights ranging from 50 g to 150 g, according to manufacturer guidelines.[150–151]

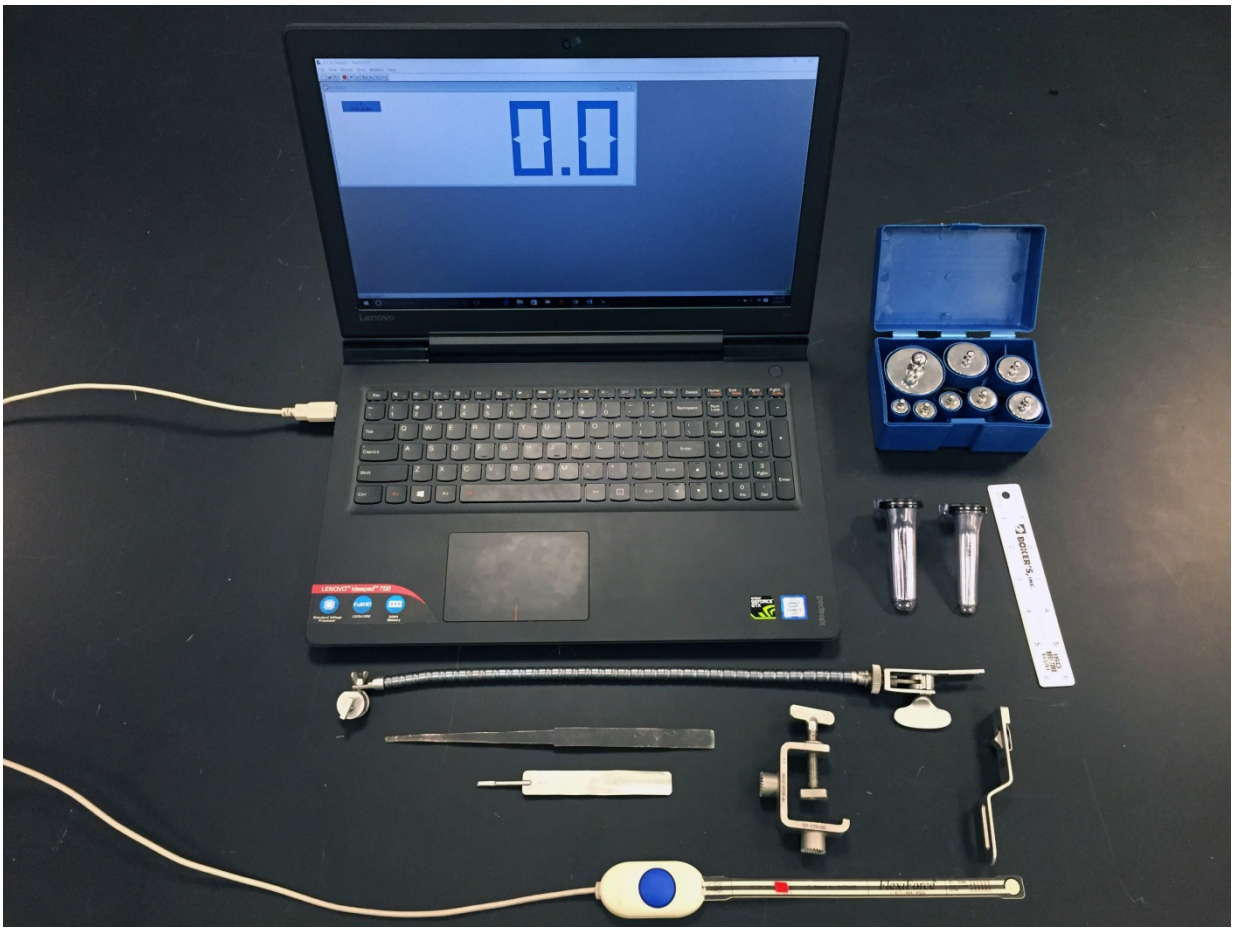

Figure 6. Tekscan FlexiForce Economical Load & Force Measurement System. Software and hardware components of the force measurement system as well as spatula and tubular retractors, calibration weights, and a self-retaining snake arm.

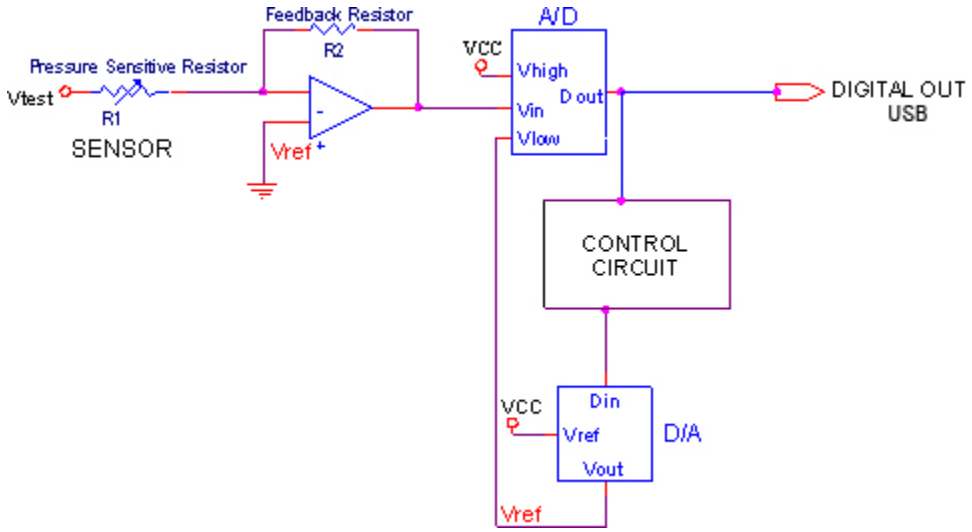

Figure 7. FlexiForce Handle Electronics Schematic. Image courtesy of Tekscan, Inc.

For the purposes of this study, mean retraction pressure (MRP) was defined as the mean quotient of the resultant force acting on the sensor and the surface area in direct contact with the tissue[22]:

$$Mean\ Retraction\ Pressure = \frac{Resultant\ Force}{Surface\ Area}$$

Wherein, the circular surface area of the force sensor was 73.9 mm^2 (radius 4.85 mm).

Craniotomy Placement and Target Visualization

For each approach, three-point fixation was achieved using a Mayfield head holder and the head was placed in a standard surgical position. Following conventional skin incisions, craniotomies were fashioned using an Anspach® EMAX® 2 Plus high-speed surgical drill (The Anspach Effort, Inc., Palm Beach Gardens, FL). Extreme care was taken to maintain dural integrity during bone removal. Each approach was performed 6 times, of which 3 were performed with tubular retraction and 3 with spatula retraction. A 229 mm long by 3–13 mm wide Greenberg® Tapered Retractor Blade (Symmetry Surgical Inc., Antioch, TN) was used for direct spatula retraction in a standard curvilinear configuration, without surgical patties or cottonoid pads, and a 12L VBAS (12×8 mm wide, 7 cm long, TC 12/7, Vycor) was used for tubular retraction in all but the retrosigmoid and middle fossa approaches, in which 12S (12×8 mm wide, 3 cm long, TC 12/3) and 17L (17×11 mm wide, 7 cm long, TC 17/7) retractors were used, respectively (Figure 4, Appendix B). Both retractors were fashioned to a non-tapered self-retraining snake arm (Mizuho America, Inc., Union City, CA); the VBAS was connected to the snake arm via the Vycor Extension Arm (Vycor) (Figure 8). Retractors were placed into the surgical corridor under direct microscopic visualization (Zeiss OPMI Neuro/NC 4 System, Carl Zeiss Meditec AG, Jena, Germany), and upon achieving target visualization, the snake arm was

locked in place and force readings were obtained and recorded. Mean retraction distance (MRD) of the brain tissue was measured using a flexible surgical ruler at the cranial opening, from the margin of the tissue in a neutral non-retracted position to its final position once the target structure was exposed using the given retraction modality, in all approaches.

Figure 8. Retraction Force Sensor. Retraction force sensor adhered to the spatula (left) and tubular (right) retractors, both connected to the self-retraining snake arm, prior to insertion into the surgical corridor. The cadaveric specimen pictured here is for illustrative purposes and was not used for experimentation.

Measurement of Retraction Force

Multiple force readings were recorded at different points along each retractor. In all approaches, 2 points of measurement, proximal and distal, were obtained along the spatula retractor, where the proximal point was located at the shallowest point of contact between the retractor and the retracted tissue, and the distal point was located at the distal tip of the retractor (Figure 9). Four points of measurement were obtained for the tubular retractor in approaches where it was placed between brain and dura or within brain (i.e. supracerebellar infratentorial, interhemispheric, and transcortical), including proximal and distal readings on both the superior

(or lateral) and inferior (or medial) sides of the retractor, in relation to the specimen (Figure 9). Two points of measurement were obtained for the tubular retractor, at proximal and distal points along the surface in contact with the retracted tissue, in approaches where the retractor was placed between brain or dura and bone (i.e. supraorbital, middle fossa, and retrosigmoid). Each measurement was repeated 4 times.

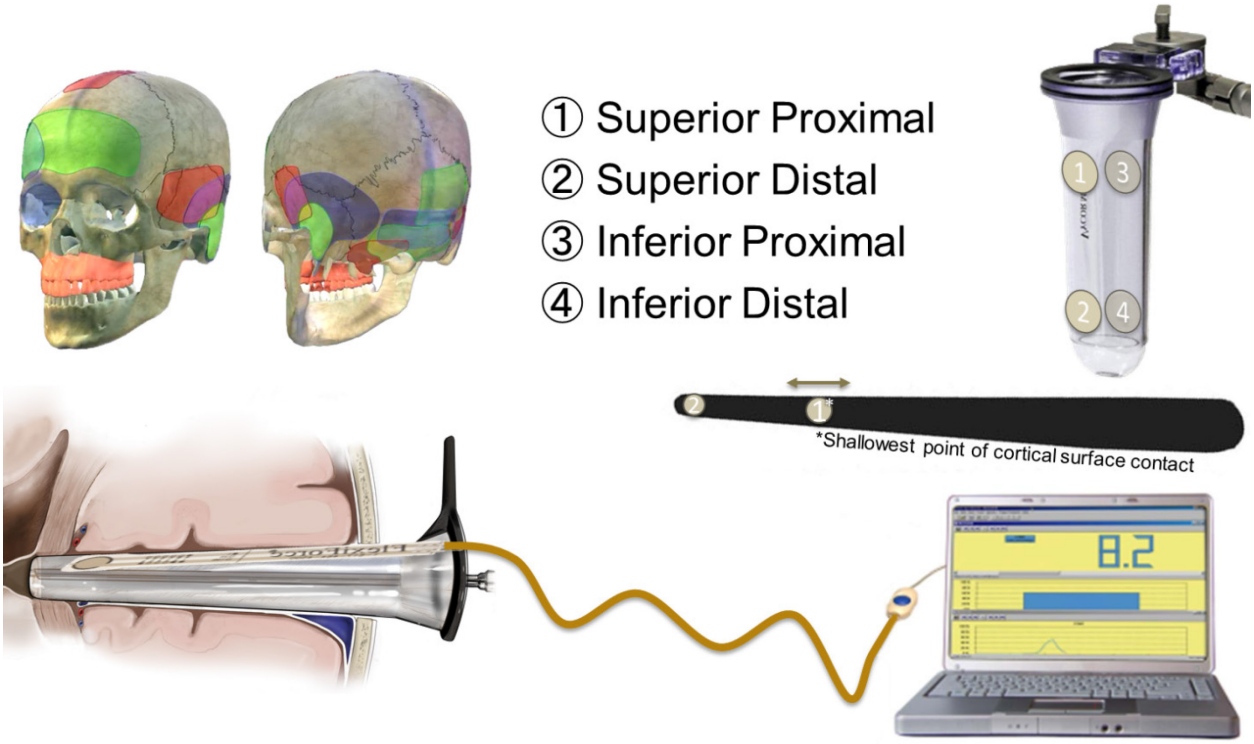

Figure 9. Location of Retraction Force Measurements. Artistic rendering of the location of force sensing points on both the spatula and tubular retractors, as well as the locations of a number of neurosurgical approaches.

Post-Retraction Microscopic Parenchymal Inspection

Upon completion of all measurements and removal of the retractor following each approach, the surgical microscope was used to visually assess for cortical tissue deformity, vessel collapse, damage to cortical surfaces, and parenchymal tearing along the surgical corridor and at the margins of the retractor.

Statistical Analysis

All obtained force values were recorded and converted into pressure values in millimeters of mercury (mmHg), and are displayed as mean ± standard error of the mean. Statistical significance of differences in MRP values were assessed using a one-tailed two-sample *t*-test. Statistical significance was considered for any *P* value less than or equal to 0.05. All analyses were performed using the Statistical Package for the Social Sciences software version 24.0 (SPSS Inc., Chicago, IL, USA).

Results

Each approach was completed bilaterally on all 3 specimens, for a total of 36 cranial openings, of which 18 were used to measure spatula retraction pressure and 18 to measure tubular retraction pressure. Target visualization was achieved in all cases with the minimum amount of brain retraction required to visually expose the given structure and retraction pressure values were successfully obtained in all 36 approaches. Collectively, MRP was 56.93% lower with the use of tubular retraction at 37.89±5.18 mmHg (range: 17.00–49.72 mmHg) compared to spatula retraction at 87.98±10.80 mmHg (range: 54.92–118.71 mmHg; $P < 0.01$). Aggregate MRP at the proximal end of the tubular retractor was 59.27% lower (mean: 41.12±2.89 mmHg, range: 13.44–63.41 mmHg) than that from the spatula retractor (mean: 100.96±5.99 mmHg, range: 56.82–129.11 mmHg), while aggregate distal MRP was 58.25% lower in the tubular group (33.31±1.87 mmHg, range: 12.68–46.93 mmHg) compared to the spatula group (mean: 75.00±5.06 mmHg, range: 52.25–113.13 mmHg; $P < 0.01$) (Figure 10). Additionally, both tubular and spatula groups demonstrated statistically significant reductions in MRP from the proximal to distal points ($P < 0.01$).

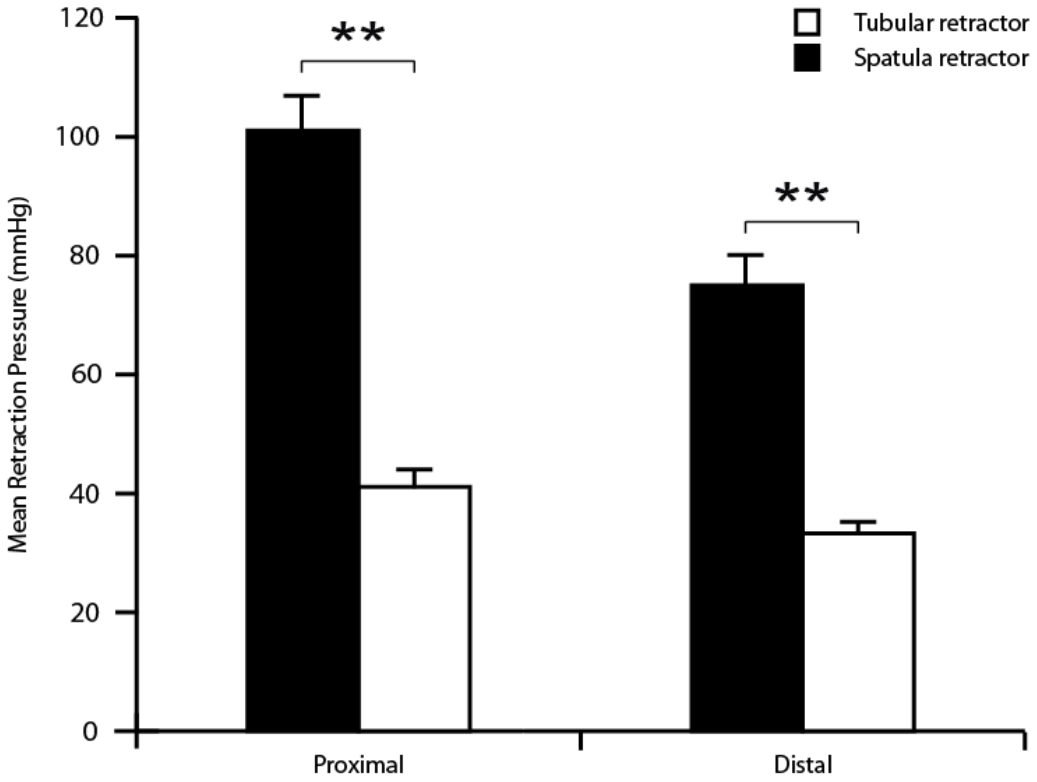

Figure 10. Aggregate Mean Retraction Pressure at Proximal and Distal Measurement Points. Statistically significant reductions in MRP from the proximal to distal points were observed within as well as between groups ($P < 0.01$).

Mean Retraction Pressure by Approach

Tubular retractors significantly reduced MRP in all approaches performed when compared to spatula retractors ($P < 0.01$) (Figure 11). The greatest reductions in MRP were observed in the supraorbital and transcortical approaches, with 66.82% and 69.05% MRP reductions from tubular retraction, respectively. In the supracerebellar infratentorial approach, MRP decreased by 60.92%, from 118.71±2.77 to 46.39±1.27 mmHg in the tubular retractor group. MRP in the middle fossa approach was 56.73% less in the tubular group, at 49.72±1.36 mmHg, than the spatula group, at 114.91±6.72 mmHg. Similarly, tubular retraction reduced MRP in the retrosigmoid approach from 93.47±7.35 to 42.11±1.87 mmHg, a change of 54.95%.

The smallest reduction in MRP from tubular retraction occurred in the interhemispheric approach, with an average reduction of 17.57 mmHg, or 28.44%.

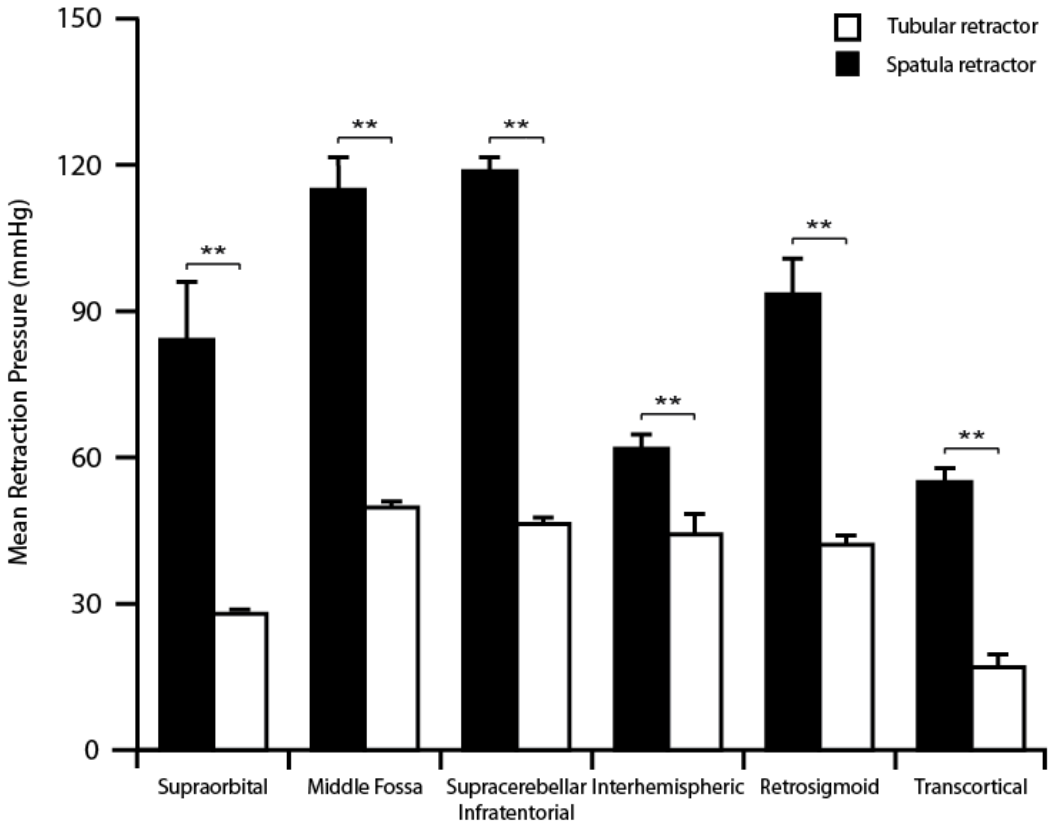

Figure 11. Mean Tubular and Spatula Retraction Pressures by Approach. $^{**}P < 0.01$.

In the spatula group, the supracerebellar infratentorial, middle fossa, and retrosigmoid approaches had the highest MRPs, whereas the middle fossa, supracerebellar infratentorial, and interhemispheric approaches had the highest MRPs in the tubular group (Table 2).

	Supraorbital	Middle Fossa	Supracerebellar Infratentorial	Interhemispheric	Retrosigmoid	Transcortical
Craniotomy Size (cm)	2.0×3.5	4.0×5.5	2.0×2.0	2.5×2.5	1.5×1.5	2.0×2.0
Tubular Retractor						
MRP (mmHg±SD)						
Proximal Superior/Lateral*	27.90±2.68	52.51±1.28	49.46±6.85	63.41±2.42	45.91±2.09	14.46±1.28
Distal Superior	27.90±2.68	46.93±3.65	46.62±4.57	30.69±4.17	38.30±5.00	27.39±5.30
Proximal Inferior/Medial**	–	–	46.04±5.58	56.82±6.14	–	13.44±1.73
Distal Inferior	–	–	43.63±5.43	25.87±1.01	–	12.68±1.76
Mean±SE	27.90±0.86	49.72±1.36	46.39±1.36	44.20±4.19	42.11±1.87	17.00±2.70
MRD (mm)†	9.00	12.00	9.00	9.00	9.00	9.00
Spatula Retractor						
MRP (mmHg±SD)						
Proximal	115.92±3.55	129.11±17.29	124.29±6.44	66.97±3.21	112.62±7.64	56.82±6.14
Distal	52.25±4.87	100.70±6.11	113.13±4.87	56.57±9.31	74.32±3.35	53.01±10.36
Mean±SE	84.09±11.89	114.91±6.72	118.71±2.77	61.77±2.95	93.47±7.35	54.92±2.83
MRD (mm±SD)	19.75±0.50	29.50±2.50	16.25±0.96	15.50±1.00	24.75±2.5	14.00±1.41
MRP Reduction (%)	70.93	59.12	61.81	31.71	58.24	70.57
P value	0.00117	< 0.01	< 0.01	0.00141	< 0.01	< 0.01
MRD Reduction (%)	54.43	59.32	44.62	41.94	63.64	35.71
P value	< 0.01	< 0.01	< 0.01	< 0.01	< 0.01	0.01501

Table 2. Mean Retraction Pressure and Distance. *Superior corresponded to lateral, or brain, in both the interhemispheric and transcortical approaches. **Inferior corresponded to medial in the interhemispheric (falx cerebri) and transcortical (brain) approaches. †Tubular MRD is a fixed value based on the distal port height of the retractor + 1 mm to account for the thickness of the port. MRP, mean retraction pressure; MRD, mean retraction distance; SD, standard deviation; SEM, standard error.

Spatula Retraction Pressure Distribution

Within the spatula retractor group, statistically significant differences in proximal and distal MRPs were observed in all but the interhemispheric and transcortical approaches, indicative of focal areas of high pressure toward the origin of the retractor (Figure 12). In the supraorbital and retrosigmoid approaches, proximal MRPs were 54.92% and 34.01% greater, respectively, than distal MRPs ($P < 0.01$); and in the middle fossa and supracerebellar infratentorial approaches, proximal MRPs were 22.00% and 8.98% greater, respectively ($P < 0.05$).

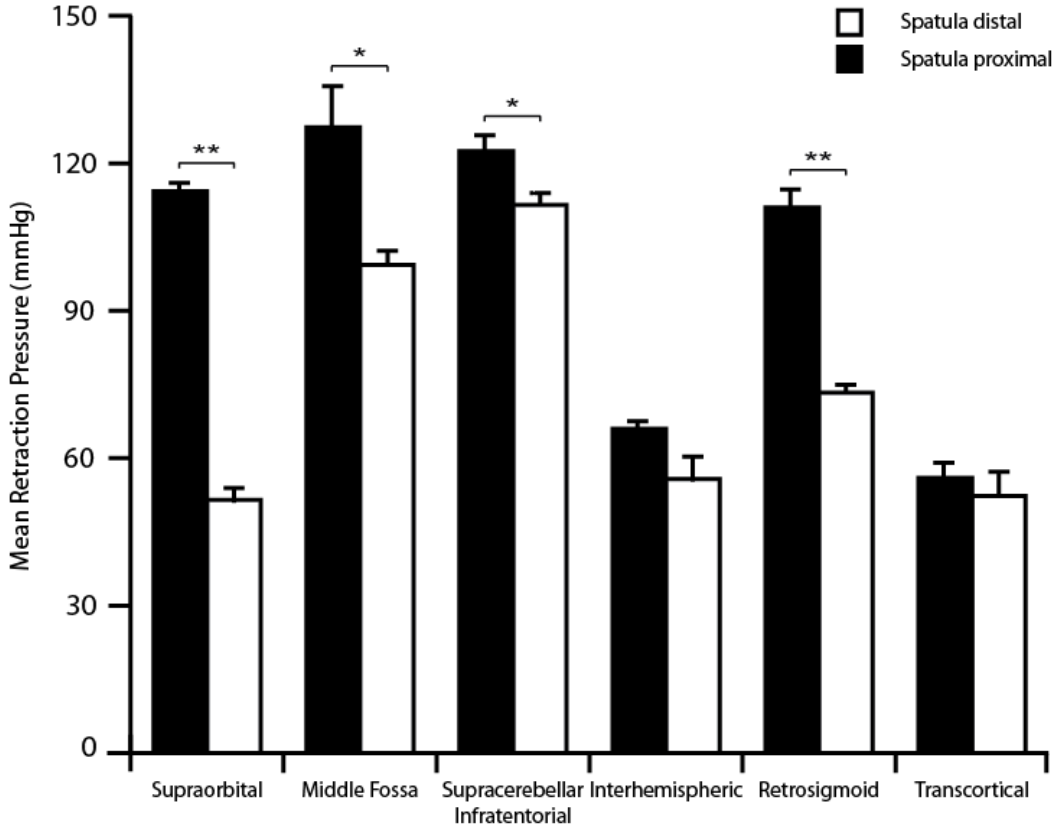

Figure 12. Pressure Distribution along the Spatula Retractor by Approach. $^{*}P < 0.05$; $^{**}P < 0.01$.

Tubular Retraction Pressure Distribution

Within the tubular retractor group, statistically significant differences in proximal and distal MRPs were only observed in the interhemispheric, middle fossa, and retrosigmoid approaches (Figure 13). In the middle fossa and retrosigmoid approaches, proximal MRPs were 10.63% and 16.57% greater, respectively, than distal MRPs ($P < 0.05$), indicative of more equal pressure distribution along the axis of the retractor; while in the interhemispheric approach, proximal MRP was 52.95% greater than distal MRP ($P < 0.01$). In the 3 approaches where measurements were taken on both sides of the retractor (Table 2), no statistically significant difference in MRP between the superior/lateral and inferior/medial aspects was observed.

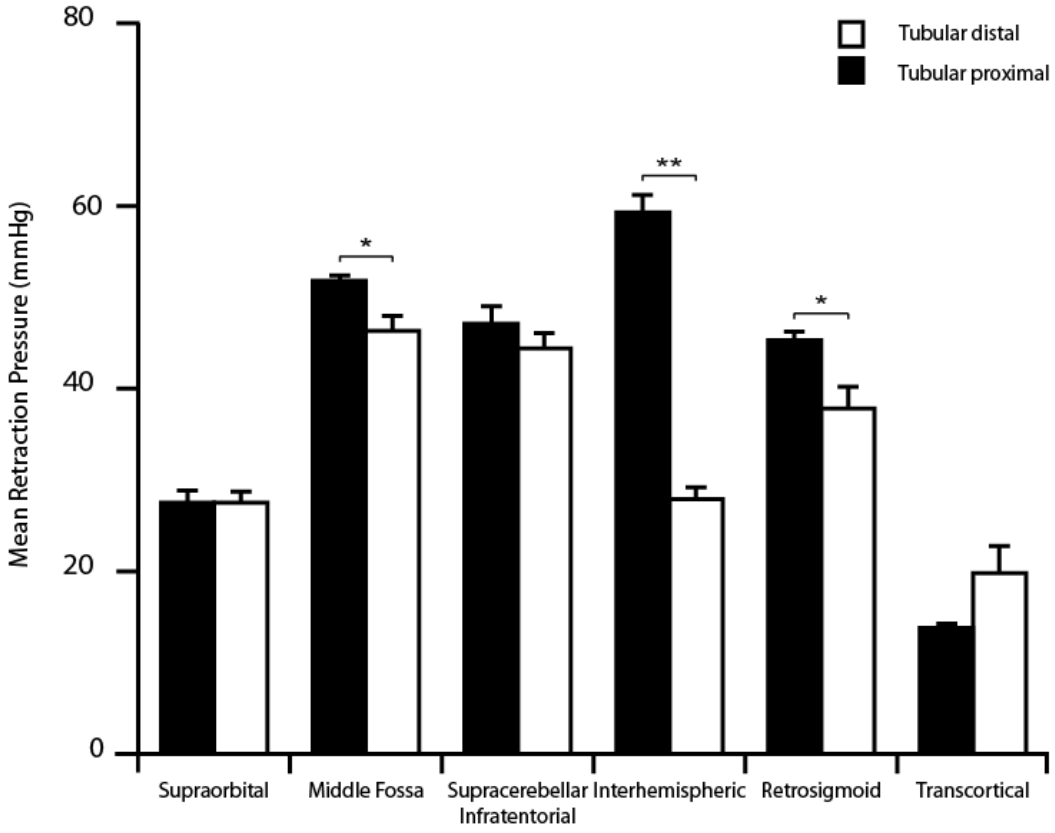

Figure 13. Pressure Distribution along the Tubular Retractor by Approach. $^{*}P < 0.05$; $^{**}P < 0.01$.

Spatula versus Tubular Retractor Pressure Distribution

The reductions in MRP provided by the tubular retractor were also statistically significant in all approaches when proximal and distal measurement points were compared independently between retractor groups (Figure 14). As such, distal tubular MRP was significantly less than the distal spatula point in each approach, and proximal tubular MRP was significantly less than the proximal spatula point in each approach.

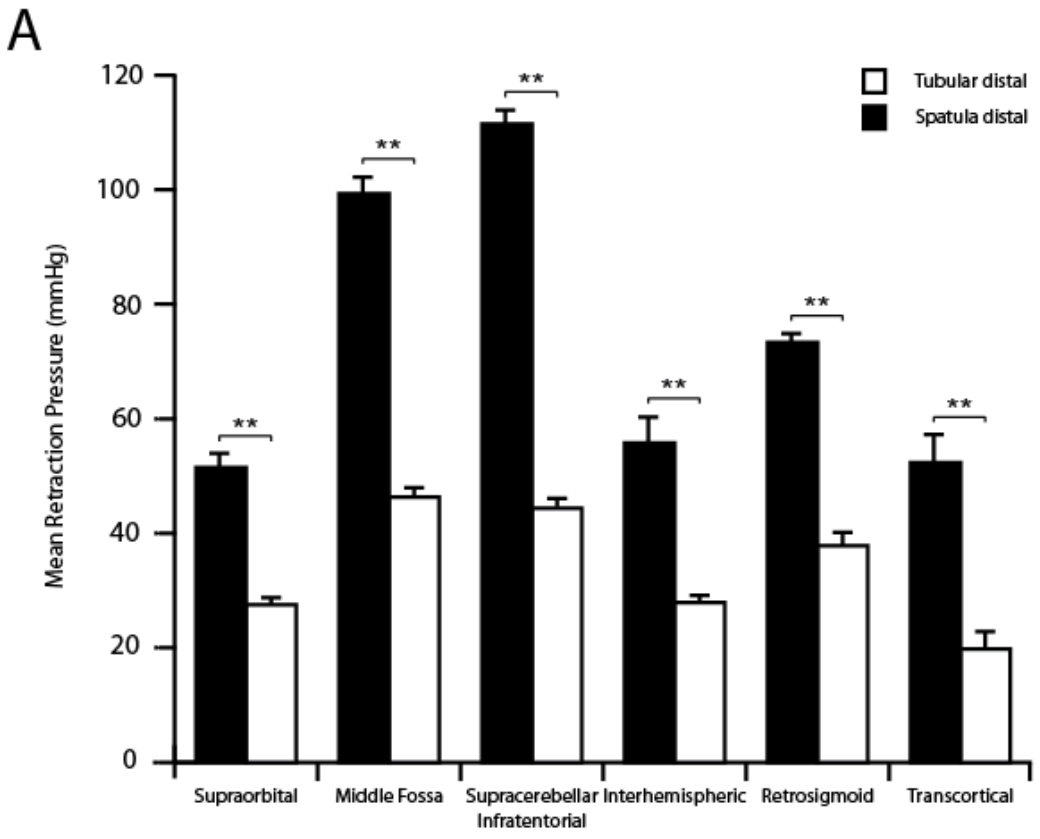

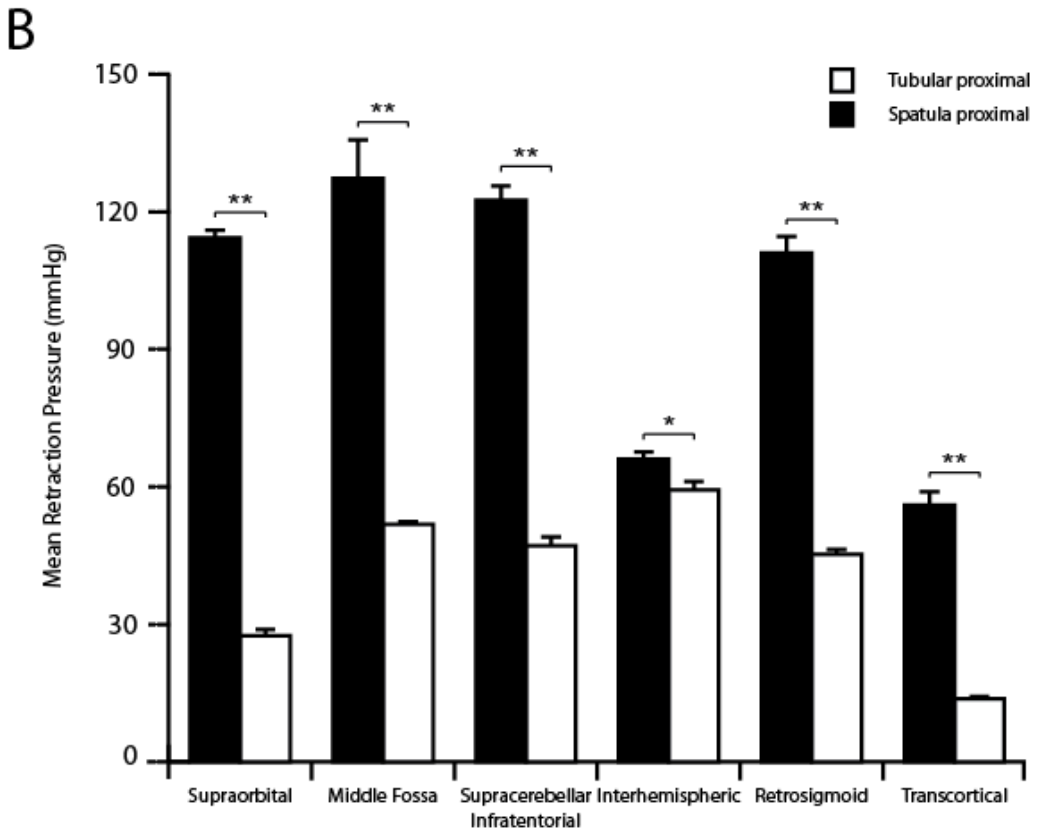

Figure 14. Spatula and Tubular Retraction Pressures by Location and Approach. (A) Distal and (B) proximal MRPs for each retractor in all approaches. $^{*}P < 0.05$; $^{**}P < 0.01$.

Retraction Pressure by Retractor Placement

In all classifications of retractor placement (Table 1), tubular MRP was significantly less than spatula MRP ($P < 0.01$) (Figure 15). For approaches where the retractors were placed between brain and dura, aggregate spatula MRP was 88.94±7.47 mmHg, whereas aggregate tubular MRP was 49.79% less at 44.66±2.16. For approaches where the retractors were placed between brain/dura and bone, aggregate spatula MRP was 96.08±5.60 mmHg and aggregate tubular MRP was 59.06% less at 39.33±2.01 mmHg. For the transcortical approach, where the retractors were placed within brain parenchyma, aggregate spatula MRP was 54.13±2.83 mmHg, compared to an aggregate tubular MRP of 16.75±1.66 mmHg, a 69.05% decrease.

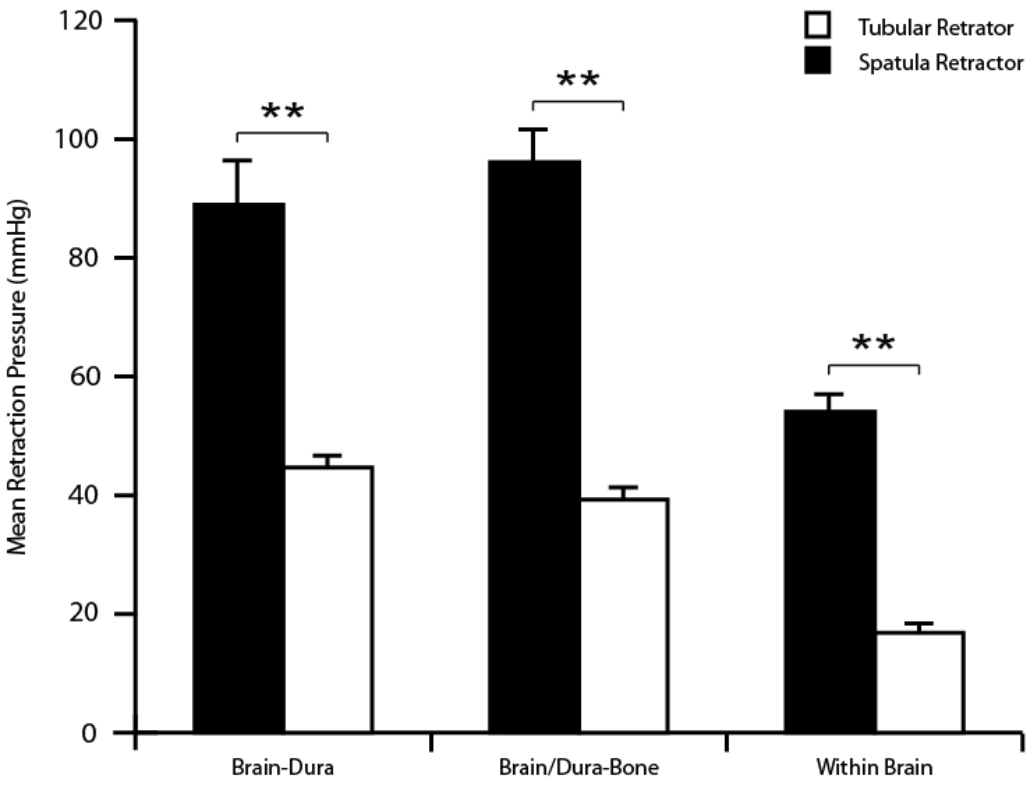

Figure 15. Spatula and Tubular Retraction Pressures by Retractor Position. $^{**}P < 0.01$.

Mean Retraction Distance

Tubular MRD was a fixed value based on the distal port height of the retractor plus 1 mm to account for the thickness of the port itself, and was 9.00 mm in all approaches except the middle fossa approach where it was 12.00 mm. Spatula MRD varied between approaches and ranged between 15.50±1.00 and 29.50±2.50 mm (Table 2). Tubular MRD was significantly less than spatula MRD in all approaches with an average reduction of 10.00±5.96 mm or 49.94±10.87%

Post-Retraction Microscopic Parenchymal Inspection

Qualitative microscopic visual inspection of the parenchymal tissue along the surgical corridor was performed following removal of the retractor at the conclusion of each approach. In

both the tubular and spatula retractor groups, tissue deformity was observed and in most cases found to be slightly less than the MRD. The deformed tissue returned to its pre-retracted position within 10 minutes following cessation of retraction. Vessels along the surgical corridor were noted to be compressed; however, the non-perfused nature of the specimen did not permit determination of vessel collapse, as the vessels were not physiologically patent. Damage to cortical surfaces was observed in both groups. In the tubular group, brain tissue was noted to have entered into the retractor through the aperture at the tip of the introducer on 3 occasions during the transcortical approach. In the spatula group, parenchymal damage and tearing was observed on 3 occasions during the middle fossa approach, 3 occasions during the transcortical approach, and on 1 occasion during the supraorbital approach; all of which were noted to be where the edges of the spatula had been placed.

Summary

Collectively, tubular retraction resulted in average brain retraction pressures that were 50 mmHg or 57% less than those resulting from spatula retraction. In all cases, retraction pressure was significantly greater at the distal, or deep, end of both the spatula and tubular retractors. Spatula-based retraction pressures were greatest in the supracerebellar infratentorial, middle fossa, and retrosigmoid approaches, as well as the supraorbital approach, with a maximum single reading of 150 mmHg, whereas tubular retraction pressures were greatest in the middle fossa, supracerebellar infratentorial, and interhemispheric approaches and no single reading exceeded 65 mmHg. In both groups, the transcortical approach had the lowest mean retraction pressures. Tubular retractors demonstrated more consistent average retraction pressures between approaches with a standard deviation (SD) of only 12.70 mmHg, compared to spatula retractors

with a SD of 26.44 mmHg. No significant differences in retraction pressure were found between the superior/lateral and inferior/medial sides of the tubular retractor. Mean retraction distance was 50% less in the tubular retraction group and, upon visual inspection, cortical tearing was observed in 39% of cases following spatula retraction.

SURGICAL FEASIBILITY OF TUBULAR RETRACTION AND TRANSTUBULAR APPROACHES

Rationale and Objective

In order to determine the full applicability of transtubular techniques in neurosurgery, we propose and investigate the surgical feasibility and efficacy of performing a series of 5 common neurosurgical approaches through percutaneous minimally invasive transtubular surgical corridors, including complex skull base approaches, in a cadaveric model using a number of different surgical adjuncts.

Experimental Design and Methods

Microscopic (5 sides) and 3-dimensional (3D) endoscopic (5 sides) percutaneous supraorbital, anterior transpetrosal, interhemispheric transcallosal, retrosigmoid, and supracerebellar infratentorial approaches were performed through a tubular retractor system on 5 preserved cadaveric heads (10 sides), previously injected with colored latex—red for arteries and blue for veins (Figure 9). Six sides were also previously injected with a synthetic intracanalicular tumor model for assessment of resection in the transtubular anterior transpetrosal approach. Dissections were completed with a neurosurgical microscope (Zeiss) and 3D endoscope (VSIII, Visionsense Ltd., New York, New York, USA) with 0°, 30°, and 90° angled optics. An Anspach eMax 2 Plus (Anspach) high-speed electric neurosurgical drill was used to perform all bone work, and was used transtubularly with a minimally invasive attachment.

Synthetic Tumor Model

Three specimens (6 sides) were preoperatively injected with synthetic tumor models (ST-540 Injection Resin, Strata-Tech, Des Moines, Iowa, USA) bilaterally using a Teflon integrated curved IV catheter through a retrosigmoid route to simulate small intracanalicular tumors (≤1.5 cm in diameter) with minimal extension into the posterior fossa.[146,152–153] The tumors were placed anterior (2 sides), posterior (2 sides), superior (1 side), and inferior (1 side) to the cranial nerve (CN) VII–VIII complex. The synthetic tumor resin was mixed with a radiopaque solution (Omnipaque [iohexol] solution, GE Healthcare Inc., Little Chalfont, United Kingdom) to appear hyperdense on CT (Figure 16).

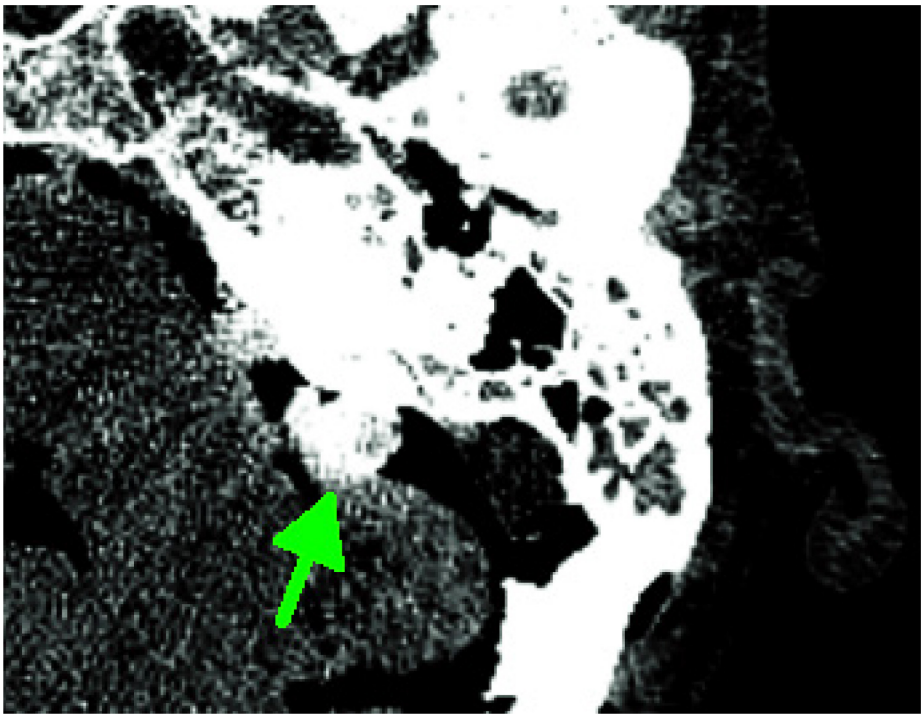

Figure 16. Synthetic Intracanalicular Tumor Model. CT scan of a cadaveric specimen with a small (≤1.5 cm in diameter) hyperdense contrast-enhancing synthetic intracanalicular tumor (green arrow) with extension into the cerebellopontine angle.

Neuronavigation

For image-guided neuronavigation, 6 radiopaque skin markers (fiducials) were affixed to the cranium. One-millimeter spiral CT axial slices (Biograph TruePoint PET•CT, Siemens AG; Munich, Germany) were obtained of each specimen and transferred to a neuronavigation workstation (Kolibri Image-Guided Surgery Platform, Brainlab AG; Feldkirchen, Germany) for spatial registration and preoperative surgical planning.

Entry and Trajectory Planning

Because of the small size of the bone openings and the rigid nature of the tubular retractor, determination of optimal entry points was important for ensuring accurate surgical trajectories, especially in the interhemispheric transcallosal and supracerebellar infratentorial approaches to prevent injury to the nearby dural venous sinuses. Preoperative trajectory planning was essential in the anterior transpetrosal approach due to the rigid surgical corridor and need for a precise path to the petrous apex.

To define an optimal entry zone for a subtemporal trajectory to the petrous apex, the lateral petroclival angle—the angle between the petrous bone and a sagittal line passing through the petroclival suture at the level of petrous ridge—and the distance from the petroclival suture to the porus acusticus internus, the petroclival-acoustic distance, were determined using the 5 cadaveric CT scans as well as an additional 20 normal adult head CT scans (50 sides).[154] A trajectory, perpendicular to the petrous ridge, was then plotted and measured from the porus acusticus internus to an external point on the skull flush with the floor of the middle fossa (Figure 17). Mean lateral petroclival angles and corresponding distances were calculated to determine an optimal entry zone. The calculated optimal entry zone was correlated to external

landmarks and then verified for target accuracy using the trajectory planning feature of the neuronavigation software on all ten cadaveric sides (Figure 18).

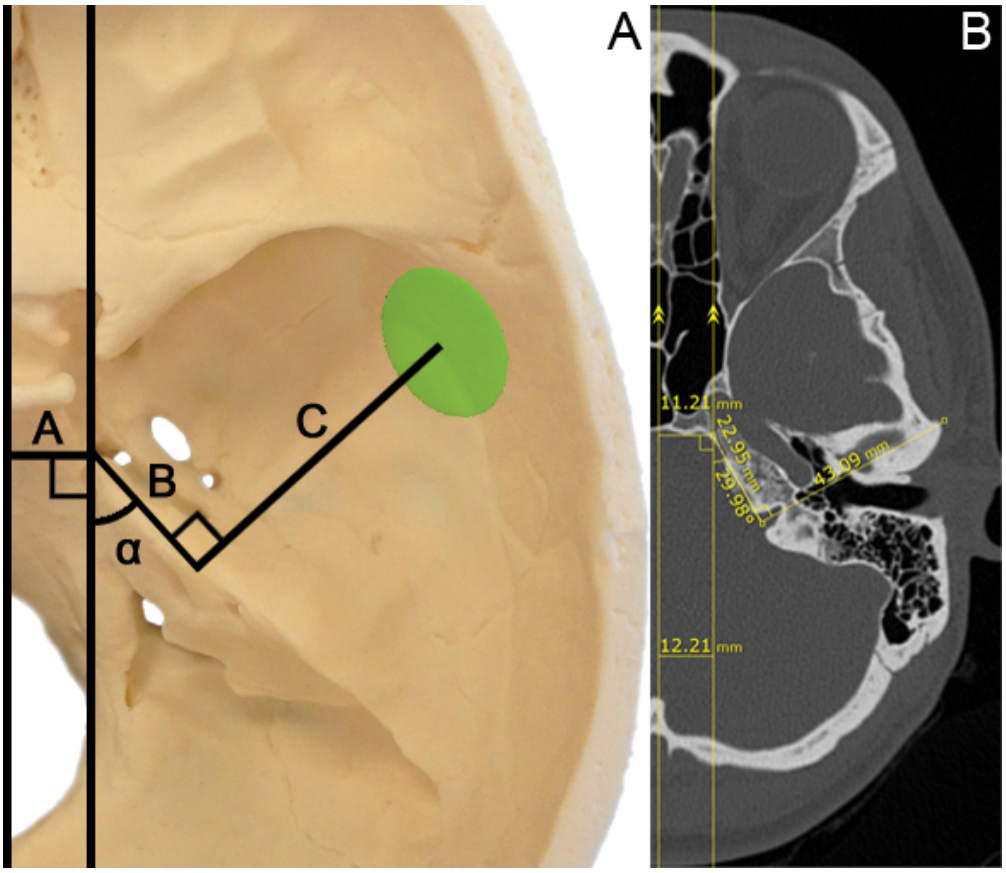

Figure 17. Entry Point Geometry. (A) A midsagittal line was drawn between the nasion and inion, and the distance, *A*, to a parallel sagittal line passing through the petroclival suture was measured. The lateral petroclival angle, α, was measured between the petrous bone and the sagittal line passing through the petroclival suture at the level of petrous ridge. The petroclival-acoustic distance, *B*, also was measured at the level of petrous ridge from the petroclival suture to the porus acusticus internus. A trajectory perpendicular to the petrous ridge, *C*, was then plotted and measured from the porus acusticus internus to an external point on the skull. (B) A representative CT scan showing collection of the midsagittal-petroclival suture distance, lateral petroclival angle, petroclival-acoustic distance, and trajectory length. (Note: To calculate the true petroclival angle—the angle between the posterior surface of the clivus and the posterior surface of the petrous bone at the level of the petrous ridge—90° should be added to the lateral petroclival angle).

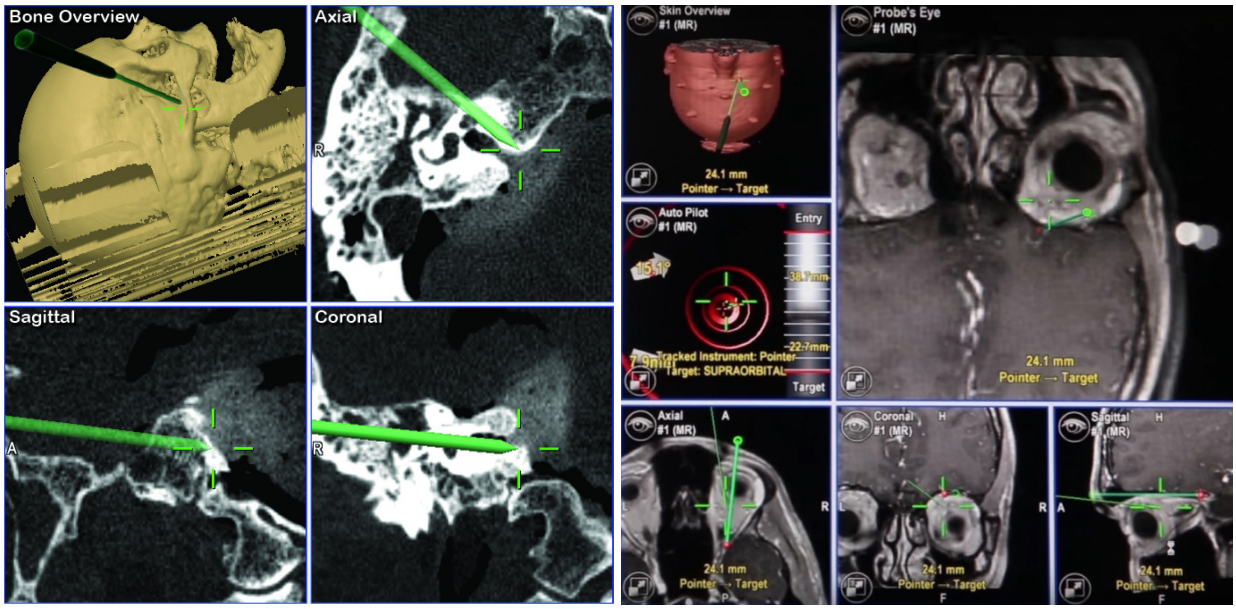

Figure 18. Neuronavigation Trajectory Planning. Verification of the optimal entry zone and surgical trajectories in the anterior transpetrosal (left) and supraorbital (right) approaches.

Positioning, Incision, and Burr Hole Placement

For each approach, three-point fixation was achieved using a Mayfield head holder and the head was placed in a standard surgical position (Figure 19). In the supraorbital approach, the head was positioned supine with 15–35° rotation to the contralateral side, 15° elevation, and 10–15° retroflection, and 10° lateroflection. In the anterior transpetrosal approach, the head was positioned supine with 90° rotation to the contralateral side to provide an unobstructed view of the middle fossa floor and 20° lateroflection to facilitate gravitational retraction of the temporal lobe. In the interhemispheric transcallosal approach, the head was positioned supine with 15–30° neck flexion; in the retrosigmoid approach, the head was positioned supine with 100° rotation to the contralateral side and 10° anteroflexion; and in the supracerebellar infratentorial approach, the head was positioned prone with 45° anteroflexion and 5–10° of rotation to the ipsilateral side.

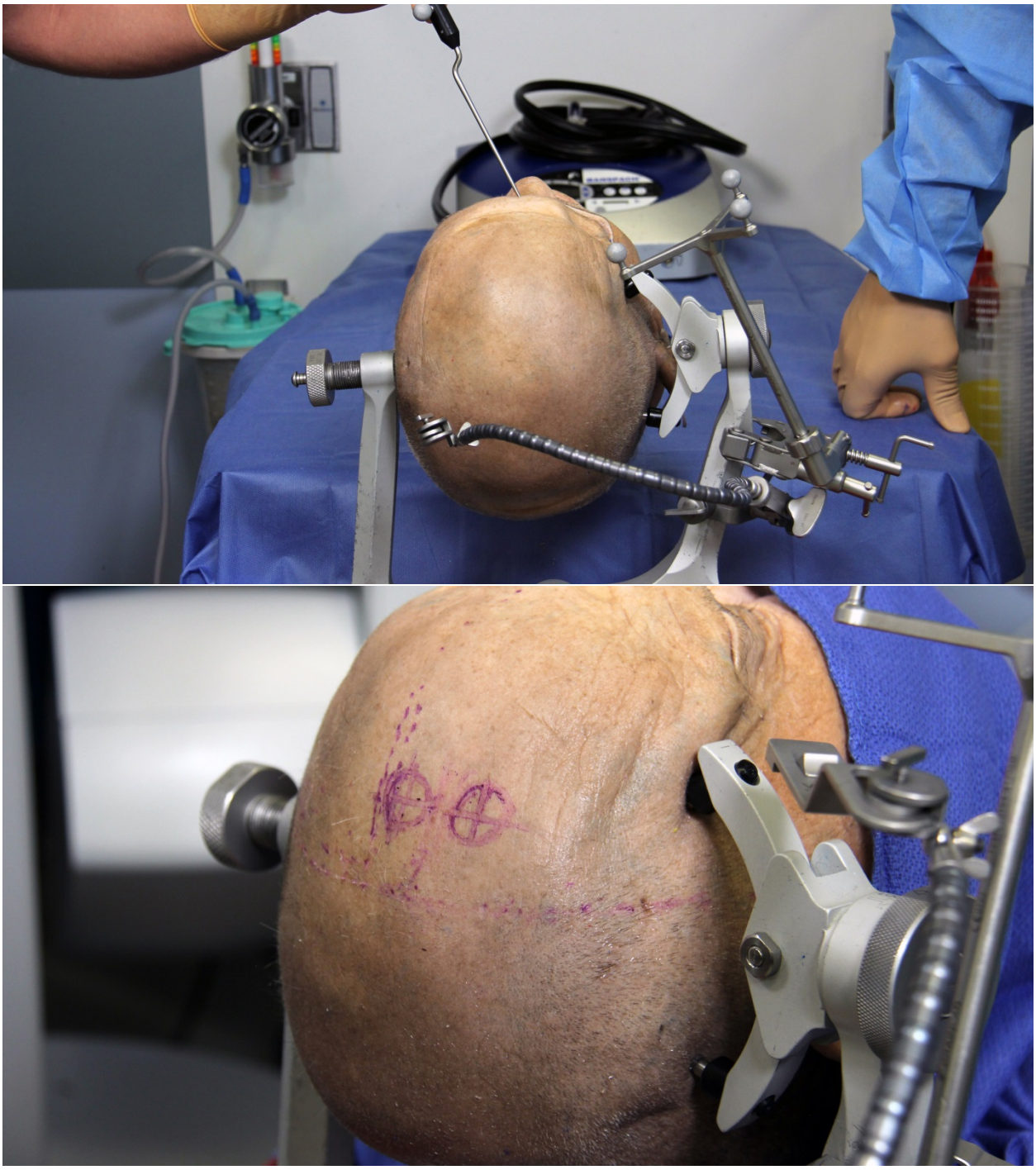

Figure 19. Patient Positioning. A neuronavigation pointer is placed for trajectory planning following positioning of the head and head holder (top), and skin markings were placed for the interhemispheric transcallosal approach (bottom).

Following 2–4 cm linear skin incisions above the craniectomy site, large burr holes or minicraniectomies were fashioned using the high-speed surgical drill. In the anterior transpetrosal approach, care was taken to preserve the frontal branch of the facial nerve, and in the supraorbital approach care was taken to preserve the supraorbital nerve. Based on the size of the tubular retractor and the predetermined optimal entry zone, a 2.5–3 cm diameter burr hole was fashioned as appropriate for each approach (Figure 20). The dura was gently detached from the inner bone table and, in all but the anterior transpetrosal approach, incised linearly.

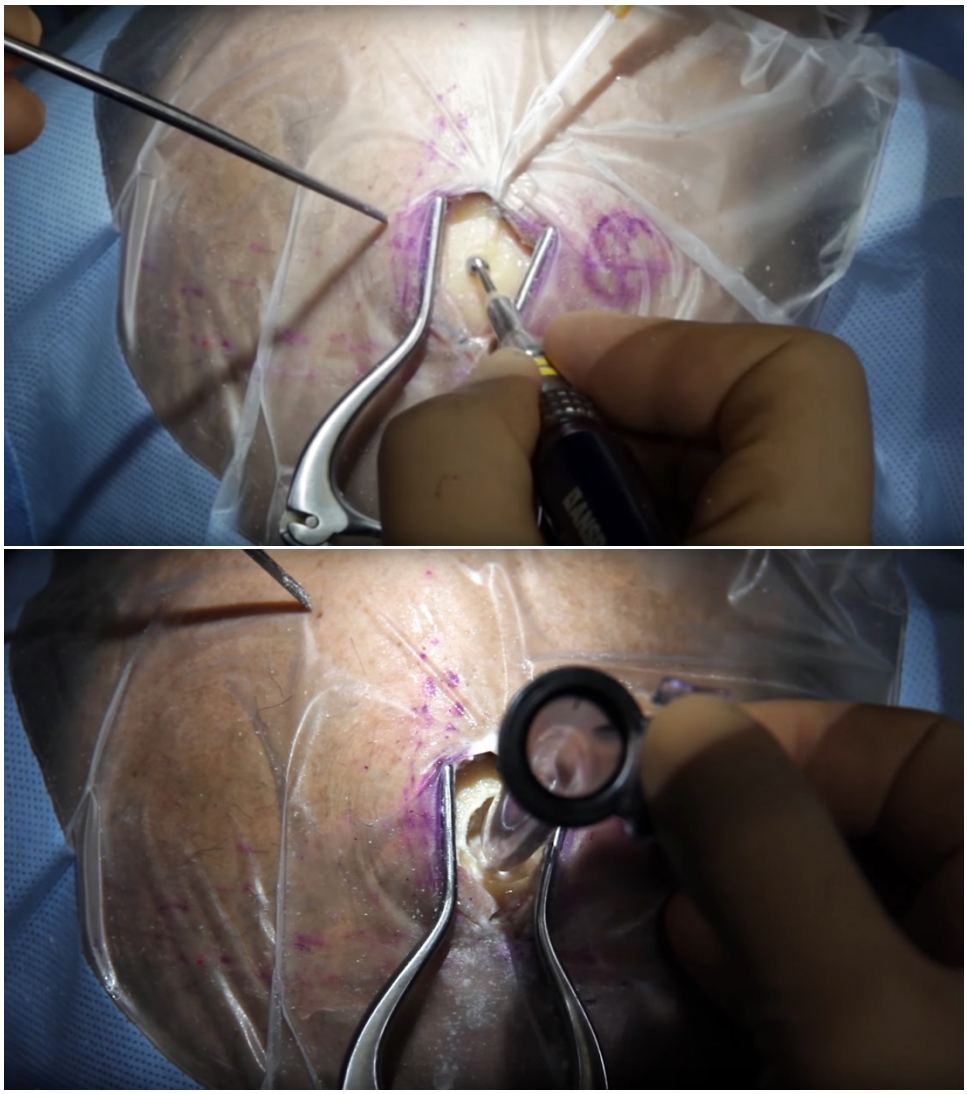

Figure 20. Burr Hole Placement. Drilling (top) and sizing (bottom) of a percutaneous burr hole.

Introduction of the Tubular Retractor System

A 12L VBAS (12×8 mm wide, 7 cm long, TC 12/7, Vycor) was used for tubular retraction in all but the retrosigmoid and anterior transpetrosal approaches, in which 12S (12×8 mm wide, 3 cm long, TC 12/3) and 17L (17×11 mm wide, 7 cm long, TC 17/7) retractors were used, respectively (Figure 4, Appendix B). The selected tubular retractor was mounted onto an extension arm (Vycor) attached to a self-retaining snake retractor (Mizuho) and gently inserted into the surgical corridor while correct advancement along the preplanned trajectory was verified using neuronavigation (Figure 21). Upon reaching the target region, the introducer was removed (Figure 22).

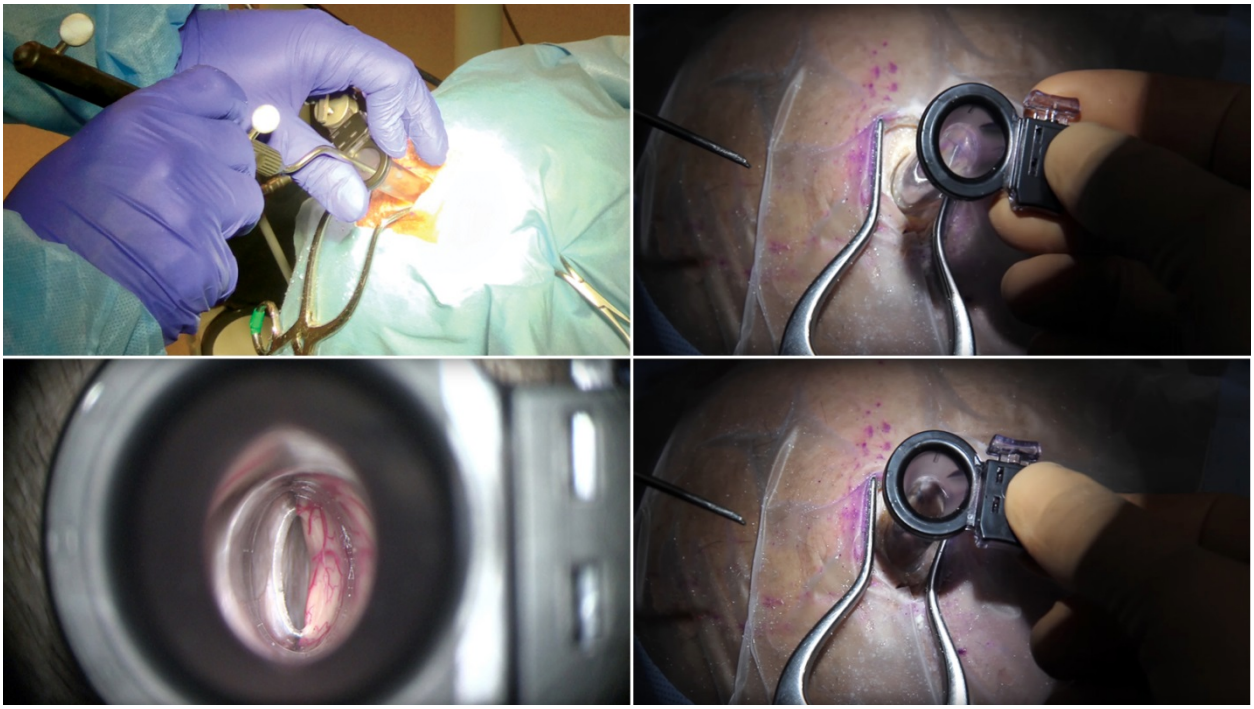

Figure 21. Insertion of the Tubular Retractor. The tubular retractor is inserted into the interhemispheric transcallosal surgical corridor.

Figure 22. Removal of the Introducer.

Intraoperative Orientation and Anatomical Quadrant Segmentation

In order to ensure proper surgical positioning of the tubular retractor before manipulation of or around the surgical target, correct anatomical alignment was ensured by verifying that the appropriate anatomical landmarks appeared within the correct visual quadrants (upper left, upper right, lower left, and lower right). At any point, to ensure correct positioning, two of these quadrants had to be lined up with correct corresponding landmarks (Figure 23).

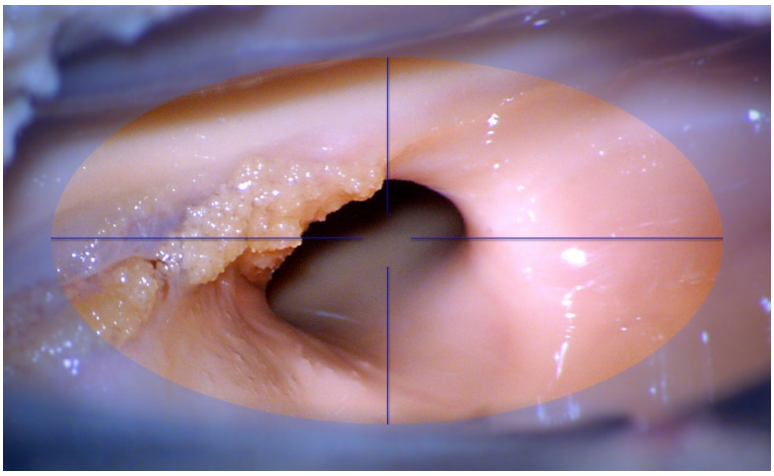

Figure 23. Transtubular Visual Field Quadrants.

For example, in the interhemispheric transcallosal approach, the following quadrant combinations may be used for proper surgical orientation when entering the lateral ventricle: upper and lower left, upper and lower right, upper left and right, lower left and right, upper left and lower right, and upper right and lower right (Figure 24). If the anatomy appeared in each quadrant and the quadrants were properly aligned, the surgical positioning was determined to be correct. Confirmation of alignment was performed during each segment of each approach to ensure a safe working area and correct anatomical awareness.

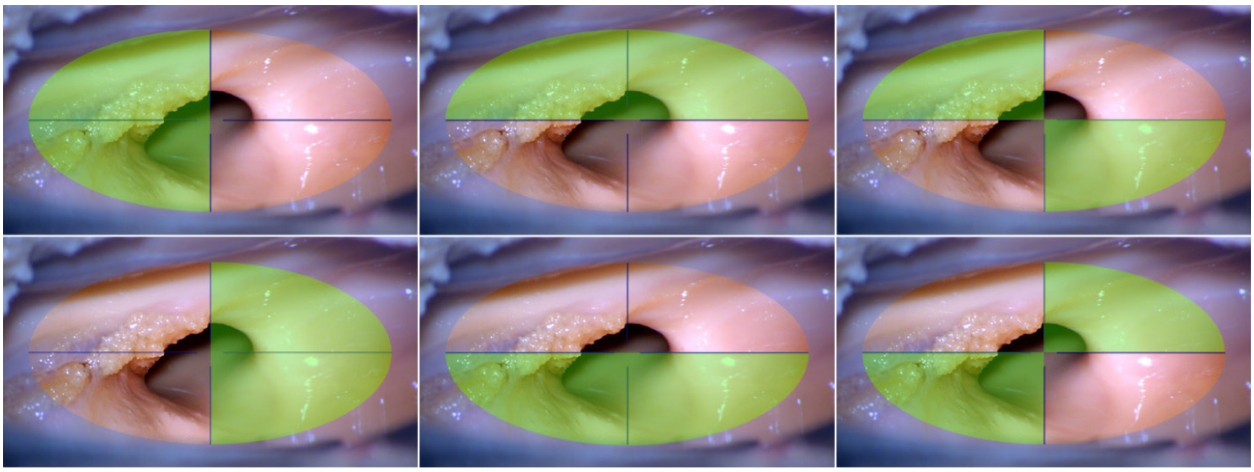

Figure 24. Transtubular Visual Field Quadrant Alignment. Potential quadrant alignment configurations in the transchoroidal or transforaminal interhemispheric transcallosal approach.

Transtubular Skull Base Dissection

To assess the feasibility of performing complex drilling through the tubular retractor at the base of the skull, transtubular anterior petrosectomies were performed and are described extensively herein in order to illustrate the principles required for transtubular skull base techniques.

After insertion of the tubular retractor, the microscope was angled so that visualization through the retractor could be achieved, the blunt end of the introducer was advanced into the opening, and the dura was gently peeled off of the floor of the middle fossa. The middle meningeal artery was identified and cut to untether the temporal lobe dura from the floor of the middle fossa. The retractor was yawed slightly along the axial plane allowing for identification of the middle meningeal artery and foramen spinosum. The greater superficial petrosal nerve (GSPN) was identified at its exit from the facial hiatus and carefully dissected from the outer layer of temporal dura and middle fossa periosteum. The tubular retractor was yawed slightly to follow the GSPN posteriorly until the arcuate eminence was identified. The introducer was removed, the working channel was positioned up against the petrous ridge, and the arcuate eminence was fully exposed (Figures 22 and 25). Improper positioning of the retractor could result in obstruction of the surgical field by temporal dura. The self-retaining snake retractor connected and locked in place, and the 3D endoscope was introduced into the tubular retractor.

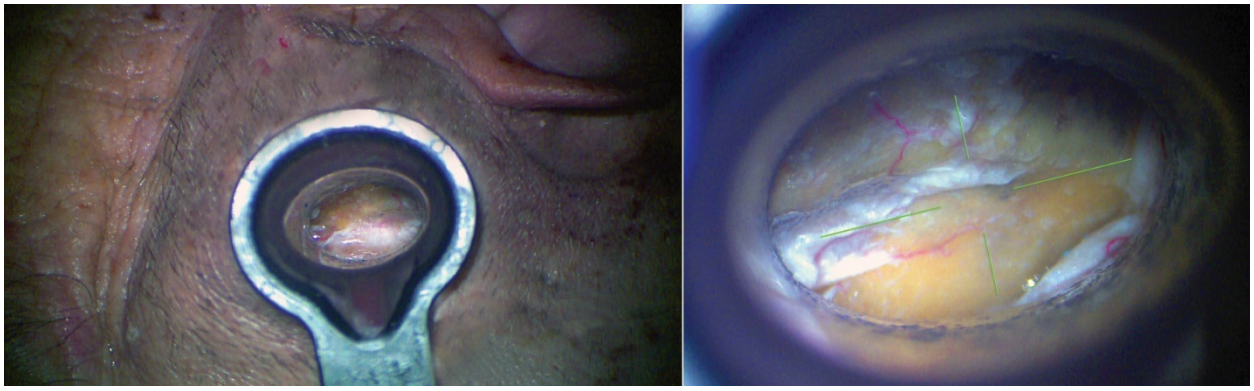

Figure 25. Placement of the Tubular Retractor along the Skull Base. The minimally invasive percutaneous surgical trajectory (left) with the working channel positioned up against the right petrous ridge and exposure of the arcuate eminence in the posterosuperior quadrant after removal of the introducer (right).

Before proceeding with dissection of the internal auditory canal (IAC), correct surgical positioning was verified by confirming that the GSPN and facial hiatus were visualized in the anterosuperior quadrant and the arcuate eminence in the posterosuperior quadrant in order to help ensure safe drilling of the petrous bone (Figure 26).

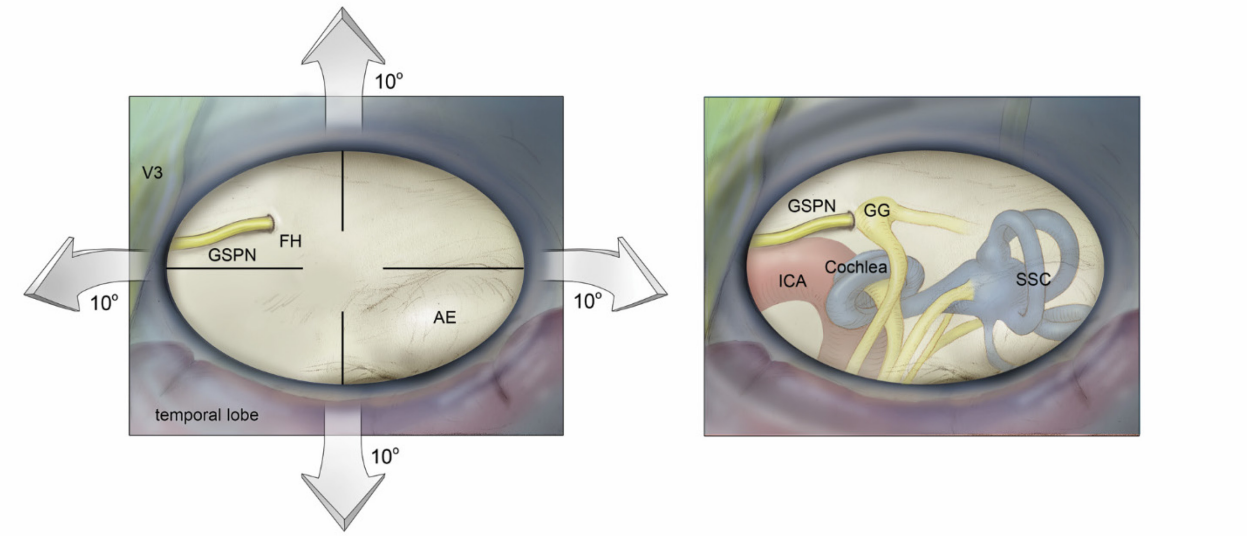

Figure 26. Transtubular Surgical Anatomy of the Anterior Temporal Bone. Anatomic orientation of the tubular retractor at the target structure in the anterior transpetrosal approach. Key surgical landmarks, including the GSPN, facial hiatus (FH), arcuate eminence (AE), mandibular nerve (V3), petrous ridge, and tegman tympani, as seen through the tubular retractor (left) and through the petrous bone (right). The tip of the retractor could achieve 20° of yaw and the opening of the retractor could achieve 10° of negative pitch (downward in relation to the visual field, superior/rostral toward to the top of the head in relation to the anatomy) at full insertion (left).

Because the arcuate eminence—a superficial landmark for the deep intrapetrous location of the superior semicircular canal—has a constant relationship to the location of the IAC, an imaginary line bisecting the angle between the arcuate eminence and the GSPN was located and corresponded to the location of the IAC. The location of the cochlea was identified at the vertex of the angle between the GSPN and the IAC, where the GSPN corresponds anatomically to the

course of the horizontal portion of the intrapetrous internal carotid artery. A minimally invasive surgical drill was used through the retractor to remove the thin layer of bone along this bisecting line to expose the entire length of the IAC from the fundus to the porus acusticus (Figure 27). Drilling of the IAC was initiated medially at the intersection with the petrous ridge, where the bone is thickest, and continued laterally toward the fundus where Bill's bar was exposed.

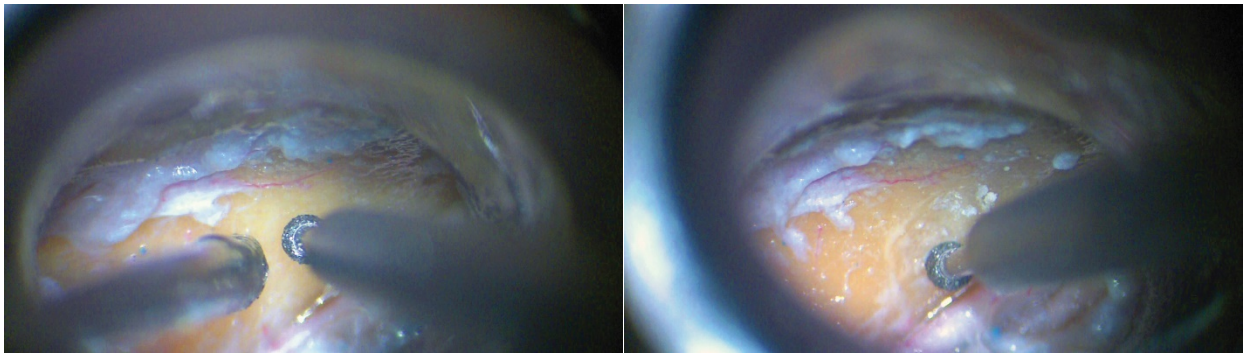

Figure 27. Drilling of the Internal Auditory Canal.

To further confirm surgical accuracy, the superior semicircular canal was blue-lined in 4 cadaveric sides and a line 60° anterior to the blue-line was used to indicate the course of the IAC. With the high-speed drill, bone was removed along this imaginary line down to the porus acusticus. As the bone became more compact and the dura of the IAC was approached, a diamond burr was used with copious irrigation to mitigate the risk of thermal injury to any neurovascular structures pushed up against the dura by mass effect from a tumor. In some cases, a thin shell of bone was left over the dura and subsequently removed using a blunt dissector or fine Kerrison punch. A curved microsuction aspirator was used to provide an unobstructed visual field and allowed for enhanced visualization of the transtubular surgical field. Drilling proceeded laterally using the diamond burr and bone was removed until Bill's bar was exposed at the fundus of the canal. At this step, extreme care was taken as the facial nerve becomes increasingly

superficial as it nears the fundus and joins the geniculate ganglion—which in some cases may be dehiscent.

Once the dura was properly identified, a cutting burr was again used to remove bone in the pre- and postmeatal triangles. Care was taken to avoid damage to the cochlea. The IAC was unroofed by approximately 270° and exposed in its entire length from the lateral aspect of the fundus to the porus acusticus. The tubular retractor adequately limited the amount of exposure needed. The dura of the IAC was exposed and incised linearly at the posterior aspect of the IAC toward the petrous ridge.

After the dura was opened, the intracanalicular segment of the facial nerve, Bill's bar, the superior vestibular nerve, the loop of the anterior inferior cerebellar artery, and the lateral surface of the pons were observed (Figure 28). The 90° medial rotation of the nerves at their entrance into the porus acusticus and the resulting anatomy, with the superior vestibular nerve posterior, the inferior vestibular nerve inferoposterior, and the cochlear nerve inferior relative to CN VII, was clearly visualized. Care was taken to preserve the internal auditory (labyrinthine) artery, which was identified between the facial and the cochlear nerves. At the fundus, Bill's bar was observed clearly dividing the superior aspect of the IAC. Anterior to Bill's bar, in the anterosuperior quadrant of the transtubular visual field, CN VII and the nervus intermedius were observed.

The cochlea was identified in the anterosuperior quadrant, the tegmen tympani in the posterosuperior quadrant, and the intrapetrous internal carotid artery—running underneath the GSPN—in the anterosuperior quadrant. The medial portion of the IAC coursed within the anteroinferior quadrant.

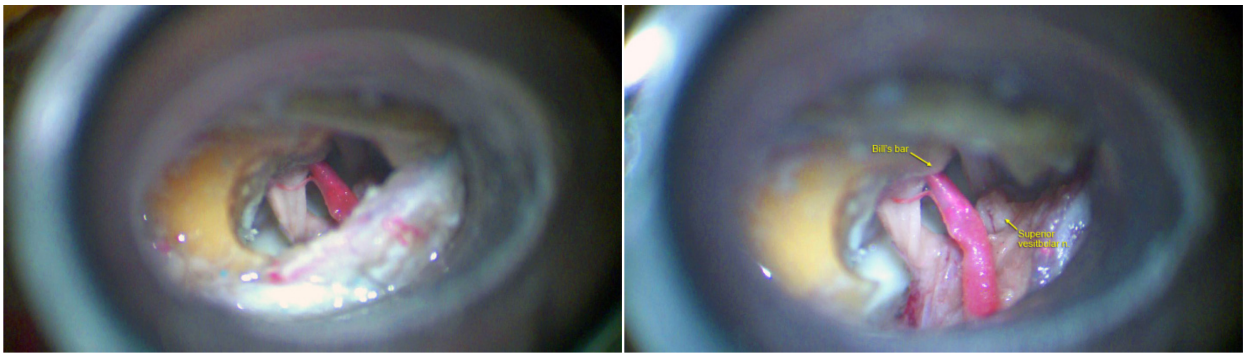

Figure 28. Intradural Exposure in the Anterior Transpetrosal Approach. The right facial nerve, Bill's bar, the superior vestibular nerve (cut to expose the inferior vestibular nerve), the loop of the anterior inferior cerebellar artery, the labyrinthine artery, and the lateral surface of the pons following dural opening.

In specimens containing a synthetic tumor model, resection was completed. After closure of the IAC, the retractor was removed and the field was copiously irrigated (Figure 29).

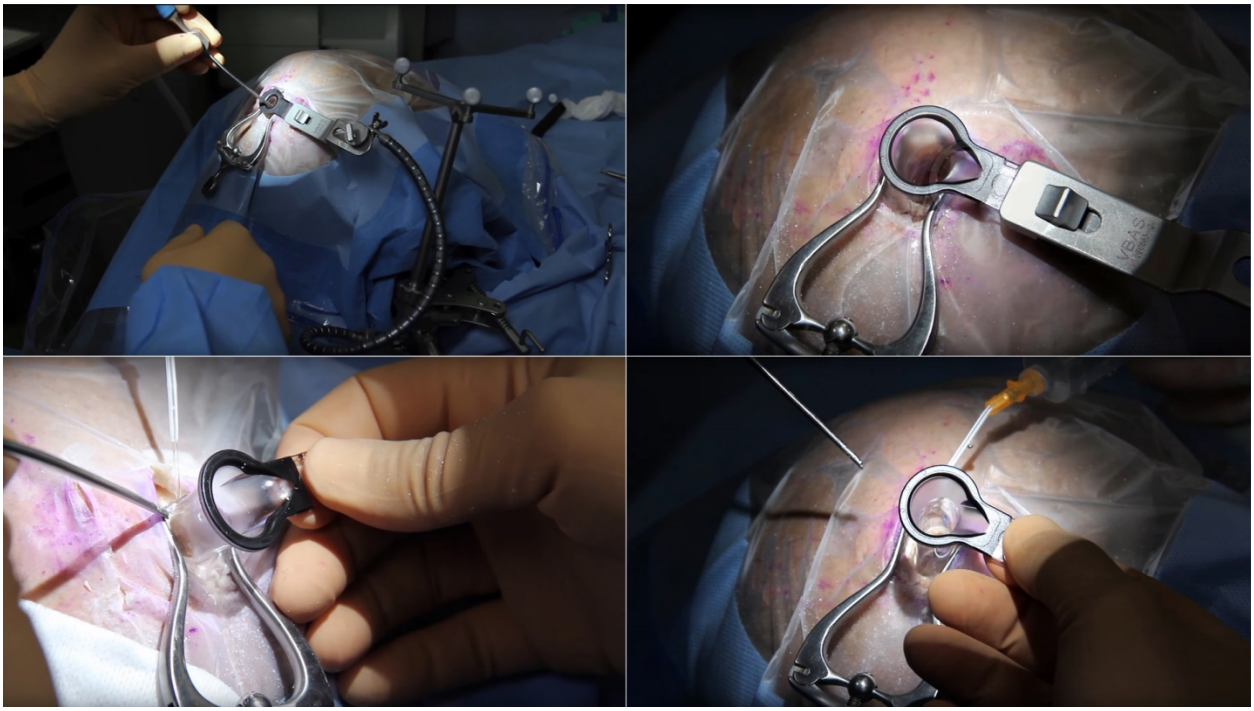

Figure 29. Removal of the Tubular Retractor.

Assessment of Tumor Resection, Exposure, and Maneuverability

The degree of tumor resection was quantitatively assessed for all specimens with synthetic intracanalicular tumors (Table 3). Additionally, the degree of exposure of important surgical landmarks was assessed to evaluate surgical freedom and maneuverability on and around key structures (Table 4).[115,146,155] Accordingly, a value of exposure less than 90° indicates that the structure can be exposed from a single angle, but circumferential control is absent and surgical maneuverability is not possible. A degree of exposure between 90° and 180° indicates that the structure can be exposed from different angles, but full circumferential control and surgical maneuverability are still somewhat difficult, particularly if the structure is completely encircled within a lesion. A degree of exposure greater than 180° indicates that the structure is fully exposed from different angles, control along its entire circumference is complete, and surgical maneuvers using a combination of microinstruments, suction, flexible instruments, bayoneted instruments, and/or tube shaft instruments through the tubular retractor are possible.

Grade	Description	Percentage Removed*
I	Gross total removal of all visible macroscopic tumor model	98-100%
II	Near total removal with only a small amount of inaccessible or unobservable tumor left in situ	91-97%
III	Subtotal removal with significant portions of inaccessible tumor left in situ	50-90%
IV	Partial removal with portions of visible tumor left in situ	< 50%
V	Biopsy-like access with removal of only a small portion of tumor	< 20%

Table 3. Synthetic Tumor Resection Scale. *Determined by weight.

Degree of Exposure	Angles Exposed	Circumferential Control
< 90°	Single	Absent
90°-180°	Multiple	Difficult
> 180°	All	Present

Table 4. Degree of Exposure Scale.

Results

All approaches, both microscopic and endoscopic, were successfully completed through the tubular retractor via minimally invasive percutaneous openings, with minimal retraction of brain tissue.

Tubular Retraction

The tubular retractors provided sufficient space to allow for simultaneous placement of the endoscope and any combination of 2 microsuction aspirators, microinstruments, bayoneted instruments, flexible instruments, and/or tube shaft instruments (Figure 30). Use of flexible, bayonetted, and/or tube shaft instruments in the retractor did not obstruct the microscopic or endoscopic visual fields (Figure 27). The conical shape of the retractor greatly facilitated its insertion and advancement, and its transparent walls provided excellent visualization of the peripheral anatomy—especially the key bony landmarks—while allowing for constant monitoring of the surrounding vasculature. Microsuction, microinstruments, and flexible, bayonetted, and tube shaft instruments were all used through the retractor without difficulty. A neuronavigation pointer was also easily used through the working channel, and irrigation was applied through the retractor as needed without difficulty.

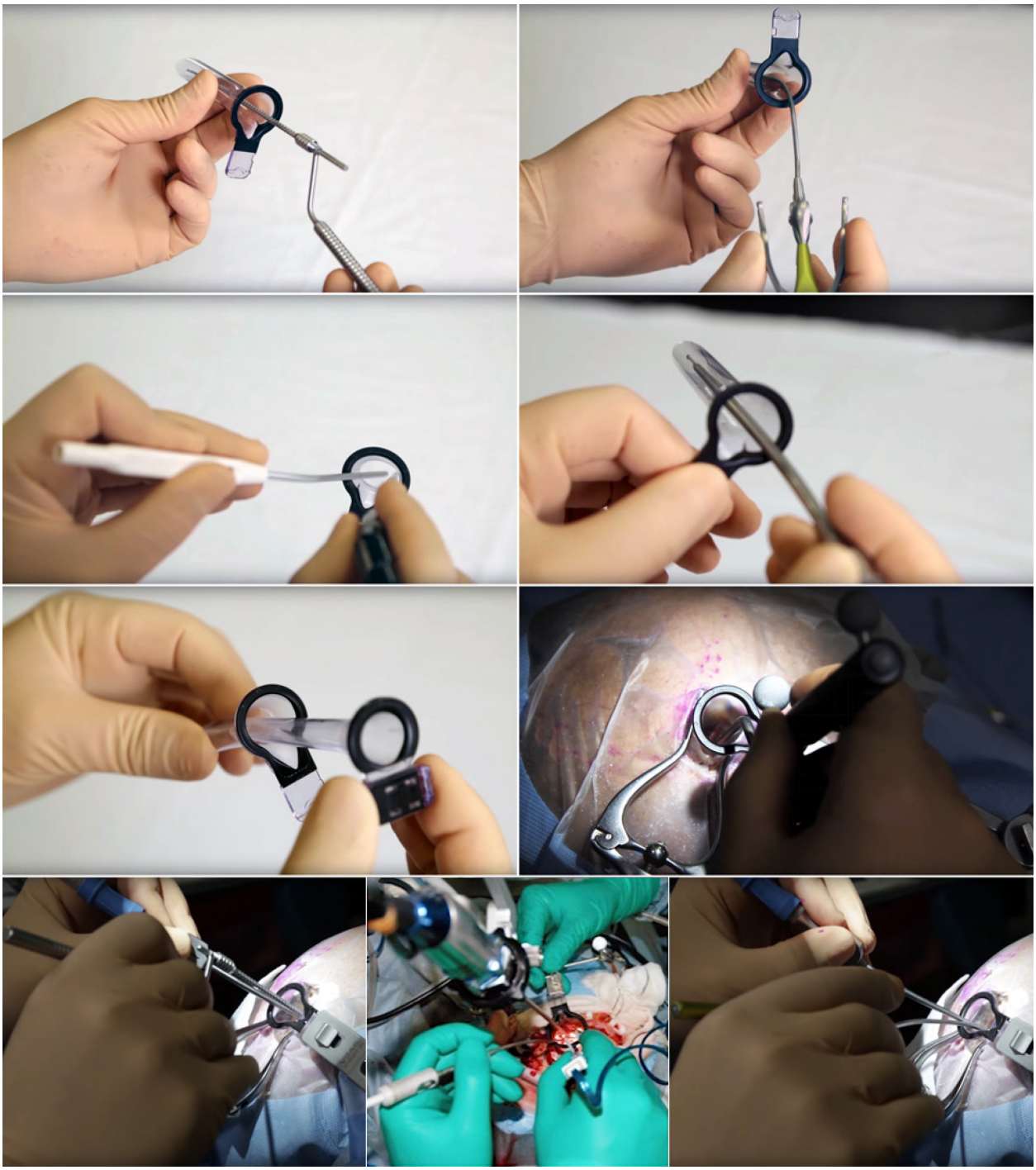

Figure 30. Surgical Instrumentation and Bimanual Transtubular Techniques. Transtubular use of bayonetted and flexible instruments (first row), suction and a minimally invasive surgical drill (second row); unlatching of the introducer and integration of a neuronavigation pointer (third row); and bimanual technique (fourth row) and integration of the endoscope (fourth row, middle).

The smooth nature of the retractor prevented adherence to any tissues and mitigated the need for underlying cottonoid pads or surgical patties, and facilitated smooth insertion into the field. The introducer was placed in situ whenever advancing the retractor deeper into the surgical corridor and irrigation with sterile water or saline was applied during any movement of the retractor. The latch that releases the introducer was tested and locked prior to insertion. When removing the introducer from the surgical field, it was important to consider that the end of the working channel was approximately 1 cm proximal to the tip of the introducer, and thus to avoid tissue obstructing the field, the introducer was unlatched from the working channel and the working channel was then slid further into the field, over the introducer, until it reached the target; the introducer was then removed from the field. This maneuver positioned the retractor at the target site in a single motion without requiring repositioning or advancement without the introducer in place.

At full insertion, the retractor provided 3–4 degrees of freedom, depending if the retractor was placed along a rigid boney surface, and in most cases, the tip of the retractor could achieve 20° of yaw and the opening of the retractor could achieve 10° of pitch, alleviating the need to pull brain tissue in any single direction (Figure 26).

Careful and precise preoperative planning, considering the ~1 cm distance from the tip of the introducer to the distal edge the working channel, and integration with neuronavigation significantly reduced the need for intraoperative repositioning, further reducing trauma to retracted tissues, and eliminated the need for so-called “wanding” of the retractor wherein the working channel is angled or transposed inside the surgical field. This maneuver was avoided unless absolutely necessary as it can cause additional bleeding and damage to cortical tissue during intraparenchymal approaches. Surgical planning also allowed for easy determination of

optimal retractor size, although having additional distal port sizes readily available clinically is advisable.

Surgical Opening and Trajectory

In the anterior transpetrosal approach, the mean lateral petroclival angle was 41±5° and the mean petroclival-acoustic distance was 21±2 mm (Appendix C). The corresponding mean optimal entry point was located 4 cm posterior to the lateral orbital wall, 2 cm anterior to the external auditory meatus, and flush with the superior rim of the zygomatic arch. This calculated optimal entry zone and trajectory was successfully verified for target accuracy on all cadaveric specimens via the trajectory planning feature of the neuronavigation software (Figure 18).

In the supracerebellar infratentorial and interhemispheric approaches, trajectories were slightly more variable, as the corridors were between brain and dura; however, neuronavigation was successfully used in call cases to avoid injury to the nearby dural venous sinuses. Placement of bone openings in the supraorbital and retrosigmoid approaches were based on the use of conventional surface landmarks coupled with neuronavigation.

Surgical Exposure and Maneuverability by Approach

The degree of circumferential exposure of important surgical landmarks was assessed in each approach to evaluate surgical freedom and maneuverability on and around key structures (Table 5).

Supraorbital Approach. The transtubular supraorbital approach provided good visualization of the anterior fossa and its neurovascular contents, as well as the supra- and parasellar regions, with minimal frontal lobe manipulation (Figure 31). The suprasellar pyramid

and carotid cistern were accessed with 15–20° contralateral rotation of the head. After the arachnoid membrane was dissected the anterolateral structures of the supraseller pyramid including the ipsilateral optic nerve, optic chiasm, anterior communication artery (ACOM), supraclinoid (ophthalmic) segment of the internal carotid artery, and A1 segment of the anterior cerebral artery were identified. After minimal retraction of the frontal lobe, the optic-carotid and intraoptic windows were visible. The Sylvian fissure was approached with the head rotated 15°to the contralateral side, and opened from medially to laterally to expose the M1 segment of the middle cerebral artery. The optic chiasm was approached with the head positioned with 20° contralateral rotation and the entire A1 segment, ACOM, lamina terminalis, and contralateral A1, as well as the Heubner artery were exposed. The pericarotid triangles were approached with the head positioned with 15–20° contralateral rotation. The anatomical windows between CN II, the internal carotid artery, CN III, and the anterior petroclinoid ligament were observed. The deep prepontine and interpeduncular cisterns were observed and approached via the optic-carotid and carotid-oculomotor surgical corridors. The interpeduncular fossa was accessed through the optic-carotid window the head positioned with 15–20° contralateral rotation to expose the ipsilateral superior cerebellar artery and basilar trunk. Contralateral structures could be approached with the head positioned with 35° contralateral rotation. With the tubular retractor pointed medially, the contralateral CN II and the internal carotid artery were exposed along with the origin of the ophthalmic artery. The internal carotid artery bifurcation was observed. As the carotid cistern was opened, the temporal lobe and contralateral A1 and M1 became visible. Accurate placement of the craniotomy, which includes the superior aspect of the supraorbital rim, is essential for basal placement of the retractor and avoiding injury to the supraorbital nerve medially and the temporal branches of the facial nerve laterally. Careful removal of the inner bone table was

necessary to provide the correct surgical trajectory and allow for insertion of the tubular retractor, as insufficient bone removal will push the retractor superiorly toward the frontal lobe. Supine positioning with the contralateral frontal area fixed with one pin allowed for free manipulation of the ipsilateral side.

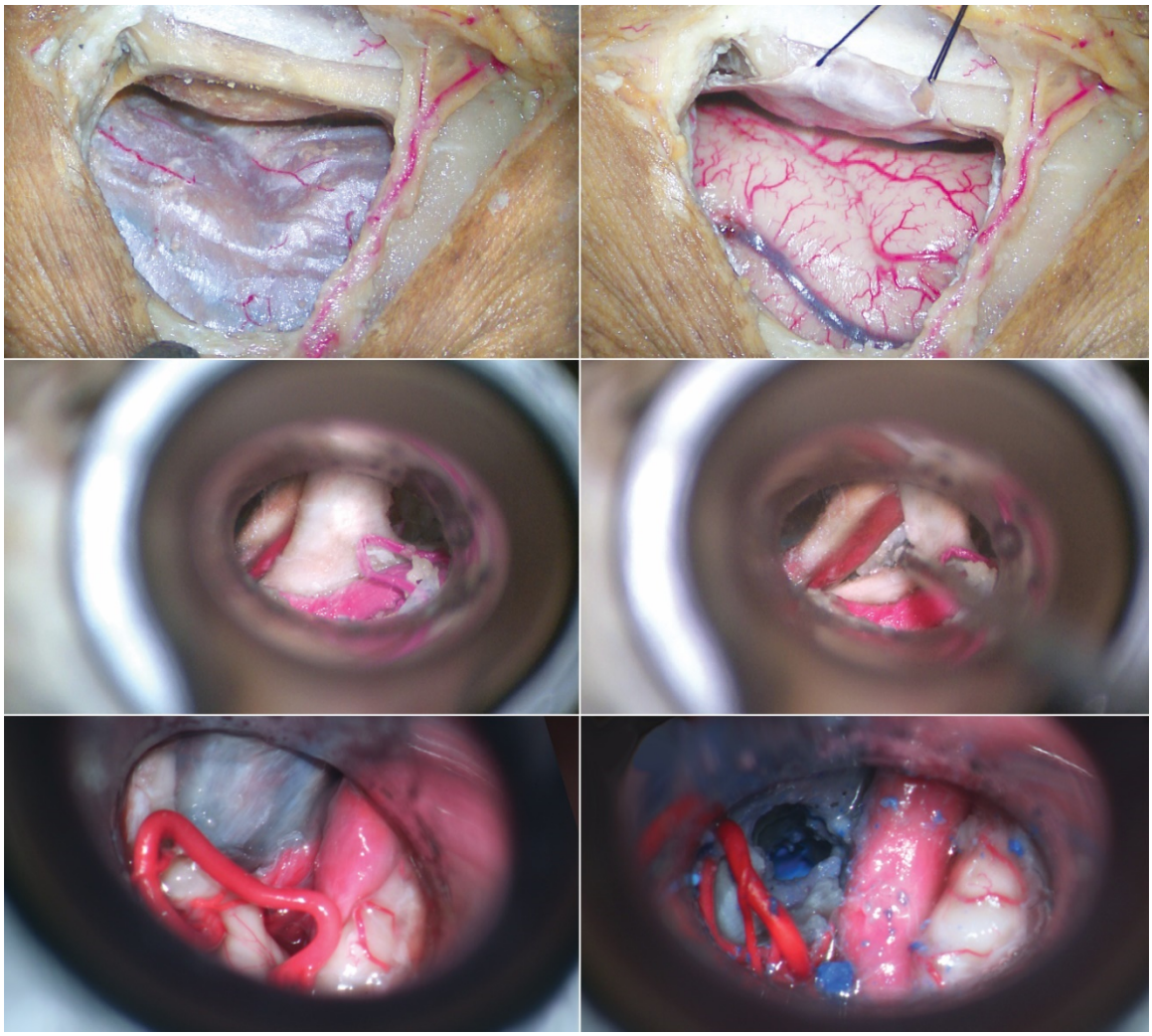

Figure 31. Transtubular Supraorbital Approach. A keyhole craniotomy was fashioned as basal as possible and included the superior aspect of the supraorbital rim (top). Anterolateral aspect of the right suprasellar area medial to the supraclinoid internal carotid artery (middle). The window between CN II, the internal carotid artery, CN III, and the anterior petroclinoid ligament (bottom, left). The ipsilateral superior cerebellar artery and basilar trunk through the optic-carotid window following posterior clinoidectomy (bottom, right).

Anterior Transpetrosal Approach. The transtubular anterior transpetrosal approach, as described extensively in the previous section, provided excellent exposure of the entire length of the IAC as well and the facial and vestibular nerves from the inner ear to the pons (Figures 25, 27–28). Placement of the bone opening flush with the floor of the middle fossa was essential for achieving minimal temporal lobe retraction. Insertion of the tubular retractor into the surgical field was performed from a lateral to medial direction with the tip aimed a few degrees anterior to the planned trajectory toward the middle meningeal artery and mandibular nerve. Due to the 45° angle between the course of the IAC and the superior surface of the petrous bone, the tubular retractor was pitched 10° superiorly in order to align the surgical trajectory as perpendicular as possible to the petrous bone and with the roof of the IAC while applying only minimal retraction of the temporal lobe. This maneuver allowed for full exposure of the fundus of the IAC. Due to the small size of the bone opening, the complexity of petrous bone anatomy, and the limited peripheral vision, accurate placement of key visible anatomical structures in the correct transtubular visual quadrants was essential for safe drilling of the petrous bone. The GSPN and facial hiatus were visualized and confirmed in the anterosuperior quadrant and the arcuate eminence in the posterosuperior quadrant. Thus, the cochlea corresponded to the anterosuperior quadrant, the tegmen tympani to the posterosuperior quadrant, and the intrapetrous internal carotid artery to the anterosuperior quadrant. The medial portion of the IAC then coursed within the anteroinferior quadrant. Extreme care was taken while drilling in case of dehiscent geniculate ganglia as well as when dissecting near the fundus where the facial nerve is partially covered by the transverse crest and visualization may be limited. Maneuvers within the IAC were performed from a medial to lateral direction in order to avoid traction of CN VIII as it entered the modiolus. Intradurally, the facial nerve, Bill's bar, the superior vestibular nerve, the loop of the anterior

inferior cerebellar artery, and the lateral surface of the pons were clearly observed. Sacrifice of the superior petrosal sinus was only necessary when there was synthetic tumor extending medially and rostrally into the cerebellopontine angle.

Interhemispheric Transcallosal Approach. The transtubular interhemispheric transcallosal approach provided excellent access to the lateral ventricle through an interhemispheric burr hole, as well as access to the third ventricle via the transforaminal, transchoroidal, or transseptal interforniceal corridors (Figures 20–21, 32). Careful placement of the burr hole was essential for avoiding the superior sagittal sinus. In some cases, a small shell of bone was left above the superior sagittal sinus to protect its lateral aspect. A small fenestration of the corpus callosum was fashioned and the tubular retractor was carefully advanced into the lateral ventricle. The normal ventricular anatomy was identified including the choroid plexus, foramen of Monro, body and columns of the fornix, thalamus, superior choroidal vein, thalamostriate vein, and septal vein. The foramen of Monro and the fornix were located by using the choroid plexus, thalamostriate vein, superior choroidal vein, septal vein, and vein of the caudate nucleus. The foramen of Monro was easily identified as an oval opening between the columns of the fornix and the anterior end of the thalamus. Just posterior to the interventricular foramen, a small bulge on the surface of the thalamus, the anterior nucleus of the thalamus, was seen. The choroid plexus was also easily identified projecting in the ventricular cavity, extending from the interventricular foramen, where it meets the plexus of the contralateral ventricle, to the end of the inferior cornu (horn). In the transchoroidal corridor, efforts were made to preserve the small perforators brunching off of the choroidal arteries and entering the thalamus. The superior and anterior thalamic veins, thalamostriate vein, and choroidal arteries were observed passing through the tenia choroidea. The body of the fornix was elevated to expose the internal cerebral

veins and the tela chorioidea. The junction between the anterior septal vein and internal cerebral vein was observed relative to the foramen of Monro, usually in a posterior position that allowed for enlargement of the foramen posteriorly along the choroidal fissure without sacrifice of neural or vascular structures. Fenestration of the corpus callosum and splitting of the septum pellucidum and forniceal columns allowed for entrance into the third ventricle. The roof of the third ventricle, formed by a thin layer of ependyma, was opened and entered with the tubular retractor to reveal the body and floor of the third ventricle.

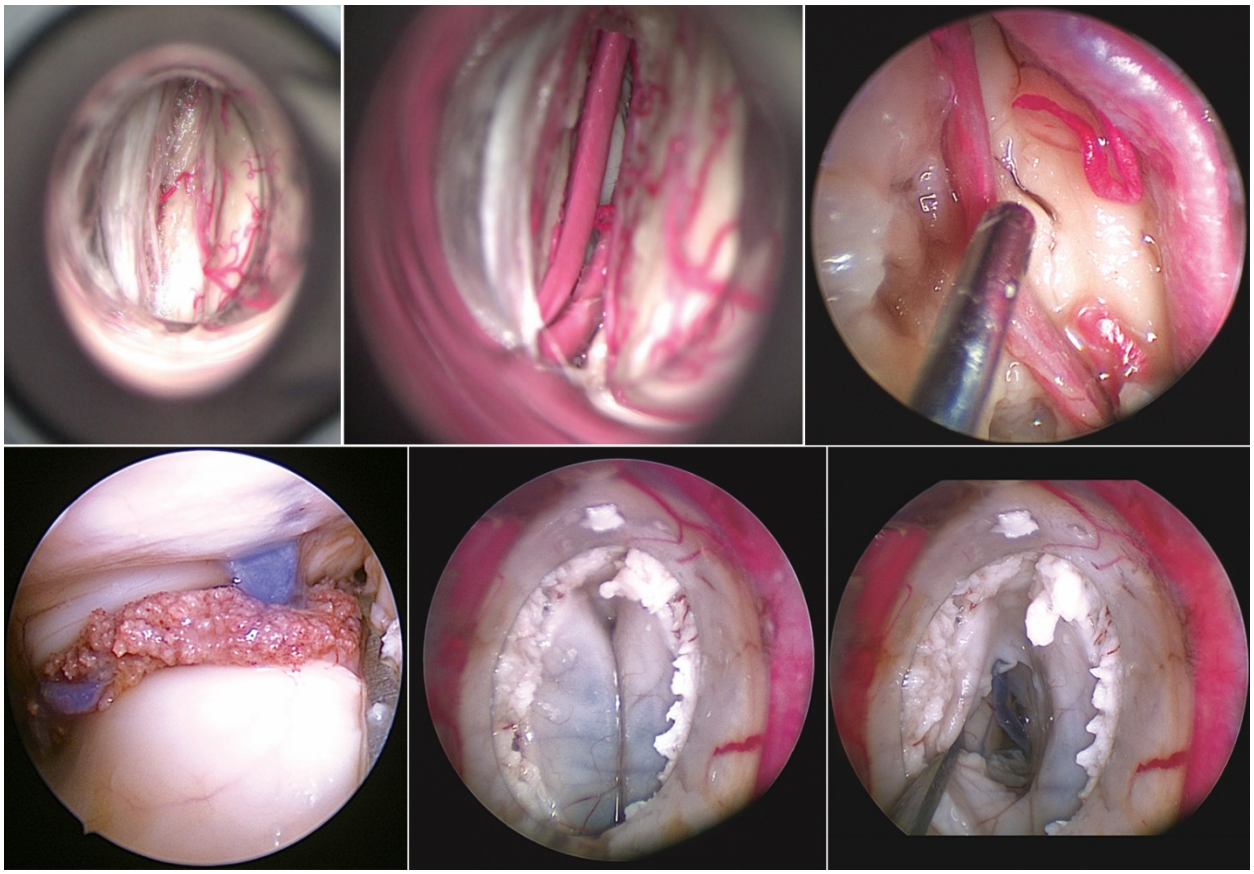

Figure 32. Transtubular Interhemispheric Transcallosal Approach. Identification of the corpus callosum and pericallosal arteries (top), fenestration of the corpus callosum (top, right), identification of the choroid plexus in the right lateral ventricle (bottom, left) and the transseptal interforniceal corridor to the third ventricle (bottom, middle and right).

Retrosigmoid Approach. The transtubular retrosigmoid approach provided full access to the cerebellopontine angle through a suboccipital keyhole craniectomy (Figure 33). Correct placement of the bone opening was essential for preservation of the underlying structures. Prior to drilling, the root of the zygoma, the mastoid tip, and the external occipital protuberance were identified and correlated with neuronavigation. The keyhole craniectomy was fashioned superiorly with its anterior border along the sigmoid sinus. Care was taken to protect the sigmoid sinus while drilling. Adequate bone removal, especially of the inner bone table, was essential for minimizing cerebellar retraction, avoiding injury to the sigmoid sinus, and providing an adequate angle of visualization. After sufficient bone removal, the dura was opened, the tubular retractor was introduced into the surgical corridor, and the arachnoid was dissected with a blunt dissector through the tip of the introducer as it was advanced deeper into the field. The angle between the tentorium and posterior surface of the petrous bone were identified and used to help facilitate a safe trajectory during insertion following the course of the superior petrosal sinus. The CN VII–VIII complex was identified in the superior aspect of the surgical corridor and the upper cerebellopontine angle, including and the superior petrosal vein, were explored. The trigeminal nerve and superior cerebellar arties were located and the trigeminal was exposed along its entire length, from the brainstem to the porus trigemini. CN III was observed deep to CN V. The relationships between CN V, VII, VIII, the superior petrosal vein, the flocculus, and the superior cerebellar artery were visualized. The transtubular surgical corridor provided excellent visualization of the neurovasculature of the cerebellopontine angle and provided a sufficient conduit for performing microvascular decompression for trigeminal neuralgia or resection of a cerebellopontine angle lesion.

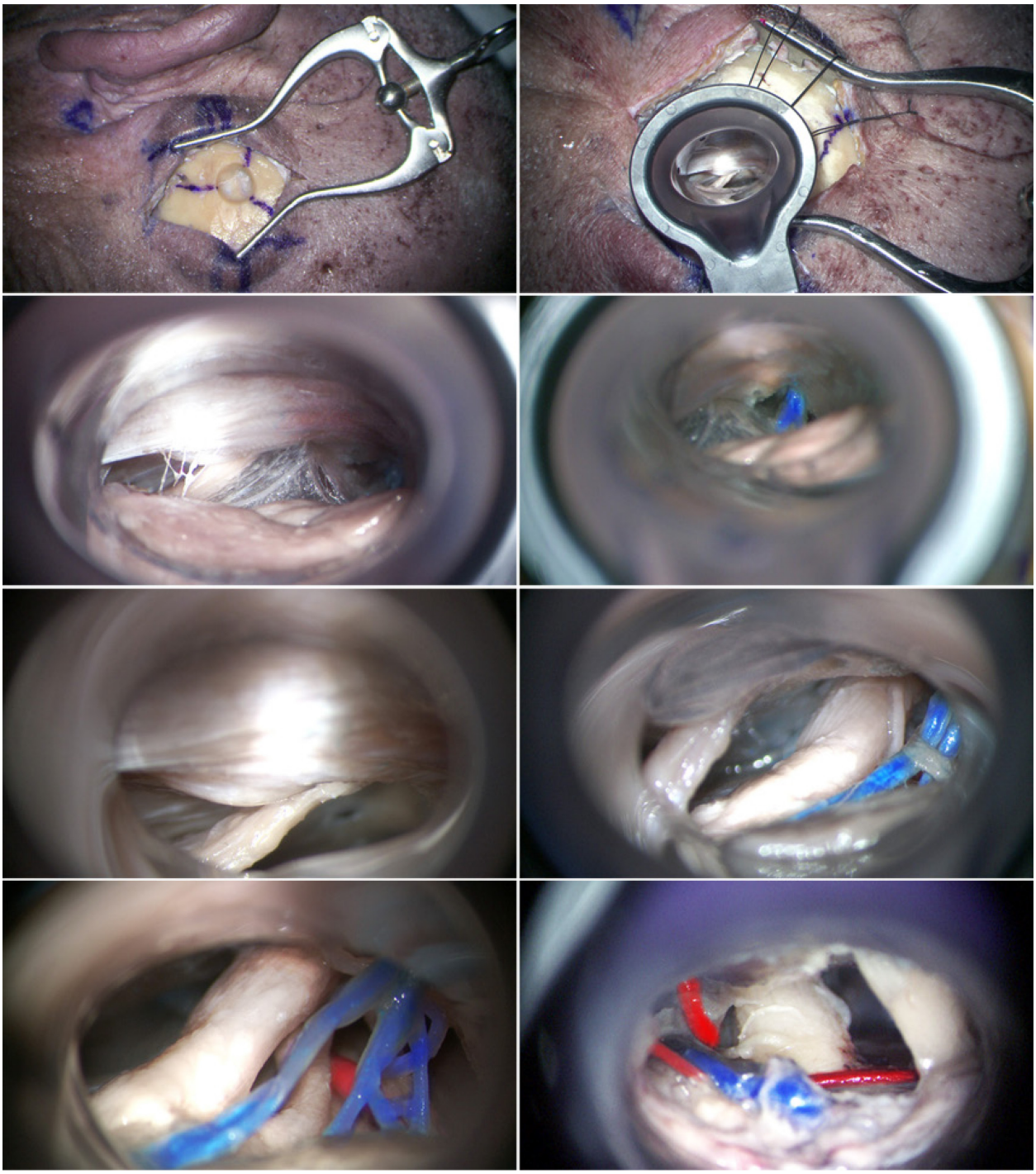

Figure 33. Transtubular Retrosigmoid Approach. Left side skin incision and introduction of the tubular retractor through the keyhole craniectomy (first row). Initial cerebellar retraction (second row, left) and opening of the arachnoid (second row, right). Identification of the facial nerve superiorly (third row). The trigeminal roots, superior petrosal vein, and superior cerebellar artery are exposed on the left side (bottom row, left), and the relationship between the superior cerebellar artery and the trigeminal on the right side (bottom row, right).

Supracerebellar Infratentorial Approach. The transtubular median and paramedian supracerebellar infratentorial approaches provided excellent exposure of the pineal region, including the superior and inferior colliculi, origin of the trochlear nerve, entire quadrigeminal plate, and posterior ambient cistern with minimal cerebellar retraction. The mini-craniectomies were fashioned at either median (5 sides) or paramedian (5 sides) locations after identification of external boney landmarks. Extreme care was taken during bone removal and opening of the dura to avoid injury to the occipital and transverse sinuses. The tubular retractor was gently inserted into the field, several bridging veins were divided, the introducer was removed, and arachnoid dissection was completed. The vein of Galen was identified and the lateral quadrigeminal cistern was exposed. The internal cerebral vein was identified and the pineal gland was exposed between the central cerebellar and internal cerebral veins. The tubular retractor provided excellent access to the entire pineal region and allowed for sufficient surgical maneuverability.

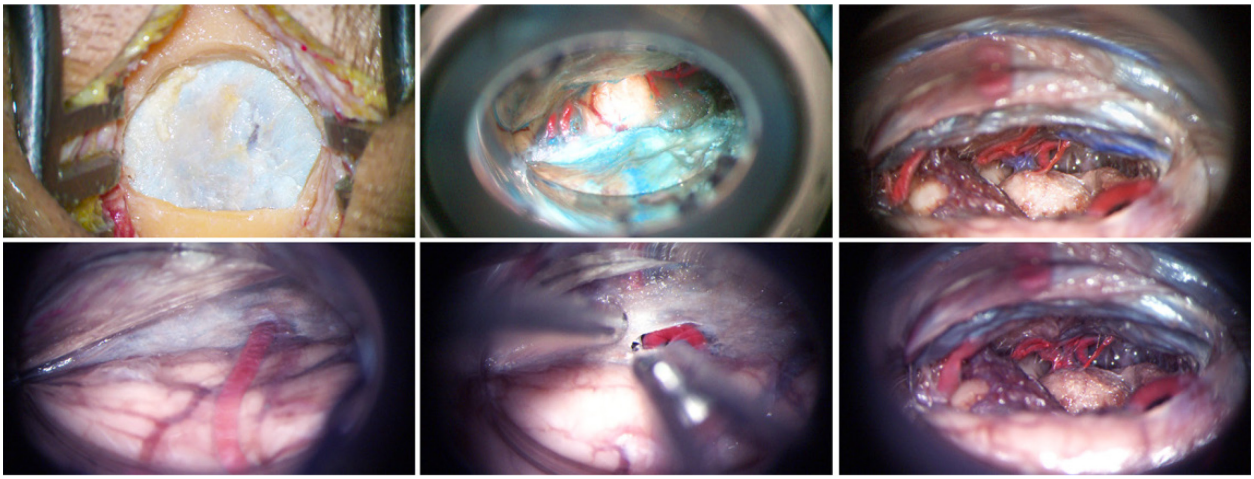

Figure 33. Transtubular Supracerebellar Infratentorial Approach. Placement of the burr hole craniectomy (top, left). Left side median supracerebellar infratentorial approach (top, middle and right). Left side paramedian supracerebellar infratentorial approach to the pineal region; before (bottom, left), during (bottom, middle), and after (bottom, right) of the arachnoid to expose the quadrigeminal cistern.

Anatomical Structure	Microscopic Exposure	Endoscopic Exposure*
Supraorbital Approach		
Optic chiasm	180°	220°
A1 segment of the anterior cerebral artery	120°	360°
Anterior communicating artery	210°	270°
Ophthalmic internal carotid artery	210°	220°
Basilar trunk	90°	180°
Anterior Transpetrosal Approach		
Anterior inferior cerebellar artery loop	220°	360°
CN VII	220°	360°
CN VIII	120°	220°
Geniculate ganglion	180°	180°
Inferior vestibular nerve	120°	220°
Superior vestibular nerve	220°	360°
Interhemispheric Transcallosal Approach		
Choroid plexus of the third ventricle	180°	300°
Mammillary bodies	60°	120°
Foramen of Monro	150°	220°
Tela choroidea	180°	220°
Forniceal columns	180°	210°
Retrosigmoid Approach		
Anterior inferior cerebellar artery	270°	360°
CN VI-VIII	180°	360°
CN V	150°	270°
Superior cerebellar artery	150°	220°
Superior petrosal vein	270°	300°
Supracerebellar Infratentorial Approach		
Superior colliculi	180°	220°
Inferior colliculi	120°	180°
Pineal gland	180°	270°
CN IV	220°	220°
Basal vein of Rosenthal	220°	270°

Table 5. Transtubular Exposure of Target Surgical Structures by Approach. *Including the use of 30° or 45° angle endoscopes.

Synthetic Tumor Resection

Of the 6 synthetic intracanalicular tumors (≤1.5 cm in diameter) resected, gross total (Grade I) resections were achieved in 5 cases with greater than 98% of the tumor recovered as determined by weight, and included the tumors placed anterior, posterior, and superior to the CN VII–VIII complex. A near-total (Grade II) resection, with 96% of the tumor recovered, was achieved in the remaining case in which the tumor was placed inferior to the CN VII–VIII complex. All minute portions of tumor that extended into the posterior fossa were resected without difficulty (Figure 35).

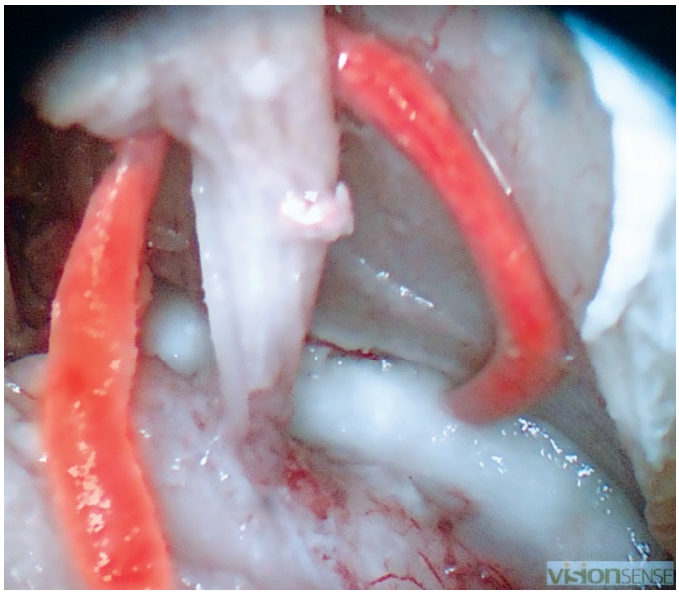

Figure 35. Synthetic Tumor Resection. Endoscopic view of the loop of the anterior inferior cerebellar artery and inferior vestibular nerve with residual tumor visible in the cerebellopontine angle.

Summary

Tubular retraction in neurosurgery provides a safe and effective conduit for the application of percutaneous minimally invasive approaches. Transtubular supraorbital, anterior

transpetrosal, interhemispheric transcallosal, retrosigmoid, and supracerebellar infratentorial approaches are all feasible and provide effective surgical corridors to the para- and suprasellar regions, internal auditory canal, lateral and third ventricles, cerebellopontine angle, and pineal region, respectively, with ample surgical exposure, freedom, and maneuverability while providing reduced retraction of brain tissue. The tubular retractor provided sufficient working space for standard bimanual surgical technique without obstruction of the visual field while using a microscope and/or an endoscope, and permitted sufficient surgical freedom in all directions not limited by bone. The transparent nature of the retractor allowed for constant monitoring of surrounding vessels and retracted surfaces, and facilitated maintenance of anatomic orientation throughout the procedure. The smooth surfaces of the working channel allowed for easy insertion and removal without impingement of retracted tissues. Additionally, the working channel limited instrumentation to the surgical corridor, thus protecting surrounding tissues from inadvertent injury. Adequate preoperative planning of the surgical trajectory was critical for facilitating a safe, direct, and practicable surgical corridor. Drilling and navigating the complex anatomical structures at the base of the skull through the tubular retractor was possible, even in the extremely restricted corridors of the anterior transpetrosal approach. The use of a synthetic tumor model provided a means for more closely simulating clinical conditions and provided an additional method for quantitatively verifying the surgical applicability of transtubular approaches through confirmation of resection ability. The magnification and angled view provided by the endoscope allowed for enhanced anatomic exposure and inspection for residual tumor.

NOVEL BONE CLOSURE TECHNIQUES FOR TRANSTUBULAR NEUROSURGERY

Rationale and Objective

The increasing availability and affordability of high-resolution 3D printers has expanded their potential for surgical application. As such, we investigate the possibility of creating on-demand intraoperative patient-specific 3D printed cranioplastic prostheses as an alternative technique for the closure of transtubular minicraniectomies where excised bone is not available for reimplantation.

Experimental Design and Methods

Miniature retrosigmoid, supraorbital, occipital, and interhemispheric craniotomies were fashioned on 3 adult cadaveric specimens (3 sides) using a high-speed surgical drill (Anspach). CT based cranioplastic implants were designed, formulated, and implanted into the cadaveric specimens, and the accuracy of development and fabrication, as well as implantation ability and fit, integration with exiting fixation devices, and incorporation of integrated seamless fixation plates was evaluated. Additionally, time required for fabrication was analyzed and compared with existing methodologies.

Computed Tomography

Following craniotomy placement, all specimens underwent half-millimeter spiral CT (Siemens). The obtained data, in Digital Imaging and Communications in Medicine file format,

was then transferred to Materialise Mimics® software (Materialise NV, Leuven, Belgium) for conversion to standard triangle language (STL) file format.

Prosthesis Design

Based on manufacturer guidelines, the STL files were imported into Materialise 3-matic® (Materialise NV, Leuven, Belgium) and the prostheses models for each craniotomy were created using a superimposition technique, wherein a model was created to fill a defined area around the surgical opening and the curvature of its surface was matched to that of the surface of the intact contralateral bone.[156] To accomplish this using the 3-matic® software, a free forming curve was created and superimposed onto the bone surrounding the defect. The area within the curve was then exported onto a 2D plane and the contralateral surface was mirrored and superimposed in order to create the correct curvature for the prosthesis. The software's prosthesis algorithm function was then used to create a 3D master implant to exact thickness specifications that adequately filled the skull defect. Following creation of the digital design, the model was refined using variable thickness and Boolean subtraction to achieve continuity with the surrounding bone. Any obstructing material on the underside was removed and the edges were smoothed and chamfered.

Several prostheses were designed with integrated fixation strips to assess the feasibility of providing seamless fixation (Figure 36). To accomplish this, adherence points were designed on a 2D plane, projected onto the prostheses, and fused using a unionizing function. These adherence, or fixation, plates were then given a thickness of 1.0 mm with 0.5 mm rounded edges. Prefabricated holes were designed into the plates to allow for titanium screw placement.

Additionally, these integrated fixation plates were projected onto the surface of the skull so that they would contour and become flush with the natural curvature of the bone.

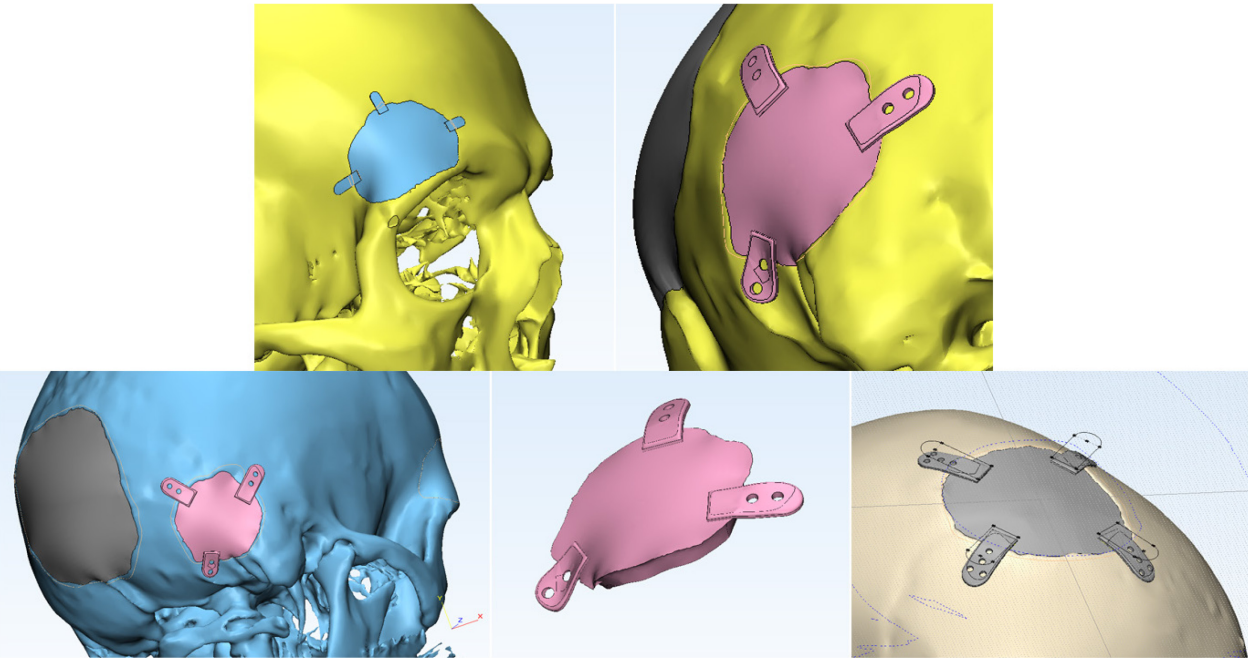

Figure 36. Design of 3D Printable Prostheses with Integrated Fixation Strips.

Design of Polymethyl Methacrylate Injection Molds

As an alternative method for creating artificial custom prostheses, 3D printed injection-molds were also developed in order to cast cranioprostheses using polymethyl methacrylate (PMMA). The box molds were constructed using a subtraction method of a previously generated cranioprosthesis within a computer generated mold box. Once the box molds were 3D printed, they were injected with PMMA (HydroSet™, Stryker Corporation, Kalamazoo, MI) and allowed to dry for 15 minutes (Figure 37).

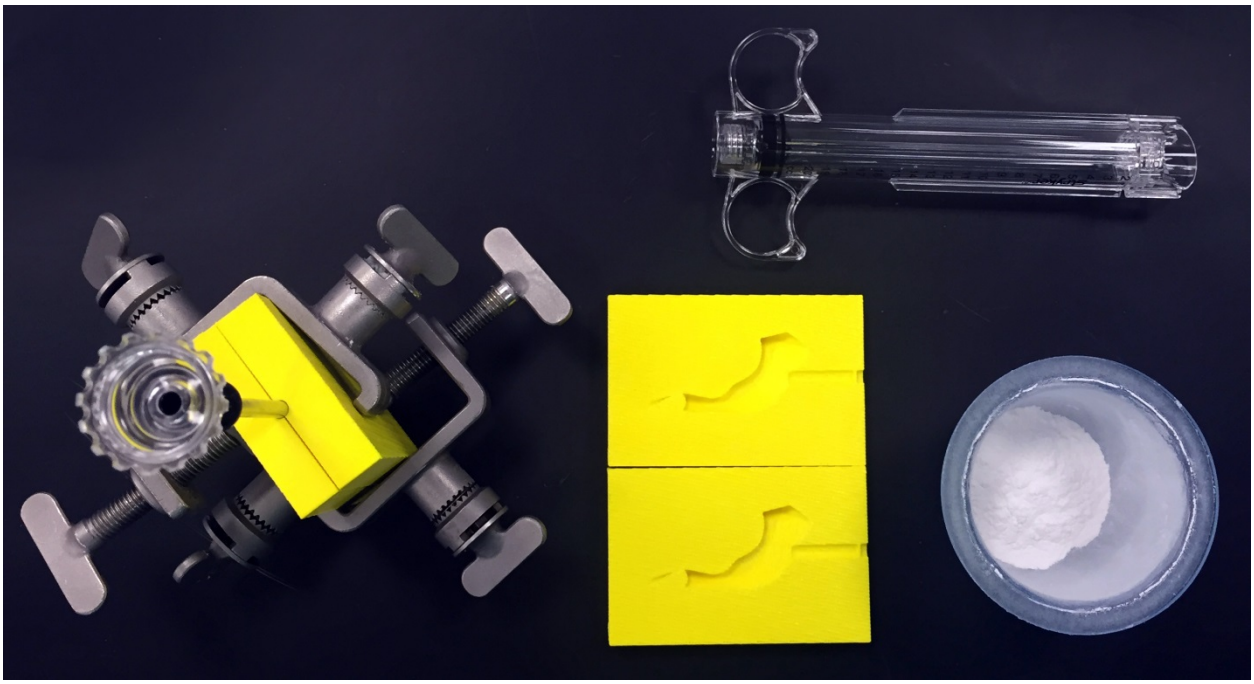

Figure 37. Polymethyl Methacrylate Cranioplasty Injection Molds.

3D Printing of Cranial Prostheses

All cranioprostheses and box molds were created using a fused deposition modeling 3D printer (Fortus 250mc, Stratasys Ltd., Eden Prairie, MN) with a production grade acrylonitrile butadiene-styrene thermoplastic (ABS*plus*™, Stratasys) material.

Prosthetic Cranial Flap Placement, Fixation, and Assessment

Each printed prostheses was implanted into its corresponding cranial opening using standard surgical techniques. The fit of the 3D printed prostheses within the opening was assessed using a surgical microscope (Zeiss) for approximation of the defect, and titanium plates and self-tapping screws (Universal Neuro 3, Stryker) were assessed for fixation to the skull. Cranioprostheses printed with integrated fixation plates were fixed to the skull with titanium screws and pressure was applied to assess fixation strength.

Results

All cranioprostheses were successfully designed using the superimposition technique and were printed and detached from the support material without difficulty (Figure 38). Support material was either dissolved away in an agitated detergent bath or simply broken away without damaging the prosthesis. The average time for design, from importation of CT data to initiation of printing was 14.6 minutes.

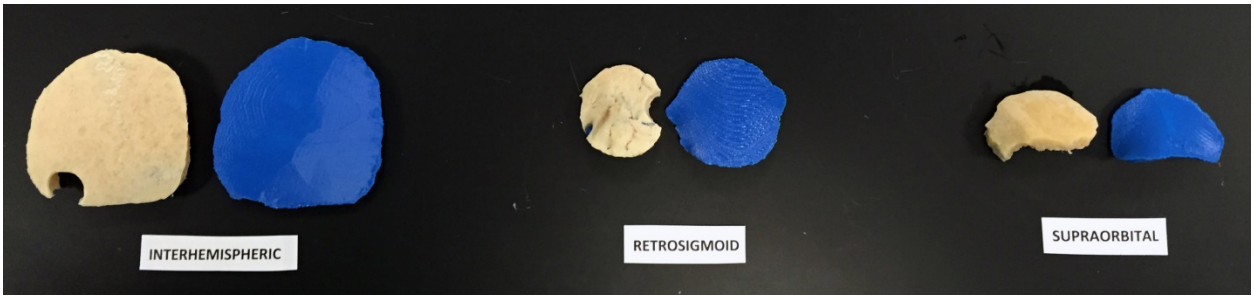

Figure 38. 3D Printed Cranial Prostheses.

Prosthetic Cranial Flap Placement and Fixation

All prostheses seamlessly approximated the outer bone table of the skull defect and were flush with the skull when inserted. Each cranioprosthesis was fixed to the skull using 3–4 points of fixation. The use of titanium plates and screws allowed for uncomplicated fixation and the screw were used in the printed material without difficulty (Figure 39).

Due to the nature of the material used, it was not possible to print integrated fixation strips less than 1 mm in thickness, so 1 mm thick fixation strips were incorporated into several printed models. These strips achieved sturdy fixation with the surrounding bone, did not break or loosen when pried with significant force, and, as they were designed to conform to the contour of the skull, did not require additional bending or shaping. However, these strips were significantly thicker than standard titanium plates and were not flush with the outer surface of the bone.

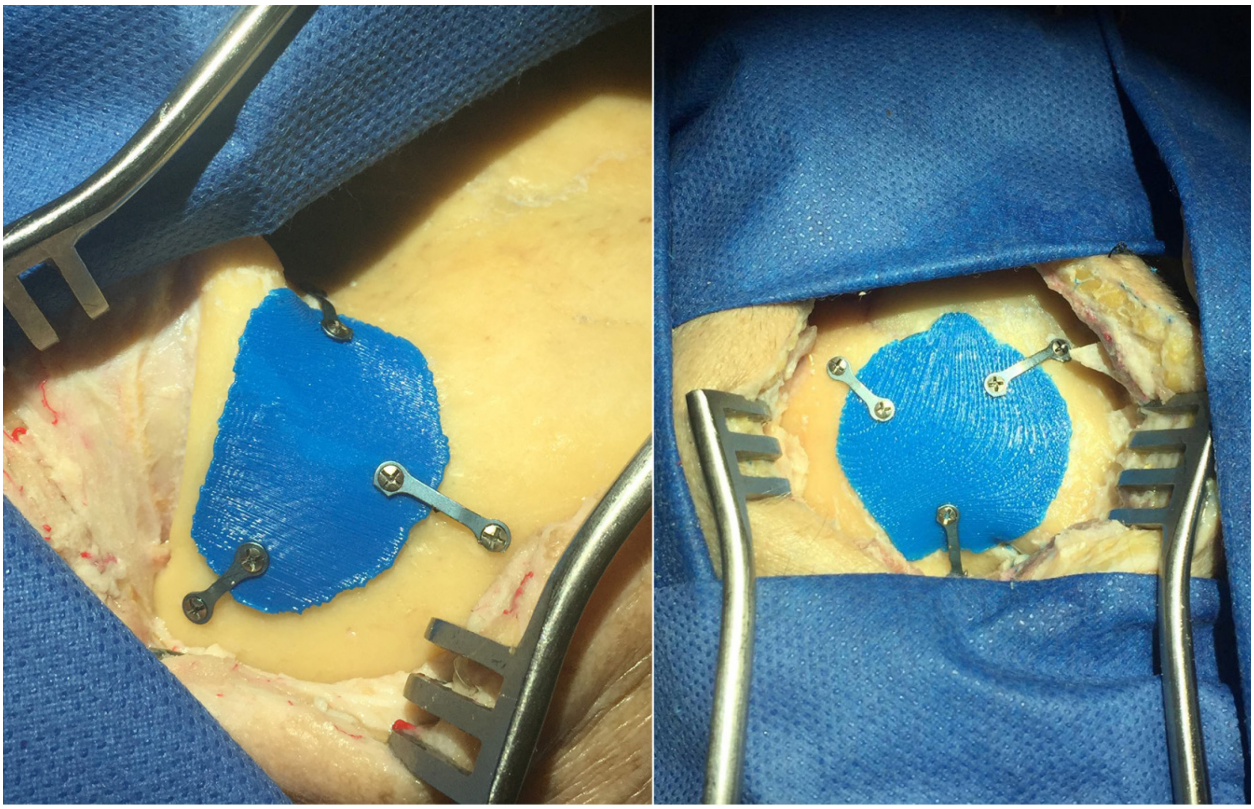

Figure 39. Implantation and Fixation of 3D Printed Cranial Prostheses.

3D Printed PMMA Injection Molds

Detailed injection molds were easily created using the 3-matic® software and PMMA was injected into the box mold without difficulty (Figure 3). To facilitate removal of the dried PMMA from the mold, the mold was covered with plastic wrap prior to injection of PMMA.[157] After removing the dried PMMA, any uneven edges were easily smoothed using the surgical drill. The mold consistently created a prosthesis that provided an exact fit within the skull defect and sat flush with the surrounding bone.

Assessment of Print Time

The average print time for all cranioprostheses was 108.6 minutes (Table 6). Print time was assessed for different resolutions, where high resolution correlated to 0.178 mm layer

thickness, medium resolution to 0.254 mm, and low resolution to 0.330 mm. At medium resolution, all cranioprostheses were printed in less than 3 hours. The addition of integrated fixation strips increased average print time by a moderate 16 minutes in the retrosigmoid approach and a substantial 62 minutes in the interhemispheric approach. This significant increase in print time in the latter was due in part to the additional support material required to stabilize the prosthesis during printing. As titanium plates and screws integrated easily with the printed material, this large increase in print time for integration of adherence strips may not be justified with currently available technologies.

Cranioplasty Site	**High Resolution (0.17 mm)**	**Medium Resolution (0.254 mm)**	**Lowest Resolution (0.33 mm)**	**Average Print Time**
Retrosigmoid	82	55	41	59
Retrosigmoid with fixation plates	92	58	42	64
Interhemispheric	92	54	96	80
Interhemispheric with fixation plates	195	126	106	142
Occipital	293	169	132	198

Table 6. 3D Printing Time versus Resolution.

Comparison of On-Demand and Commercial Prosthesis Development

Currently, commercially produced custom designed craniofacial implants are extremely expensive, at greater than $10,000 per unit, and can take weeks to design and obtain (Figure 40).[158–159] The rapid prototyping and fabrication process described here could be performed bedside by in-house personnel after minimal training, provide a significant reduction in cost, and produce a prosthesis ready for implantation in 2.5 to 3 hours, while providing all of the same clinical benefits as commercially produced variants.

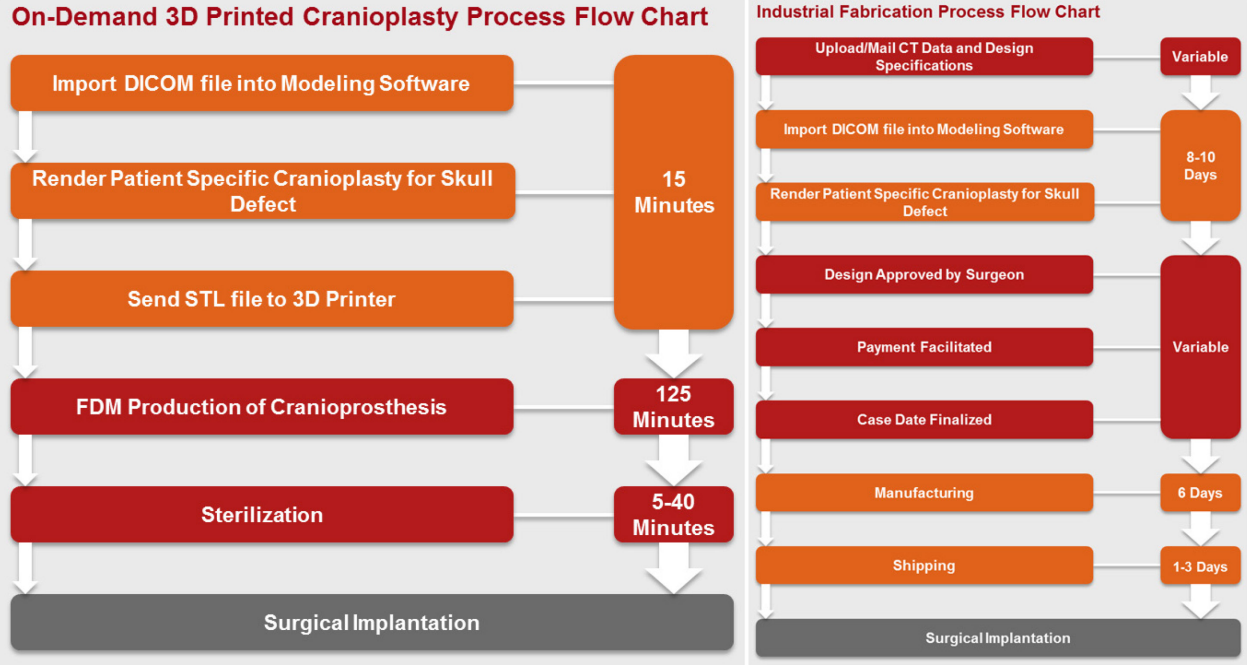

Figure 40. Comparison of On-Demand and Commercial Prosthesis Development.

Summary

On-demand 3D printing of cranial prostheses is a simple, feasible, inexpensive, and rapid solution with a number of potential clinical benefits. The technical difficulty of developing these prostheses is minimal and implantation is technically comparable and potentially easier than current fixation techniques. Low fabrication times highlight the advancement of user-friendly rapid prototyping software and underscore the ability for rapid production of patient-specific prostheses. In the future, these concepts could be applied intraoperatively wherein a rapid CT or surface scan of the bone opening is performed and a custom cranioprosthesis is designed and 3D printed during the remainder of the operation. On-demand printing of custom prostheses may help improve cosmetic outcomes, decrease operative times, reduce costs and production time, and decrease perioperative complications including infection and resorption. Clinical studies are necessary to determine full practicability of this technique as well as to evaluate the potential for incorporation of antibiotic and biomaterials, including osteoblasts, and

integration of intracranial pressure monitors and flexible materials for use in decompressive craniotomies, among others possibilities.

DISCUSSION

Since the introduction of stereotactic cylindrical retractors by Kelly et al. in 1988,[89–90] transtubular excision of intraparenchymal lesions via transcortical routes has been aptly described in the literature.[91,96–100,103–143]

In 2008 Greenfield et al. reported their findings on transtubular resection of deep brain lesions in 10 patients in which radiographic gross total resection was achieved in all cases.[103] In 2011, Raza, Recinos, and colleagues published 2 studies in which VBAS was used for deep intracranial lesions in 13 adult and pediatric patients wherein satisfactory resection or biopsy was obtained in all cases and no new neurological deficits were observed postoperatively.[107,109] The same year, Jo et al. reported on 21 patients who underwent endoscopic transtubular resection of deep-seated lesions, in which gross total resection was achieved in 66% of cases and partial resection in 19%, and discussed their difficulty with resection of large calcified lesions but concluded that transtubular techniques can minimize brain retraction and provide satisfactory visualization.[108] In 2015, Akiyama and colleagues contributed data from an additional 18 patients to the literature, in which no complications were observed, helping to establish the safety of transtubular techniques.[120]

In 2015, Przybylowski et al. and Wang et al. both published some of the first findings on transtubular intracrerebral hemorrhage evacuation.[130,132] Wang and colleagues reported their findings from 21 patients and, although the hematoma evacuation rates were similar between the endoscope (90%) and craniotomy (85%) groups, they found that median intensive care unit stay

decreased from 11 to 6 days due to reduced surgical invasiveness—representing an important advancement in the treatment of spontaneous supratentorial ICH, which is the subject of the ongoing MiSPACE trial.[130,136]

The following year Hong et al. reported the first comparison of endoscope- versus microscope-assisted transtubular tumor resection in a series of 20 patients, wherein total or near total resection was achieved in 90% of cases.[117] Eliyas et al. also reported in 2016 on 21 patients who underwent transsulcal resection of intraventricular and periventricular lesions using the NICO BrainPath®, in which gross total resection was achieved in 17 patients.[116]

The same year, Bander and colleagues performed a quantitative analysis of FLAIR hyperintensity and apparent diffusion coefficient maps on 21 patients who underwent transtubular transcortical resection of deep intraparenchymal lesions, and found that tubular retractors did not significantly increase FLAIR signal in the brain, indicating minimal trauma to surrounding white matter.[114]

Despite the adoption of minimally invasive transtubular transcortical approaches in neurosurgery, as of yet there have been no reports on the application of transtubular techniques in non-transcortical approaches or studies comparing brain retraction pressures between retraction modalities.

In comparing the retraction pressure induced by spatula and tubular retractors in a cadaveric model, we observed herein a substantial 57% decrease in mean brain retraction pressure in the tubular group compared to the spatula group in 6 different neurosurgical approaches collectively. Mean retraction distance was 50% less in the tubular retraction group and, upon visual inspection, cortical tearing was observed in 39% of cases following spatula retraction. Notably, tubular retractors demonstrated more consistent average retraction pressures

between approaches compared to spatula retractors, potentially indicative of increased stability. Furthermore, the tubular retractor provided nearly equal pressure distribution between its proximal and distal ends in the supraorbital, middle fossa, supracerebellar infratentorial, and retrosigmoid approaches. These findings confirm that tubular retraction provides reduced and symmetrically, or conically, distributed pressure onto retracted brain tissue, reduces the risk of parenchymal injury and cortical tearing, and can thus help decrease the incidence of retraction injury. Additionally, several other studies have shown that the blunt tip of the introducer provides progressive dilation that minimizes retraction injury to white matter tracts in transcortical or transcallosal corridors.[103,114,166]

The tubular retractor provided sufficient working space for standard bimanual surgical technique without obstruction of the visual field while using a microscope and/or an endoscope, and permitted sufficient surgical freedom (Figures 26 and 30). In addition, by limiting the range of instrument movement and protecting the surrounding tissues from instruments within the working channel, the tubular retractor may reduce inadvertent iatrogenic instrumental injury and thermal injury from the endoscope light or electrocautery.[115,146] Compared with freehand manipulation of the retractor, the use of self-retaining snake and extension arms may also decrease the risk of injury from torque effect (Figure 41).[101]

Figure 41. Fixation of the Tubular Retractor. Clinical integration of VBAS with self-retaining snake and extension arms in a transcortical approach.

The transparent construction of the retractor allowed for visual monitoring of the retracted surfaces, including any vessels in contact with the working channel, throughout the procedure and facilitated maintenance of anatomic orientation by allowing for good visualization of the surrounding anatomy through the walls of the channel. The smooth surfaces of the working channel allowed for easy insertion and removal without impingement of retracted tissues, and optimally distribute light so that it does not reflect back into the microscope or endoscope.

The tubular retractor provided sufficient space within the working channel to allow for simultaneous placement of an endoscope and any combination of 2 microsuction aspirators, microinstruments, bayoneted instruments, flexible instruments, and/or tube shaft instruments without visually obstructing the surgical field. Instruments could be interchanged easily and quickly—with the surrounding tissues protected from accidental injury. If the use of a larger instrument or device, including an ultrasonic aspirator, is necessary, a retractor with a larger distal port size may be used, but would necessitate a larger bone opening. Flexible, tube shaft, bayonetted, and long endoscopic instruments were the most efficient geometrically and ergonomically, and provided more space for movement within the retractor.

In all, the tubular retractor minimizes brain retraction, reduces compression of cortical venous networks, allows for constant monitoring of retracted tissues, lessens the potential for target shift, helps prevent inadvertent injury to surrounding tissues, provides a direct route to the surgical target, and allows for significantly smaller and less invasive skin incisions and boney openings, which have been associated with shorter recovery times, reduced hospital stays, and reduced costs (Figure 42).[130]

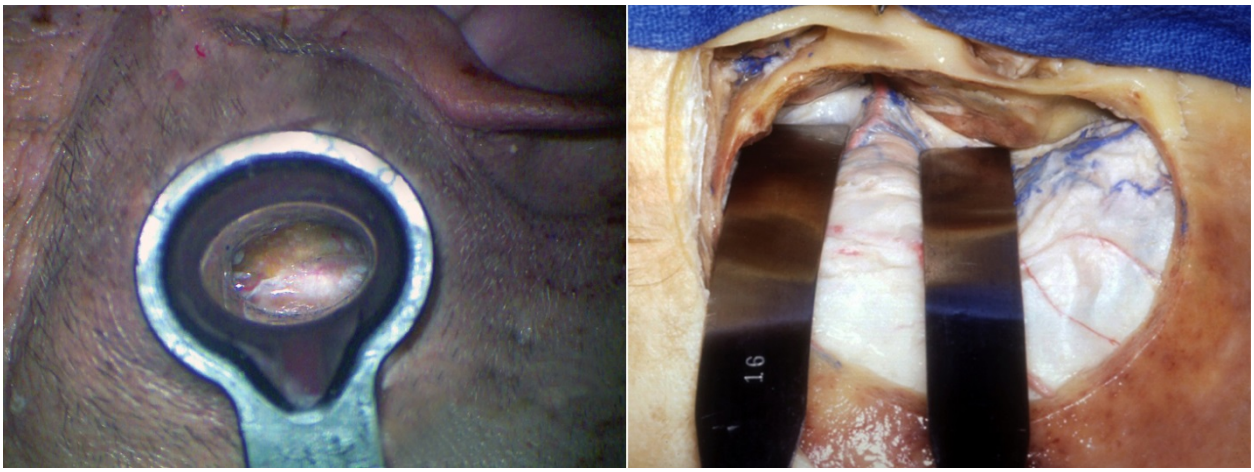

Figure 42. Transtubular versus Conventional Anterior Transpetrosal Craniotomy. Right image courtesy of the Rhoton Collection.

In examining the feasibility and applicability of transtubular approaches and techniques in neurosurgery, we found that tubular retractors provide a safe and effective conduit for the application of percutaneous minimally invasive approaches. Transtubular supraorbital, anterior transpetrosal, interhemispheric transcallosal, retrosigmoid, and supracerebellar infratentorial approaches were all successfully completed and represent feasible and effective corridors to their respective targets with ample surgical exposure, freedom, and maneuverability, and minimal parenchymal retraction. Drilling and navigating the complex anatomical structures of the skull base through the tubular retractor was possible, even in the extremely restricted corridors of the anterior transpetrosal approach.[160] The interhemispheric transcallosal approach further facilitated controlled aspiration of ventricular cerebrospinal fluid and formation of an air medium that provided better intraoperative visualization.[101,122] The use of a synthetic tumor model provided a means for more closely simulating clinical conditions and provided an additional method for quantitatively verifying the surgical applicability of transtubular approaches through confirmation of resection ability.

Adequate preoperative planning of the surgical trajectory and intraoperative navigation was critical for facilitating a safe, direct, and practicable surgical corridor. While the neuronavigation pointer was used without difficulty through the retractor (Figure 43), a tubular retractor system with integrated neuronavigation markers would greatly ease insertion and enable constant monitoring of position and trajectory relative to anatomical landmarks. Emerging technologies related to transtubular surgery, including integration of the tubular-specific trajectory into the planning software and use of robotic exoscopy will facilitate increased applications of transtubular techniques.[161–162] One of these technologies is BrightMatter™ from Synaptive Medical, an optical robotic exoscopy system designed for transtubular neurosurgery and coupled to a trajectory-centric planning and navigation system with integration of white matter tractography (Figure 44).

Figure 43. VBAS Integration with Neuronavigation.

The exoscopic robot system is a potential replacement for the surgical microscope that provides hands free movement of the camera and can automatically align to a surgical tool in the field. This device will allow for improved efficiency, as the surgeon is able to control visualization without letting go of the surgical instruments. While these systems are able to replace the traditional surgical microscope, especially with integration of stereoscopic displays, they still cannot offer the angled views provided by the endoscope, which in this study allowed for enhanced anatomic exposure of the target region and inspection for residual tumor.

Figure 44. Synaptive BrightMatter™. Synaptive Medical's integrated robotic exoscopy surgical camera and white matter tractographic navigation system for transtubular neurosurgery. Image courtesy of Synaptive Medical.

Despite the detailed multiangled anatomical exposure provided by the endoscope, surgeons should be extremely familiar with the associated anatomy, as well as the use of instruments through a tubular retractor, before attempting a transtubular approach. The

transtubular surgical field is substantially narrowed compared to conventional approaches and necessitates a thorough understanding of key surgical landmarks (Figure 45). Although the retractor provides a safe corridor for the approach, it should not provide the surgeon with a false sense of safety—awareness of the position and anatomical surroundings of each instrument is still paramount for preventing iatrogenic tissue damage. It is advisable to spend several hours practicing the use of different instruments to handle objects, such as small paper cubes and tissue paper, through the retractor in order to gain familiarity with transtubular techniques before attempting them. Despite the learning curve associated with transtubular techniques, the principles are mainly the same as those of microsurgery.[101,109,115]

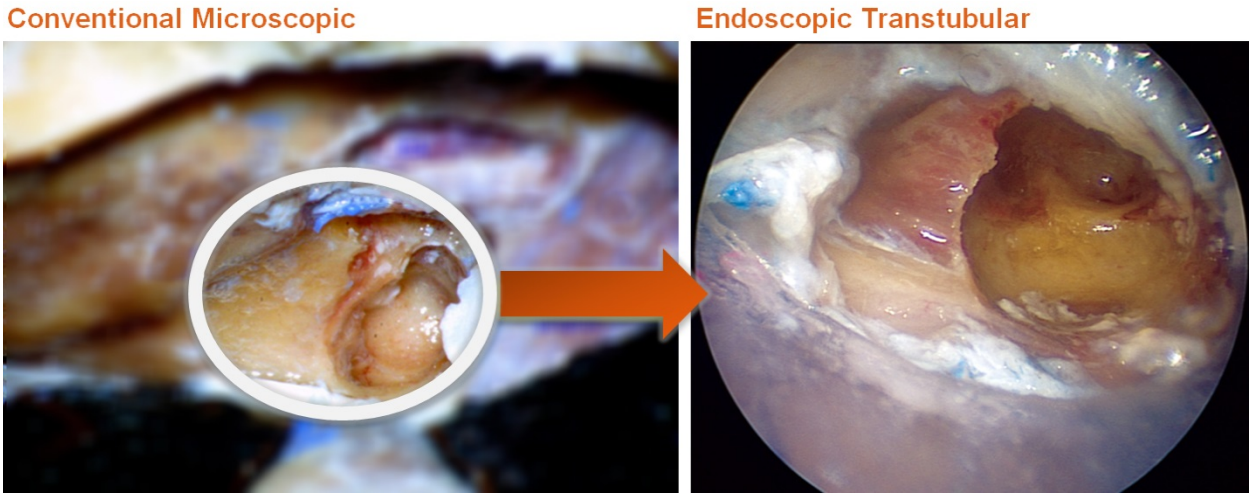

Figure 45. Reduced Field of View in Transtubular Neurosurgery.

Future tubular retractor designs may benefit from additional lengths, diameters, and shapes, as well as multiple beveled tip options for retraction along different surfaces. Further development of instruments and training devices specifically designed to accompany this system would contribute to the safety of this technique (Figure 46).

Figure 46. Synaptive Brightmatter™ Brain Simulator.

The use of on-demand 3D printing to produce patient-specific cranial prostheses for closure of transtubular minicraniectomies represents a feasible and novel technique that is rapid, simple, and inexpensive. The ability for the surgical team to easily build and incorporate a real-time form-fitting and patient-specific cranioprosthesis could help improve postoperative cosmetic appearances and mitigate the risk of post-cranioplasty complications.[158,163] Additionally, design and fabrication of patient-specific implants by clinical personnel would significantly lower associated costs and allow for wider use of custom designed implants, especially in developing regions. However, these findings must be further verified using clinically approved materials.

While the data reported herein on mean tubular retraction pressure is quite promising, additional studies are necessary to determine clinical tubular retraction dynamics. The use of more sophisticated sensors could help determine how tubular retraction pressure varies over time

in a clinical model, and the roles of cerebral profusion pressure and systemic intraoperative factors on retraction pressure and injury. Additionally, this study is limited by its cadaveric nature, the potential for brain atrophy and its effect on retraction distances, and the use of preserved and potentially stiffer tissue, even when reporting relative values. As transtubular neurosurgery likely represents the next incarnation of minimally invasive neurosurgery, and transtubular techniques are applied in various neurosurgical disciplines and subspecialties, continued research, training, and refinement are essential for the development of improved clinical proficiency and outcomes while furthering the development of these techniques.

CONCLUSION

This body of work establishes the safety and efficacy of minimally invasive transtubular neurosurgery. Application of tubular retractors significantly reduces brain retraction pressure in a range of neurosurgical approaches, results in less damage to retracted tissues, and provides a safe, valid, and transparent conduit for the application of microscopic and/or endoscopic miniaturized percutaneous approaches that can achieve improved cosmetic outcomes, while protecting surrounding tissues from inadvertent instrumental or thermal injury. Advances in neuronavigation and other supplementary surgical technologies will continue to expand the indications for tubular retraction in neurosurgery and will help pave the way for the eventual application of transtubular surgical robotics.

APPENDIX A

Timeline of Published Research on Tubular Retraction in Cranial Surgery

Year	First Author	Title
1988	Kelly PJ	The Stereotaxic Retractor in Computer-Assisted Stereotaxtic Microsurgery: Technical Note
1990	Otsuki T	Stereotactic Guiding Tube for Open-System Endoscopy: A New Approach for the Stereotactic Endoscopic Resection of Intra-Axial Brain Tumors
1991	Eiras J	Stereotactic Open Craniotomy And Laser Resection of Brain Tumors A Five Years Experience
1993	Ross DA	A Simple Stereotactic Retractor for Use with the Leksell Stereotactic System
1995	Cabbell KL	Stereotactic Microsurgical Craniotomy for the Treatment of Third Ventricular Colloid Cysts
1994	Barlas O	A Simple Stereotactic Retractor for Use with the Leksell System
1996	Cabell KL	Stereotactic Microsurgical Craniotomy for the Treatment of Third Ventricular Colloid Cysts
2002	Jho HD	Endoscopic Removal of Third Ventricular Tumors: A Technical Note
2004	Barlas O	Stereotactically Guided Microsurgical Removal of Colloid Cysts
2005	Harris AE	Microsurgical Removal of Intraventricular Lesions Using Endoscopic Visualization and Stereotactic Guidance
2006	Ogura K	New Microsurgical Technique for Intraparenchymal Lesions of the Brain: Transcylinder Approach
2008	Akai T	Intra-Parenchymal Tumor Biopsy Using Neuroendoscopy with Navigation
2008	Greenfield JP	Stereotactic Minimally Invasive Tubular Retractor System for Deep Brain Lesions
2008	Dorman JK	Tumor Resection Utilizing a Minimally Invasive Spinal Retractor with a Novel Cranial Adaptor
2009	Fahim DK	Transtubular Microendoscopic Approach for Resection of a Choroidal Arteriovenous Malformation
2009	Singh L	Cylindrical Channel Retractor for Intraventricular Tumour Surgery–A Simple and Inexpensive Device
2010	Ichinose T	Microroll Retractor for Surgical Resection of Brainstem Cavernomas
2010	Herrera SR	Use of Transparent Plastic Tubular Retractor in Surgery for Deep Brain Lesions: A Case Series
2011	Jo KW	Efficacy of Endoport-Guided Endoscopic Resection for Deep-Seated Brain Lesions
2011	Recinos PF	Use of a Minimally Invasive Tubular Retraction System for Deep-Seated Tumors in Pediatric Patients

2011	Raza SM	Minimally Invasive Trans-Portal Resection of Deep Intracranial Lesions
2012	Almenawer SA	Minimal Access to Deep Intracranial Lesions Using a Serial Dilatation Technique
2013	Cohen-Gadol AA	Minitubular Transcortical Microsurgical Approach for Gross Total Resection of Third Ventricular Colloid Cysts: Technique and Assessment
2014	Ajlan AM	Endoscopic Transtubular Resection of a Colloid Cyst
2015	Ding D	Endoport-Assisted Microsurgical Resection of Cerebral Cavernous Malformations
2015	Nagatani K	High-Definition Exoscope System for Microneurosurgery: Use Of an Exoscope in Combination with Tubular Retraction and Frameless Neuronavigation for Microsurgical Resection of Deep Brain Lesions
2015	Shoakazemi A	A 3D Endoscopic Transtubular Transcallosal Approach to the Third Ventricle
2015	Bernardo A	A Percutaneous Transtubular Middle Fossa Approach for Intracanalicular Tumors
2015	Akiyama Y	Rigid Endoscopic Resection of Deep-Seated or Intraventricular Brain Tumors
2015	Wang WH	Endoscopic Hematoma Evacuation in Patients with Spontaneous Supratentorial Intracerebral Hemorrhage
2015	Rymarczuk GN	Use of a Minimally Invasive Retractor System for Retrieval of Intracranial Fragments in Wartime Trauma
2015	Ding D	A Minimally Invasive Anterior Skull Base Approach for Evacuation of a Basal Ganglia Hemorrhage
2015	Przybylowski CJ	Endoport-Assisted Surgery for the Management of Spontaneous Intracerebral Hemorrhage
2016	Bander ED	Utility of Tubular Retractors to Minimize Surgical Brain Injury in the Removal of Deep Intraparenchymal Lesions: A Quantitative Analysis of FLAIR Hyperintensity and Apparent Diffusion Coefficient
2016	Eliyas JK	Minimally Invasive Transsulcal Resection of Intraventricular and Periventricular Lesions through a Tubular Retractor System: Multicentric Experience and Results
2016	Angileri FF	Fully Endoscopic Freehand Evacuation of Spontaneous Supratentorial Intraparenchymal Hemorrhage
2016	Hong CS	Comparison of Endoscope- versus Microscope-Assisted Resection of Deep-Seated Intracranial Lesions Using a Minimally Invasive Port Retractor System
2016	Ratre S	Microendoscopic Removal of Deep-Seated Brain Tumors Using Tubular Retractions System
2016	Eibach S	Less Traumatic Technique to Access Deep Brain Lesions with the “Doigt-De-Dieu”
2016	Kutlay M	Fully Endoscopic Resection of Intra-Axial Brain Lesions Using Neuronavigated Pediatric Anoscope
2017	Habboub G	A Novel Combination of Two Minimally Invasive Surgical Techniques in the Management of Refractory Radiation Necrosis: Technical Note
2017	White T	Frameless Stereotactic Insertion of Viewsite Brain Access System with Microscope-Mounted Tracking Device for Resection of Deep Brain Lesions: Technical Report

APPENDIX B

Vycor Medical ViewSite Brain Access System (VBAS) Sizing Chart

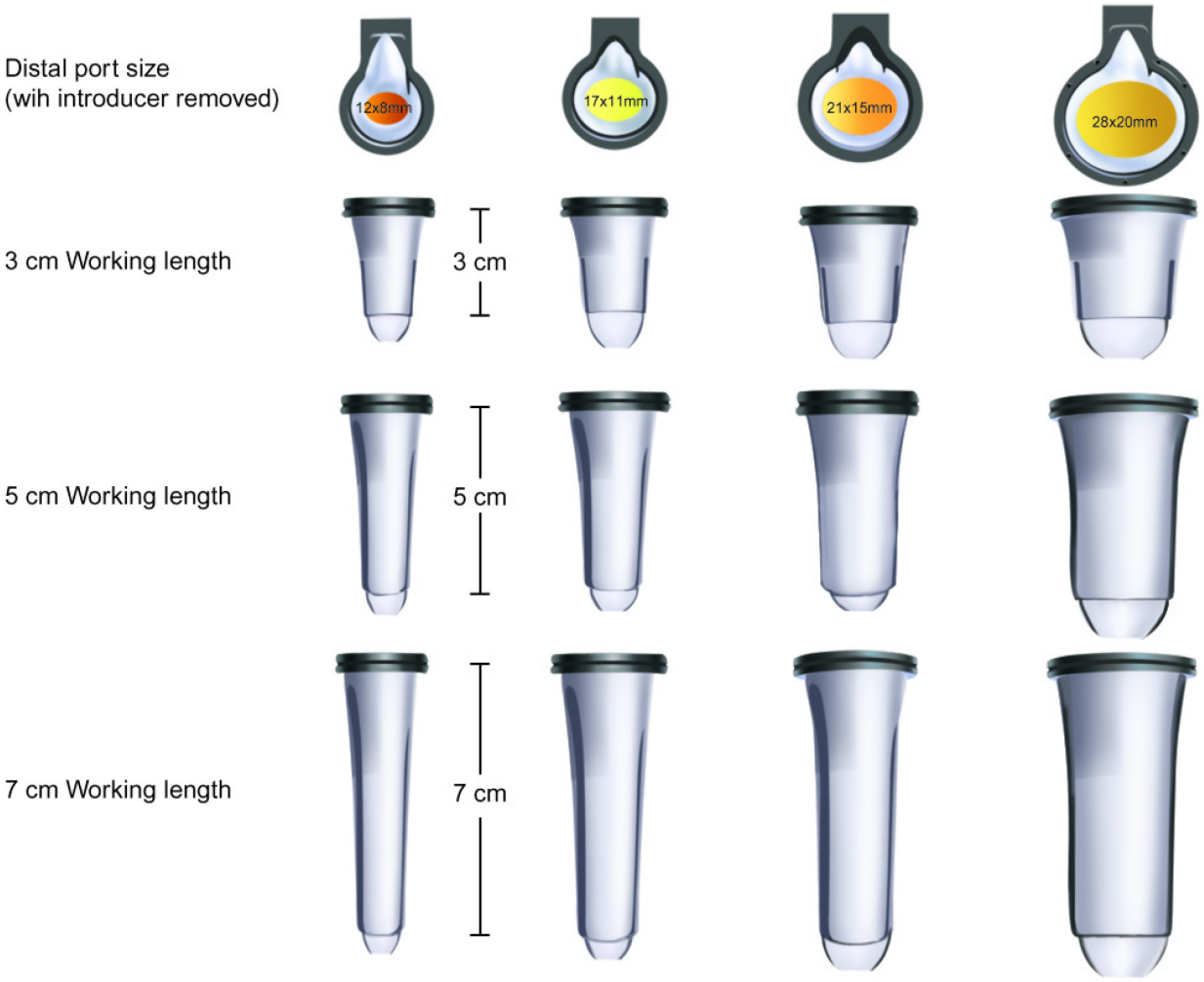

APPENDIX C

Petroclival Angles and Petroclival-Auditory Distance Findings

Patient No.	Midsagittal*-Petroclival Suture Distance (mm)	Lateral Petroclival Angle (°)†	Petroclival-Acoustic Distance (mm)	Trajectory Length (mm)
1	11	39	22	42
2	10	31	23	44
3	11	43	21	42
4	9	41	21	37
5	10	44	21	37
6	9	34	22	39
7	10	43	27	40
8	10	28	25	38
9	12	43	23	43
10	12	45	24	40
11	10	36	23	43
12	10	39	22	44
13	12	40	20	39
14	11	39	21	41
15	11	40	22	41
16	10	46	22	41
17	12	33	22	42
18	10	36	23	43
19	12	48	21	37
20	11	47	21	36
21	10	48	19	38
22	10	44	19	39
23	9	37	20	39
24	9	35	20	39
25	11	41	21	42
26	11	42	23	40
27	10	44	18	34
28	10	41	20	36
29	8	42	20	43
30	9	41	21	42
31	10	41	19	33
32	10	45	20	35
33	11	38	21	36
34	11	45	24	40
35	11	44	20	47
36	11	32	21	46
37	12	42	18	44
38	12	45	23	42
39	10	41	21	40
40	10	37	21	38
41	11	42	19	39
42	11	45	20	40
43	11	37	21	39
44	10	36	21	38
45	8	33	20	38
46	8	32	20	40
47	12	46	22	47
48	11	42	23	47
49	11	49	24	37
50	12	48	24	39
Mean*	**10 ± 1**	**41 ± 5**	**21 ± 2**	**40 ± 3**
Range	**8–12**	**28–49**	**18–27**	**33–47**

**The midsagittal line was placed between the nasion and the inion.*

†The true petroclival angle can calculated by adding 90° to the lateral petroclival angle.

REFERENCES

1. Assina R, Rubino S, Sarris CE, Gandhi CD, Prestigiacomo CJ. The History of Brain Retractors throughout the Development of Neurological Surgery. *Neurosurg Focus*. 2014;36(4):E8.

2. Kirkpatrick DB. The First Primary Brain-Tumor Operation. *J Neurosurg*. 1984;61(5):809–813.

3. Bennett H, Godlee RJ. Article 5110: Bennett and Godlee on Cerebral Tumor. In: Hart E, ed. *The London Medical Record: A Review of the Progress of Medicine, Surgery, Obstetrics and the allied sciences*. Volume XIV. London, UK: Smith, Elder, & CO.; 1886: 65–66.

4. Fraser A. *A Guide to Operations on the Brain London*. London, UK: Churchill; 1890.

5. Goodrich JT. History of Posterior Fossa Tumor Surgery. In: Özek MM, Cinalli G, Maixner W, Sainte-Rose C, eds. *Posterior Fossa Tumors in Children*. Cham, Switzerland: Springer International Publishing; 2015: 38.

6. Frazier CH. The Intracranial Surgery of the Fifth (Trigeminal) and the Eighth (Auditory) Nerves. In: Keen WW, Da Costa JC, eds. *Surgery, Its Principles and Practice: Vascular; Gynecology; Anesthesia; X-rays; Operative & Plastic; Infections; Legal Pathologic Relations; Hospital Organization*. Volume 5. Philadelphia, PA: W.B. Saunders Company; 1909.

7. Transactions of the Philadelphia Academy of Surgery. December 1, 1902: Stated Meeting. *Ann Surg*. 1903;37(3):456–462.

8. Horsley V. On The Technique of Operations on the Central Nervous System. *Br Med J*. 1906;2(2382):411–423.

9. Cushing H. A Method of Combining Exploration and Decompression for Cerebral Tumors which Prove to be Inoperable [originally published in *Surg Gynecol Obstet*. 1909;9:1–5]. Neurosurgical Classics–VI. *J Neurosurg*. 1963;20(4):368–369.

10. Dujovny M, Ibe O, Perlin A, Ryder T. Brain Retractor Systems. *Neurol Res*. 2010;32(7):675–683.

11. Yasargil MG. *Microneurosurgery*. New York, NY: George Thieme Verlag; 1984.

12. Greenberg IM. Self-Retaining Retractor and Handrest System for Neurosurgery. *Neurosurgery*. 1981;8(2):205–208.

13. Sugita K, Hirota T, Mizutani T, Mutsuga N, Shibuya M, Tsugane R. A Newly Designed Multipurpose Microneurosurgical Head Frame. Technical Note. *J Neurosurg*. 1978;48(4):656–675.

14. Yokon A, Sugita K, Kobayashi S. Clinical Study of Brain Retraction in Different Approaches and Disease. *Acta Neurochir (Wien)*. 1987;87(3–4):134–139.

15. Mangiardi JR, inventor; Vycor Medical LLC, assignee. Surgical Access Methods for Use with Delicate Tissues. US patent 8,409,083 B2. April 2, 2013.

16. Ferrara-Hoffman DL, Krizman SJ: Neurosurgery. In: Rothrock JC, ed. *Alexander's Care of the Patient in Surgery*. 14th ed. St. Louis, MS: Elsevier Mosby; 2011.

17. Schulte RR, Portnoy HD, inventors; Heyer-Schulte Corporation, assignee. Retractor for Soft Tissue for Example Brain Tissue. US patent 3,882,855. May 13, 1975.

18. Hansen KV, Brix L, Pedersen CF, Haase JP, Larsen OV. Modelling Of Interaction between a Spatula and a Human Brain. *Med Image Anal*. 2004;8(1):23–33.

19. Andrews RJ, Bringas JR. A Review of Brain Retraction and Recommendations for Minimizing Intraoperative Brain Injury. *Neurosurgery*. 1993;33(6):1052–1064.

20. Albin MS, Bunegin L, Bennett MH, Dujovny M, Jannetta PJ. Physiopathological Responses to Graded Brain Retractor Pressure Under Induced Hypotension. *Proc Am Assoc Neurol Surg*. 1976; 23.

21. Bennett MH, Albin MS, Bunegin L, Dujovny M, Hellstrom H, Jannetta PJ. Evoked Potential Changes During Brain Retraction In Dogs. *Stroke*. 1977;8(4):487–492.

22. Zhong J, Dujovny M, Perlin AR, Perez-Arjona E, Park HK, Diaz FG. Brain Retraction Injury. *Neurol Res*. 2003;25(8):831–838.

23. Lamprich BK, Miga MI. Analysis of Model-Updated MR Images to Correct for Brain Deformation Due to Tissue Retraction. Paper presented at: Proc. SPIE 5029, Medical Imaging 2003: Visualization, Image-Guided Procedures, and Display; May 30, 2003; San Diego, CA

24. Xu W, Mellergård P, Ungerstedt U, Nordström CH. Local Changes in Cerebral Energy Metabolism Due to Brain Retraction During Routine Neurosurgical Procedures. *Acta Neurochir (Wien)*. 2002;144(7):679–683.

25. Kasama A, Kanno T. A Pitfall in the Interhemispheric Translamina Terminalis Approach for the Removal of a Craniopharyngioma. Significance of Preserving Draining Veins. Part II. Experimental Study. *Surg Neurol*. 1989;32(2):116–120.

26. Sindou M. The "Dangerous" Intracranial Veins. In: Sindou M, ed. *Practical Handbook of Neurosurgery: From Leading Neurosurgeons, Volume 1*. Vienna, Austria: Springer Vienna; 2009:71–83.

27. Andrew SL, Liu S, Beeman S, Sankar T, et al. Brain Retraction and Thickness of Cerebral Neocortex: An Automated Technique for Detecting Retraction-Induced Anatomic Changes Using Magnetic Resonance Imaging. *Neurosurgery*. 2010;67(3 Suppl Operative):ons277–282.

28. Albin MS, Bunegin L, Helsel P, Marlin A, Babinski M. Intracranial Pressure and Regional Cerebral Blood Flow Responses to Experimental Brain Retraction Pressure. In: Shulman K, Marmarou A, Miller JD, Becker DP, Hochwald GM, Brock M eds. *Intracranial Pressure IV*. Heidelberg, Germany: Springer Berlin Heidelberg; 1980:131–135.

29. Numoto M, Donaghy RMP. Effects of Local Pressure on Cortical Electrical Activity and Cortical Vessels in the Dog. *J Neurosurg*. 1970;33(4):381–387.

30. Miller JD, Stanek AE, Langfitt TW. Cerebral Blood Flow Regulation During Experimental Brain Compression. *J Neurosurg*. 1973;39(2):186–196.

31. Kaido T, Nakase H, Nagata K, Otsuka H, Sakaki T. Intermittent Isometric Exposure Prevents Brain Retraction Injury Under Venous Circulatory Impairment. *Neurol Res*. 2001;23(7):739–744.

32. Rosenørn J. Self-Retaining Brain Retractor Pressure During Intracranial Procedures. *Acta Neurochir (Wien)*. 1987;85(1–2):17–22.

33. Lownie S, Wu X, Karlik S, Gelb AW. Brain Retractor Edema During Induced Hypotension: The Effect of the Rate of Return of Blood Pressure. *Neurosurgery*. 1990;27(6):901–906.

34. Rosenørn J, Diemer NH. Reduction of Regional Cerebral Blood Flow During Brain Retraction Pressure in the Rat. *J Neurosurg*. 1982;56(6):826–829.

35. Andrews RJ, Muto RP. Retraction Brain Ischaemia: Cerebral Blood Flow, Evoked Potentials, Hypotension and Hyperventilation in a New Animal Model. *Neurol Res*. 1992;14(1):12–18.

36. Hongo K, Kobayashi S, Yokoh A, Sugita K. Monitoring Retraction Pressure on the Brain. An Experimental and Clinical Study. *J Neurosurg*. 1987;66(2):270–275.

37. Rosenørn J, Diemer N. The Risk of Cerebral Damage During Graded Brain Retractor Pressure in the Rat. *J Neurosurg*. 1985;63(4):608–611.

38. Rosenørn J, Diemer NH. The Influence of the Profile of Brain Retractors on Regional Cerebral Blood Flow in the Rat. *Acta Neurochir (Wien)*. 1987;87(3–4):140–143.

39. Spatz M, Yasuma Y, Strasser A, McCarron RM. Cerebral Postischemic Hypoperfusion is Mediated by ETA Receptors. *Brain Res*. 1996;726(1–2):242–246.

40. Stahel PF, Morganti-Kossmann MC, Kossmann T. The Role of the Complement System in Traumatic Brain Injury. *Brain Res Brain Res Rev*. 1998;27(3):243–256.

41. Rosenørn J. The Risk of Ischaemic Brain Damage During the use of Self-Retaining Brain Retractors. *Acta Neurol Scand*. 1989; 79(Suppl. 120):1–30.

42. Hoffman WE, Charbel FT, Portillo GG, Edelman G, Ausman JI. Regional Tissue pO2, pCO2, pH and Temperature Measurement. *Neurol Res*. 1998;20(Suppl 1):S81–S84.

43. Mendelowitsch A, Langemann H, Alessandri B, Kanner A, Landolt H, Gratzl O. Microdialytic Monitoring Of The Cortex During Neurovascular Surgery. *Acta Neurochir Suppl*. 1996;67:48–52.

44. Buchthal A, Belopavlovic M. Somatosensory Evoked Potentials in Cerebral Aneurysm Surgery. *Eur J Anaesthesiol*. 1992;9(6):493–497.

45. Viñas FC, Zamorano L, Mueller RA, et al. [15O]-Water PET and Intraoperative Brain Mapping: A Comparison in the Localization of Eloquent Cortex. *Neurol Res*. 1997;19(6):601–608.

46. Ningyi J, Jihui L, Suocheng Guo, Jiugen L, Xianping L, Bin L. Assessment of Brain Retraction Injury from Tumor Operation with $^{99}Tc^{m}$-ECD Brain SPECT Imaging. *Chin J Nucl Med*. 1999;19(4):216–218.

47. Spetzler RF, Sanai N. The Quiet Revolution: Retractorless Surgery for Complex Vascular and Skull Base Lesions. *J Neurosurg*. 2012;116(2):291–300.

48. Schaller C, Klemm E, Haun D, Schramm J, Meyer B. The Transsylvian Approach is "Minimally Invasive" but Not "Atraumatic". *Neurosurgery*. 2002;51(4):971–977.

49. Bell BA, Symon L, Branston NM. CBF and Time Thresholds for the Formation of Ischemic Cerebral Edema, and Effect of Reperfusion in Baboons. *J Neurosurg*. 1985;62(1):31–41.

50. Laha RK, Dujovny M, Rao S, et al. Cerebellar Retraction: Significance and Sequelae. *Surg Neurol*. 1979;12(3):209–215.

51. Yundt KD, Grubb RL, Diringer MN, Powers WJ. Cerebral Hemodynamic and Metabolic Changes Caused by Brain Retraction after Aneurysmal Subarachnoid Hemorrhage. *Neurosurgery*. 1997;40(3):442–451.

52. Krayenbühl N, Oinas M, Erdem E, Krisht AF. The Impact of Minimizing Brain Retraction in Aneurysm Surgery: Evaluation Using Magnetic Resonance Imaging. *Neurosurgery*. 2011;69(2):344–348.

53. Krayenbühl N, Erdem E, Oinas M, Krisht AF. Symptomatic and Silent Ischemia Associated with Microsurgical Clipping of Intracranial Aneurysms: Evaluation with Diffusion-Weighted MRI. *Stroke*. 2009;40(1):129–133.

54. Yoshimoto K, Araki Y, Amano T, Matsumoto K, Nakamizo A, Sasaki T. Clinical Features and Pathophysiological Mechanism of the Hemianoptic Complication After the Occipital Transtentorial Approach. *Clin Neurol Neurosurg*. 2013;115(8):1250–1256.

55. Ramaurthi R, Sridhar K, Vasudevan MC, eds. *Textbook of Operative Neurosurgery*. Volume 1. New Delhi, India: BI Publications Pvt Ltd; 2005.

56. Kim HH, Johnston R, Wiet RJ, Kumar A. Long-Term Effects of Cerebellar Retraction in the Microsurgical Resection of Vestibular Schwannomas. *Laryngoscope*. 2004;114(2):323–266.

57. Burkhart CS, Strebel SP, Steiner LA. Altered Mental Status in Neurosurgical Critical Care. In: Brambrink AM, Kirsch JR, eds. *Essentials of Neurosurgical Anesthesia & Critical Care*. New York, NY: Springer New York; 2012:735.

58. Fukumachi A, Koizumi H, Nukui H. Postoperative Intracerebral Hemorrhages: A Survey of Computed Tomographic Findings After 1074 Intracranial Operations. *Surg Neurol*. 1985;23(6):575–580.

59. Kalfas IH, Little JR. Postoperative Hemorrhage: A Survey of 4992 Intracranial Procedures. *Neurosurgery*. 1988;23(3):343–347.

60. Rice BJ, Peerless SJ, Drake CG. Surgical Treatment of Unruptured Aneurysms of the Posterior Circulation. *J Neurosurg*. 1990;73(2):165–173.

61. Sekhar LN, Nanda A, Sen CN, Snyderman CN, Janecka IP. The Extended Frontal Approach to Tumors of the Anterior, Middle, and Posterior Skull Base. *J Neurosurg*. 1992;76(2):198–206.

62. Sekhar LN, Pomeranz S, Janecka IP, Hirsch B, Ramasastry BH. Temporal Bone Neoplasms: A Report on 20 Surgically Treated Cases. *J Neurosurg*. 1992;76(4):578–587.

63. Yokoh A, Sugita K, Kobayashi S. Clinical Study of Brain Retraction in Different Approaches and Diseases. *Acta Neurochir (Wien)*. 1987;87(3–4):134–139.

64. Spetzler RF, Daspit CP, Pappas CTE. The Combined Supra- and Infratentorial Approach for Lesions of the Petrous and Clival Regions: Experience with 46 Cases. *J Neurosurg*. 1992;76(4):588–599.

65. Proust F, Hannequin D, Langlois O, Creissard P. Causes Of Morbidity and Mortality After Ruptured Aneurysm Surgery in a Series of 230 Patients: The Importance of Control Angiography. *Stroke*. 1995;26(9):1553–1557.

66. Nazzaro JM, Shults WT, Neuwelt EA. Neuro-Ophthalmological Function of Patients with Pineal Region Tumors Approached Transtentorially in the Semisitting Position. *J Neurosurg*. 1992;76(5):746–751.

67. Jenkins A, Hadley DM, Teasdale GM, Condon B, Macpherson P, Patterson J. Magnetic Resonance Imaging of Acute Subarachnoid Hemorrhage. *J Neurosurg*. 1988;68(5):731–736.

68. Romner B, Sonesson B, Ljunggren B, Brandt L, Säveland H, Holtås S. Late Magnetic Resonance Imaging Related to Neurobehavioral Functioning After Aneurysmal Subarachnoid Hemorrhage. *Neurosurgery*. 1989;25(3):390–397.

69. Kivisaari RP, Salonen O, Ohman J. Basal Brain Injury in Aneurysm Surgery. *Neurosurgery*. 2000;46(5):1070–1076.

70. *AANS National Neurosurgical Procedural Statistics*. Rolling Meadows, IL: American Association of Neurological Surgeons; 2013.

71. Iyer RV, Likhith AM, Mclean JA, Perera S, Davis CH. Audit of Operating Theatre Time Utilization in Neurosurgery. *Br J Neurosurg*. 2004;18(4):333–337.

72. Di Maio S, Ramanathan D, Garcia-Lopez R, et al. Evolution and Future of Skull Base Surgery: The Paradigm of Skull Base Meningiomas. *World Neurosurg*. 2012;78(3–4):260–275.

73. Teo C. The Concept Of Minimally Invasive Neurosurgery. *Neurosurg Clin N Am*. 2010;21(4):583–584, v.

74. Perneczky A, Reisch R. *Keyhole Approaches in Neurosurgery: Volume I Concept and Surgical Technique*. Vienna, Austria: Springer-Verlag; 2008.

75. Proctor MR, Black PM, eds. *Minimally Invasive Neurosurgery*. Totowa, New Jersey: Humana Press; 2005.

76. Liu JK, Das K, Weiss MH, Laws ER, Couldwell WT. The History and Evolution of Transsphenoidal Surgery. *J Neurosurg*. 2001;95(6):1083–1096.

77. Carrau RL, Jho HD, Ko Y. Transnasal-Transsphenoidal Endoscopic Surgery of yhe Pituitary Gland. *Laryngoscope*. 1996;106(7):914–918.

78. Jho HD, Carrau RL, Ko Y, Daly MA. Endoscopic Pituitary Surgery: An Early Experience. *Surg Neurol*. 1997;47(3):213–222.

79. Alfieri A. Endoscopic Endonasal Transsphenoidal Approach to the Sellar Region: Technical Evolution of the Methodology and Refinement of a Dedicated Instrumentation. *J Neurosurg Sci*. 1999;43(2):85–92.

80. Prevedello DM, Doglietto F, Jane JA, Jagannathan J, Han J, Laws ER. History of Endoscopic Skull Base Surgery: Its Evolution and Current Reality. *J Neurosurg*. 2007;107(1):206–213.

81. Hardy J. [Surgery of the Pituitary Gland, Using the Trans-Sphenoidal Approach. Comparative Study of 2 Technical Methods]. *Union Med Can*. 1967;96(6):702–712.

82. Perneczky A, Fries G. Endoscope-Assisted Brain Surgery: Part 1--Evolution, Basic Concept, and Current Technique. *Neurosurgery*. 1998;42(2):219–225.

83. Fries G, Perneczky A. Endoscope-Assisted Brain Surgery: Part 2--Analysis of 380 Procedures. *Neurosurgery*. 1998;42(2):226–232.

84. Grunert P. From the Idea to its Realization: The Evolution of Minimally Invasive Techniques in Neurosurgery. *Minim Invasive Surg*. 2013;2013:171369.

85. Fitzpatrick JM, Wickham JE. Minimally Invasive Surgery. *Br J Surg*. 1990;77(7):721–722.

86. Bauer BL, Hellwig D. Preface. In: Bauer BL, Hellwig D, eds. *Minimally Invasive Neurosurgery I*. Vienna, Austria: Springer Vienna; 1992.

87. Badie B, Brooks N, Souweidane MM. Endoscopic and Minimally Invasive Microsurgical Approaches for Treating Brain Tumor Patients. *J Neurooncol*. 2004;69(1–3):209–219.

88. Lanzino G. Retractorless Brain Surgery. *J Neurosurg*. 2012;116(2):290.

89. Kelly PJ, Goerss SJ, Kall BA. The Stereotaxic Retractor in Computer-Assisted Stereotaxic Microsurgery. Technical Note. *J Neurosurg*. 1988;69(2):301–306.

90. Gildenberg PL. Stereotactic Surgery: Applications in Neurologic Disease. *Semin Neurol*. 1989;9(3):249–256.

91. Otsuki T, Jokura H, Yoshimoto T. Stereotactic Guiding Tube for Open-System Endoscopy: A New Approach for the Stereotactic Endoscopic Resection of Intra-Axial Brain Tumors. *Neurosurgery*. 1990;27(2):326–330.

92. Faubert C, Caspar W. Lumbar Percutaneous Discectomy. Initial Experience in 28 Cases. *Neuroradiology*. 1991;33(5):407–410.

93. Thongtrangan I, Le H, Park J, Kim DH. Minimally Invasive Spinal Surgery: A Historical Perspective. *Neurosurg Focus*. 2004;16(1):E13.

94. Oppenheimer JH, Decastro I, Mcdonnell DE. Minimally Invasive Spine Technology and Minimally Invasive Spine Surgery: A Historical Review. *Neurosurg Focus*. 2009;27(3):E9.

95. Evins AI, Banu MA, Njoku I, et al. Endoscopic Lumbar Foraminotomy. *J Clin Neurosci*. 2015;22(4):730–734.

96. Eiras J, Alberdi J, Carcavilla LI, Gomez J, Cantero J. Stereotactic Open Craniotomy and Laser Resection of Brain Tumours. A Five Years Experience. *Acta Neurochir Suppl (Wien)*. 1991;52:15–18.

97. Ross DA. A Simple Stereotactic Retractor for Use with the Leksell Stereotactic System. *Neurosurgery*. 1993;32(3):475–476.

98. Barlas O. A Simple Stereotactic Retractor for Use with the Leksell System. *Neurosurgery*. 1994;34(2):381.

99. Cabbell KL, Ross DA. Stereotactic Microsurgical Craniotomy for the Treatment of Third Ventricular Colloid Cysts. *Neurosurgery*. 1996;38(2):301–307.

100. Barlas O, Karadereler S. Stereotactically Guided Microsurgical Removal Of Colloid Cysts. *Acta Neurochir (Wien)*. 2004;146(11):1199–1204.

101. Harris AE, Hadjipanayis CG, Lunsford LD, Lunsford AK, Kassam AB. Microsurgical Removal of Intraventricular Lesions Using Endoscopic Visualization and Stereotactic Guidance. *Neurosurgery*. 2005;56(1 Suppl):125–132.

102. Schwartz TH, Anand VK. The Endoscopic, Transsphenoidal Transplanum, Transtuberculum Approach to the Suprasellar Cistern. In: Anand VK, Schwartz TH, eds.

Practical Endoscopic Skull Base Surgery. San Diego, CA: Plural Publishing; 2007:105–122.

103. Greenfield JP, Cobb WS, Tsouris AJ, Schwartz TH. Stereotactic Minimally Invasive Tubular Retractor System for Deep Brain Lesions. Neurosurgery. 2008;63(4 Suppl 2):334–340.
104. Akai T, Shiraga S, Sasagawa Y, Okamoto K, Tachibana O, Lizuka H. Intra-Parenchymal Tumor Biopsy Using Neuroendoscopy with Navigation. *Minim Invasive Neurosurg*. 2008;51(2):83–86.
105. Kassam AB, Engh JA, Mintz AH, Prevedello DM. Completely Endoscopic Resection of Intraparenchymal Brain Tumors. *J Neurosurg*. 2009;110(1):116–123.
106. Herrera SR, Shin JH, Chan M, Kouloumberis P, Goellner E, Slavin KV. Use of Transparent Plastic Tubular Retractor in Surgery for Deep Brain Lesions: A Case Series. *Surg Technol Int*. 2010;19:47–50.
107. Recinos PF, Raza SM, Jallo GI, Recinos VR. Use of a Minimally Invasive Tubular Retraction System for Deep-Seated Tumors in Pediatric Patients. *J Neurosurg Pediatr*. 2011;7(5):516–521.
108. Jo KW, Shin HJ, Nam DH, et al. Efficacy of Endoport-Guided Endoscopic Resection for Deep-Seated Brain Lesions. *Neurosurg Rev*. 2011;34(4):457–463.
109. Raza SM, Recinos PF, Avendano J, Adams H, Jallo GI, Quinones-hinojosa A. Minimally Invasive Trans-Portal Resection of Deep Intracranial Lesions. *Minim Invasive Neurosurg*. 2011;54(1):5–11.

110. Almenawer SA, Crevier L, Murty N, Kassam A, Reddy K. Minimal Access to Deep Intracranial Lesions Using a Serial Dilatation Technique: Case-Series and Review of Brain Tubular Retractor Systems. *Neurosurg Rev*. 2013;36(2):321–330.

111. Cohen-Gadol AA. Minitubular Transcortical Microsurgical Approach for Gross Total Resection of Third Ventricular Colloid Cysts: Technique and Assessment. *World Neurosurg*. 2013;79(1):207.e7–10.

112. Ajlan AM, Kalani MA, Harsh GR. Endoscopic Transtubular Resection of a Colloid Cyst. *Neurosciences (Riyadh)*. 2014;19(1):43–46.

113. Ding D, Starke RM, Crowley RW, Liu KC. Endoport-Assisted Microsurgical Resection of Cerebral Cavernous Malformations. *J Clin Neurosci*. 2015;22(6):1025–1029.

114. Bander ED, Jones SH, Kovanlikaya I, Schwartz TH. Utility of Tubular Retractors to Minimize Surgical Brain Injury in the Removal of Deep Intraparenchymal Lesions: A Quantitative Analysis of FLAIR Hyperintensity and Apparent Diffusion Coefficient Maps. *J Neurosurg*. 2016;124(4):1053–1060.

115. Shoakazemi A, Evins AI, Burrell JC, Stieg PE, Bernardo A. A 3D Endoscopic Transtubular Transcallosal Approach to the Third Ventricle. *J Neurosurg*. 2015;122(3):564–573.

116. Eliyas JK, Glynn R, Kulwin CG, et al. Minimally Invasive Transsulcal Resection of Intraventricular and Periventricular Lesions through a Tubular Retractor System: Multicentric Experience and Results. *World Neurosurg*. 2016;90:556–564.

117. Hong CS, Prevedello DM, Elder JB. Comparison of Endoscope- Versus Microscope-Assisted Resection of Deep-Seated Intracranial Lesions Using a Minimally Invasive Port Retractor System. *J Neurosurg*. 2016;124(3):799–810.

118. Chakravarthia SS, Zbacnikb A, Jennings J, et al. White Matter Tract Recovery Following Medial Temporal Lobectomy and Selective Amygdalohippocampectomy for Tumor Resection via a ROVOT-M Port-Guided Technique: A Case Report and Review of Literature. *Interdiscip Neurosurg*. 2016;6:55–61.

119. Scranton RA, Fung SH, Britz GW. Transulcal Parafascicular Minimally Invasive Approach to Deep and Subcortical Cavernomas: Technical Note. *J Neurosurg*. 2016;125(6):1360–1366.

120. Akiyama Y, Wanibuchi M, Mikami T, et al. Rigid Endoscopic Resection of Deep-Seated or Intraventricular Brain Tumors. *Neurol Res*. 2015;37(3):278–282.

121. Tao X, Siyi W, Xiaoyi C, et al. [Microsurgical Resection for Lateral Ventricular Meningiomas with Neuronavigation and Tubular Retractor System]. *Chin J Neurosurg*. 2015;31(4):332–336.

122. Jho HD, Alfieri A. Endoscopic Removal of Third Ventricular Tumors: A Technical Note. *Minim Invasive Neurosurg*. 2002;45(2):114–119.

123. Ogura K, Tachibana E, Aoshima C, Sumitomo M. New Microsurgical Technique for Intraparenchymal Lesions of the Brain: Transcylinder Approach. *Acta Neurochir (Wien)*. 2006;148(7):779–785.

124. Fahim DK, Relyea K, Nayar VV, et al. Transtubular Microendoscopic Approach for Resection of a Choroidal Arteriovenous Malformation. *J Neurosurg Pediatr*. 2009;3(2):101–104.

125. Singh L, Agrawal N. Cylindrical Channel Retractor for Intraventricular Tumour Surgery—A Simple and Inexpensive Device. *Acta Neurochir (Wien)*. 2009;151(11):1493–1497.

126. Ichinose T, Goto T, Morisako H, Takami T, Ohata K. Microroll Retractor for Surgical Resection of Brainstem Cavernomas. *World Neurosurg*. 2010;73(5):520–522.

127. Ratre S, Yadav YR, Parihar VS, Kher Y. Microendoscopic Removal of Deep-Seated Brain Tumors Using Tubular Retraction System. *J Neurol Surg A Cent Eur Neurosurg*. 2016;77(4):312–320.

128. Kutlay M, Kural C, Solmaz I, et al. Fully Endoscopic Resection of Intra-Axial Brain Lesions Using Neuronavigated Pediatric Anoscope. *Turk Neurosurg*. 2016;26(4):491–499.

129. Jo KI, Chung SB, Jo KW, Kong DS, Seol HJ, Shin HJ. Microsurgical Resection of Deep-Seated Lesions Using Transparent Tubular Retractor: Pediatric Case Series. *Childs Nerv Syst*. 2011;27(11):1989–1994.

130. Wang WH, Hung YC, Hsu SP, et al. Endoscopic Hematoma Evacuation in Patients With Spontaneous Supratentorial Intracerebral Hemorrhage. *J Chin Med Assoc*. 2015;78(2):101–107.

131. Ding D, Przybylowski CJ, Starke RM, et al. A Minimally Invasive Anterior Skull Base Approach for Evacuation of a Basal Ganglia Hemorrhage. *J Clin Neurosci*. 2015;22(11):1816–1819.

132. Przybylowski CJ, Ding D, Starke RM, Webster crowley R, Liu KC. Endoport-Assisted Surgery for the Management of Spontaneous Intracerebral Hemorrhage. *J Clin Neurosci*. 2015;22(11):1727–1732.

133. Angileri FF, Esposito F, Priola SM, et al. Fully Endoscopic Freehand Evacuation of Spontaneous Supratentorial Intraparenchymal Hemorrhage. *World Neurosurg*. 2016;94:268–272.

134. Chen JW, Paff MR, Abrams-alexandru D, Kaloostian SW. Decreasing the Cerebral Edema Associated with Traumatic Intracerebral Hemorrhages: Use of a Minimally Invasive Technique. *Acta Neurochir Suppl*. 2016;121:279–84.

135. Rymarczuk GN, Davidson L, Severson MA, Armonda RA. Use of a Minimally Invasive Retractor System for Retrieval of Intracranial Fragments in Wartime Trauma. *World Neurosurg*. 2015;84(4):1055–1061.

136. Kassam AB. Evaluation of Minimally Invasive Subcortical Parafascicular Access for Clot Evacuation (MiSPACE). In: ClinicalTrials.gov [Internet]. Bethesda (MD): National Library of Medicine (US). 2014- [cited 2017 Feb 1]. Available from: https://clinicaltrials.gov/show/NCT02331719 NLM Identifier: NCT02331719.

137. OSF Healthcare System. Clinical Outcomes Following Parafascicular Surgical Evacuation of Intracerebral Hemorrhage: A Pilot Study (MISPACE). In: ClinicalTrials.gov [Internet]. Bethesda (MD): National Library of Medicine (US). 2013- [cited 2017 Feb 1]. Available from: https://clinicaltrials.gov/show/NCT01971359 NLM Identifier: NCT01971359.

138. Fiorella D, Arthur A, Bain M, Mocco J. Minimally Invasive Surgery for Intracerebral and Intraventricular Hemorrhage: Rationale, Review of Existing Data and Emerging Technologies. *Stroke*. 2016;47(5):1399–1406.

139. Ritsma B, Kassam A, Dowlatshahi D, Nguyen T, Stotts G. Minimally Invasive Subcortical Parafascicular Transsulcal Access for Clot Evacuation (Mi SPACE) for Intracerebral Hemorrhage. *Case Rep Neurol Med.* 2014;2014:102307.

140. Ziai W, Nyquist P, Hanley DF. Surgical Strategies for Spontaneous Intracerebral Hemorrhage. *Semin Neurol*. 2016;36(3):261–268.

141. Kim H, Edwards NJ, Choi HA, Chang TR, Jo KW, Lee K. Treatment Strategies to Attenuate Perihematomal Edema in Patients With Intracerebral Hemorrhage. *World Neurosurg*. 2016;94:32–41.

142. Britz GW, Kassam A, Labib M, et al. Abstract W MP120: Minimally Invasive Subcortical Parafascicular Access for Clot Evacuation. A Paradigm Shift. *Stroke*. 2015;46 (Suppl 1):AWMP120.

143. Moore NZ, Bain M. Minimally Invasive Hemorrhage Evacuation. *World Neurosurg*. 2016;89:713–715.

144. Osada H, Nagatani K, Toyooka T, et al. [Exoscope-Assisted Surgery for Deep-Seated Intraparenchymal Tumor]. *Jpn J Neurosurg*. 2015;24(9):623–631.

145. Nagatani K, Takeuchi S, Feng D, Mori K, Day JD. [High-Definition Exoscope System for Microneurosurgery: Use of an Exoscope in Combination with Tubular Retraction and Frameless Neuronavigation for Microsurgical Resection of Deep Brain Lesions]. *No Shinkei Geka*. 2015;43(7):611–617.

146. Bernardo A, Evins AI, Tsiouris AJ, Stieg PE. A Percutaneous Transtubular Middle Fossa Approach for Intracanalicular Tumors. *World Neurosurg*. 2015;84(1):132–146.

147. Vycor ViewSite Brain Access System (VBAS) [package insert]. Boca Raton, FL: Vycor Medical Inc.; 2013.

148. NICO BrainPath and Accessories [510(k) Summary]. Indianapolis, IN: NICO Corporation; 2015.

149. Yi-ning Z, Xiao-lei C. Endoscopic Treatment of Hypertensive Intracerebral Hemorrhage: A Technical Review. *Chron Dis Transl Med*. 2016;2(3):140–146.

150. Tekscan, Inc. *ELF™ User Manual: Single Handle, Multi-Handle, Wireless, and HiSpeed Systems v. 4.3x (Rev N)*. South Boston, MA: Tekscan, Inc.; 2015.

151. Brimacombe JM, Wilson DR, Hodgson AJ, Ho KC, Anglin C. Effect of Calibration Method on Tekscan Sensor Accuracy. *J Biomech Eng*. 2009;131(3):034503.

152. Gragnaniello C, Nader R, Van doormaal T, et al. Skull Base Tumor Model. *J Neurosurg*. 2010;113(5):1106–1111.

153. Baidya NB, Berhouma M, Ammirati M. Endoscope-Assisted Retrosigmoid Resection of a Medium Size Vestibular Schwannoma Tumor Model: A Cadaveric Study. *Clin Neurol Neurosurg*. 2014;119:35–38.

154. Abdel aziz KM, Sanan A, Van loveren HR, Tew JM, Keller JT, Pensak ML. Petroclival Meningiomas: Predictive Parameters for Transpetrosal Approaches. *Neurosurgery*. 2000;47(1):139–152.

155. Bernardo A, Evins AI, Visca A, Stieg PE. The Intracranial Facial Nerve as Seen Through Different Surgical Windows: An Extensive Anatomosurgical Study. *Neurosurgery*. 2013;72(2 Suppl Operative):ons194–207.

156. Materialise Medical. How to Design a Patient-Specific Cranial Plate | Tutorial | Materialise 3-matic [Video]. YouTube. https://youtu.be/r0ExCSr2ThE. Published Jan 25, 2017. Accessed Jan 25, 2017.

157. Gerber N, Stieglitz L, Peterhans M, Nolte LP, Raabe A, Weber S. Using Rapid Prototyping Molds to Create Patient Specific Polymethylmethacrylate Implants in Cranioplasty. *Conf Proc IEEE Eng Med Biol Soc*. 2010;2010:3357–3360.

158. Honeybul S, Morrison DA, Ho KM, Lind CR, Geelhoed E. A Randomized Controlled Trial Comparing Autologous Cranioplasty with Custom-Made Titanium Cranioplasty. *J Neurosurg*. 2017;126(1):81–90.

159. HTR-PEKK Patient-Match Implant [Product Brochure]. Warsaw, IN: Biomet, Inc.; 2013.

160. Driscoll CL, Jackler RK, Pitts LH, Banthia V. Extradural Temporal Lobe Retraction in the Middle Fossa Approach to the Internal Auditory Canal: Biomechanical Analysis. *Am J Otol*. 1999;20(3):373–380.

161. Habboub G, Sharma M, Barnett GH, Mohammadi AM. A Novel Combination of Two Minimally Invasive Surgical Techniques in the Management of Refractory Radiation Necrosis: Technical Note. *J Clin Neurosci*. 2017;35:117–121.

162. White T, Chakraborty S, Lall R, Fanous AA, Boockvar J, Langer DJ. Frameless Stereotactic Insertion of Viewsite Brain Access System with Microscope-Mounted Tracking Device for Resection of Deep Brain Lesions: Technical Report. *Cureus*. 2017; 9(2):e1012.

163. Evins AI, Boeris D, Burrell JC, Ducati A. Postoperative Intracranial Hypotension-Associated Venous Congestion: Case Report and Literature Review. *Clin Neurol Neurosurg*. 2013;115(10):2243–2246.